Dissertation zur Erlangung des Doktorgrades

der Fakultät für Chemie und Pharmazie

der Ludwig-Maximilians-Universität München

Genetic, biochemical and preclinical studies on a tandem cluster of two human serpins: alpha-1-antitrypsin and serpina2

Jessica Tanja Tamara Götzfried

aus

Wolfratshausen

2018

Erklärung

Diese Dissertation wurde im Sinne von § 7 der Promotionsordnung vom 28. November 2011 von Herrn Prof. Dr. Karl-Peter Hopfner betreut.

Eidesstattliche Versicherung

Diese Dissertation wurde eigenständig und ohne unerlaubte Hilfe erarbeitet.

München, 23.01.2018

.....

Jessica Tanja Tamara Götzfried

Dissertation eingereicht am	27.02.2018
1. Gutachter:	Prof. Dr. Karl-Peter Hopfner
2. Gutachter:	PD Dr. Dietmar Martin
Mündliche Prüfung am	15.05.2018

„Das Schönste, was wir erleben können, ist das Geheimnisvolle.“

Albert Einstein

Table of contents

1. Summary

In my thesis I focused on novel aspects of alpha-1-antitrypsin (AAT or serpina1) and its close relative, serpina2 (alpha-1-antitrypsin related protein), a gene in physical proximity to the AAT gene.

Put in a nutshell, in the first described project we found that serpina2 is not a pseudogene as previously suggested. In a recent publication on serpina2, a broad tissue distribution was reported and a protease inhibiting function for serpina2 was discussed, but specific analytical tools were not available at that time. The goal of this study was to develop appropriate tools and procedures to clarify the role of serpina2 as a potential modifier of inflammatory diseases. We used cDNA of many human tissues in qPCR experiments and found serpina2 mRNA exclusively expressed in the epididymis. In addition, we explored recombinant expression of serpina2 and established rat monoclonal antibodies, which were used for immune histology, Western blots and a sandwich ELISA. To search for potential target proteases we used fluorescence resonance energy transfer (FRET) substrates derived from the reactive center loop of serpina2 in activity assays. After transfection of HEK 293 cells, the vast majority of the protein remained inside in association with the host cells, while only small amounts of the normally secreted protein were found in the culture supernatant, suggesting that poor folding and aggregation propensity of serpina2 may contribute to cellular stress and tissue inflammation, like a well-known coding variant of serpina1. With our monoclonal antibodies we were able to detect serpina2 in epididymal tissue lysates of men. A serpina1 chimera, carrying the reactive center loop of serpina2, was cleaved by chymotrypsin suggesting chymotrypsin-like proteases are putative targets of serpina2. In conclusion, serpina2 is not a pseudogene; it is an epididymis specific potential inhibitor of chymotrypsin-like proteases and may improve sperm maturation, male fertility and reproductive success.

In the second project, we characterized two common coding variants of AAT by comparing them in a hydrogen/deuterium exchange experiment combined with mass spectrometry. We revealed that a common single-amino acid variation is not functionally neutral, but affects the overall structural flexibility of the variants and their ability to fulfill their role as protease inhibitor.

In the third project we describe a new method to improve storage of donor lungs by adding AAT to the perfusion and storage solution, which could allow extended storage and better preservation before implantation. Primary graft dysfunction and vascular damage of donor lungs immediately after blood reperfusion in the recipient increases with prolonged preservation times. Hence, cold ischemic storage for only six hours is generally accepted, after lungs are cooled down and conserved in an extracellular, colloid-based electrolyte solution. Natural AAT, a highly abundant human plasma proteinase inhibitor with additional putative functions *in vivo*, has been approved as a therapeutic in AAT deficiency patients. Using a realistic clinically oriented murine model of lung transplantation and adding AAT with a functional reactive center loop to a widely used preservation solution (Perfadex), we found that ischemic storage times of lung grafts at 4 degrees can be extended to 18 h with improved graft function after reperfusion in recipient mice. Double knockout recipients that lack elastase-like activities in neutrophils were also protected from early reperfusion injury, but not those lung grafts that were perfused with a reactive center mutant of AAT devoid of elastase-inhibiting activity. We conclude that the proteinase 3 and elastase inhibiting classical function of tissue AAT reduces the early reperfusion-related injury of transplanted lungs after extended ischemic storage, which makes it a promising strategy for improvement of organ preservation.

2. Introduction

2.1 The superfamily of Serpins

The primary function of serpins is the inhibition of serine proteases. In fact, the term serpin is an acronym for serine protease inhibitor and was coined by Robin Carrell and Jim Travis in 1985[1]. The term is somewhat misleading since not all serpins are inhibitors of serine proteases, some also inhibit cysteine proteases (cross-class inhibition) and several members of the family carry out other important biological functions such as molecular chaperoning (HSP47)[2], hormone carriage (thyroxine- or cortisol-binding-protein[3]) or presumably storage (ovalbumin in egg-white). Despite their different functions, all members of the superfamily are called serpins because of their shared structure and common evolutionary origin[4]. Serpins are present in all kingdoms of life[5-7]. With approximately 1,500 members they represent the largest family of protease inhibitors[8]. In the human genome 35 putatively functional serpins (including at least 29 with inhibitory function) plus five putative pseudogenes were identified[9,10]. The superfamily is divided into clades and numbers based upon a phylogenetic analysis. For instance, serpina1 belongs to clade A and one is the number of the protein within the clade.

The serpin secondary structure is highly conserved, they consist of 8 or more alpha helices, three ß-sheets (A, B and C) and a reactive center loop (RCL), which serves as bait for target proteases[11]. The 20 – 24 amino acid long RCL is flexible and exposed, and therefore easily accessible for proteases[12]. Most serpins are secreted and circulate in their native metastable state with an intact RCL. They inhibit their target proteases in a very unique way by using an unusual conformational change that disrupts the protease structure depriving it of its activity. The major conformational change converts the serpin from a stressed state (high energy) to a relaxed state (low energy), which is also called the S to R transition. During this transition the RCL is inserted into ß-sheet A leading to significantly increased thermal stability (**Figure 2.1**)[10,13].

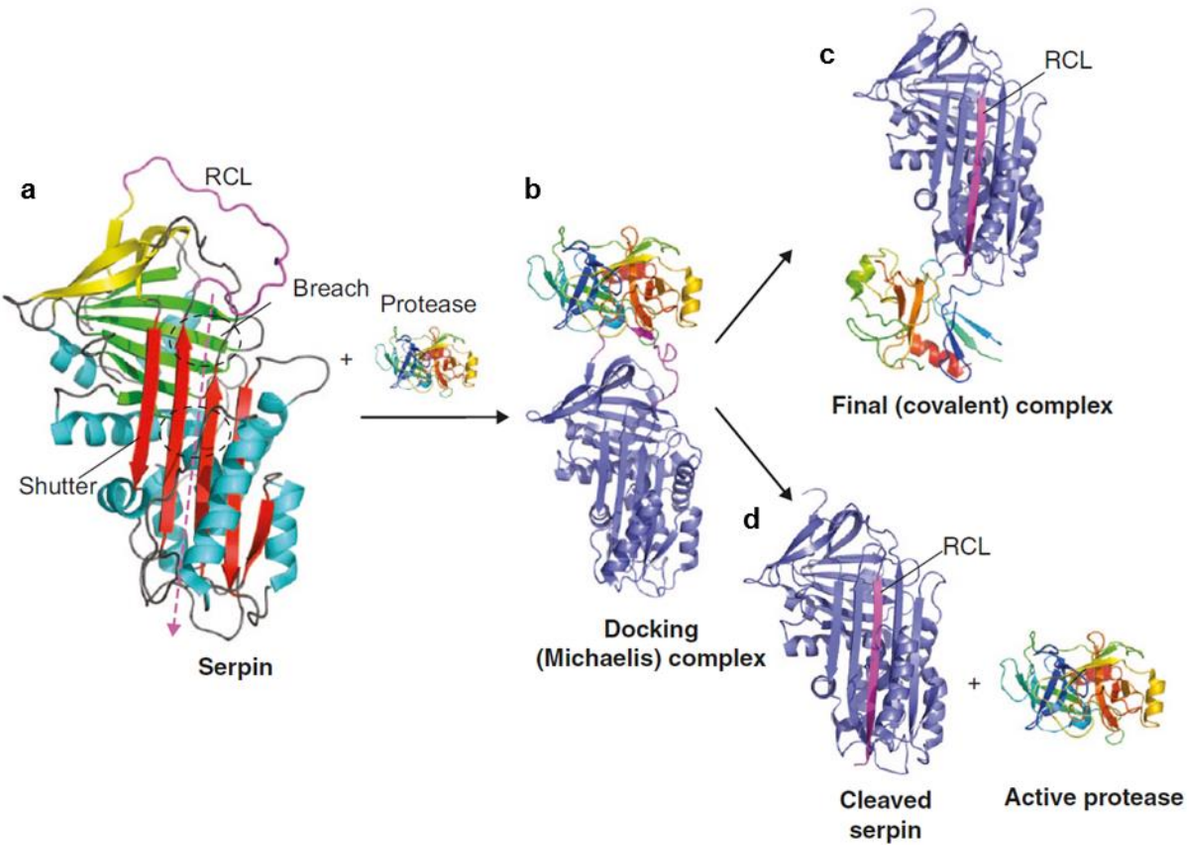

Figure 2.1 Structure and inhibitory mechanism of serpins. (**a**) Native serpina1 (alpha1-antitrypsin) based on PDB IQLP), red: A-sheet, green: B-sheet, yellow: C-sheet, blue: helices, magenta: RCL (reactive center loop) and dashed line marking the path of the RCL insertion into ß-sheet A. (**b**) Michaelis or docking complex between serpina1 and trypsin (based on PDB IOPH). After docking with an active protease two pathways are possible: (**c**) The irreversible serpin-enzyme complex (based on PDB IEZX). S to R transition took place, the serpin rapidly transforms to the energetically favorable relaxed state by inserting the reactive center loop into ß-sheet A. (**d**) Cleaved structure of serpina1 (based on PDB 7API). (Modified from Law *et al.*[8])

The serpin mechanism of protease inhibition has been studied extensively by structural biologists and biochemists (reviewed in[4,11,12]). Initially, a non-covalent protease-inhibitor Michaelis complex is formed. Subsequently, the peptide bond in the serpin's RCL is cleaved through a nucleophilic attack by the catalytic triad (Asp, His, Ser/Cys) of the protease. The Schechter-Berger nomenclature for protease substrate interaction is used to number the RCL residues (P-residues) and the respective protease subsites close to the active site (S-regions). The scissile bond (cleavage site) is located between P1 and P1'[14]. The S1 pocket of the protease interacts with the specificity-determining P1 residue of the inhibitor[15-17]. P17 – P1 are used for numbering the N-terminal side of the scissile bond and P1' – P6' for the C-terminal side[14]. The second step of the interaction is the formation of an ester bond between the enzyme and the substrate or the pseudo-substrate. For usual substrates the ester bond is hydrolyzed and the protease is set free. When the substrate happens to be a serpin (pseudo-substrate), the RCL inserts into ß-sheet A resulting in a relocation of the protease from one end to the distal end. Thereby the acyl-enzyme intermediate becomes kinetically trapped leading to an irreversible inhibition of the protease. This process leads to a destruction of the oxyanion hole by distorting the active center of the protease[11,12] Serpins are not only classed as irreversible inhibitors, but also as suicide inhibitors since they can only inactivate a single protease molecule and are no longer active after their dissociation from the protease. Their inhibitory activity cannot be recovered by dissociation from the protease.

2.2 Alpha-1-antitrypsin (AAT or serpina1)

One of the best studied serpins is alpha-1-antitrypsin. It is one of the most abundant proteins in human blood (20 – 53 µM) making up 10 % of all plasma proteins[18-20]. It is expressed primarily in hepatocytes in the liver and then distributed via the blood throughout the body. Its major physiological role is the inhibition of excessive proteases. When the protease inhibitor was first recognized as an inhibitor of trypsin, it was called alpha-1-antitrypsin, but further studies revealed that it is the most efficient inhibitor of neutrophil elastase[21]. Very high levels of alpha-1-antitrypsin are required to inhibit proteases effectively. In an acute phase response normal plasma levels are dramatically increased by enhanced de novo synthesis in the liver. These higher systemic levels protect connective tissue fibers more efficiently against elastase released by activated neutrophil granulocytes.

2.3 Alpha-1-antitrypsin deficiency

Tight regulation of proteases is very important and in a healthy system the inhibitor concentration is much higher than the protease concentration. Proteases are not properly inhibited when there is an imbalance between inhibitors and proteases as it happens in individuals with lower levels of alpha-1-antitrypsin, who are predisposed towards the development of pulmonary emphysema. Alpha-1-antitrypsin deficiency is an inherited disease. Two codominant alleles determine the concentration of alpha-1-antitrypsin in the blood stream. The most common and well characterized mutation in individuals with European ancestry is the so called Z variant ($Glu^{342} \rightarrow Lys^{342}$)[22,23]. Individuals homozygous for the Z-allele show only 10 - 15% of normal levels and develop emphysema in 80 - 90% of cases (according to Orphanet, a European rare disease database). Additionally, the Z-type of alpha-1-antitrypsin accumulates in hepatocytes due to misfolding and the mutation sometimes results in liver cirrhosis[24].

Patients are treated intravenously with purified human alpha-1-antitrypsin to raise the level in the blood and lungs (augmentation therapy). The ultimate treatment of end stage lung and liver disease is the transplantation of these organs.

2.4 Objectives of this dissertation

Alpha-1-antitrypsin has been studied extensively, however, very little is known about its direct neighbor gene serpina2, which was originally thought to be a pseudogene. In recent studies serpina2 expression was proposed again and in this thesis we evaluated the new data on serpina2 with the goal to study the protein and its function as putative protease inhibitor.

The second part of this dissertation characterizes common coding variants of alpha-1-antitrypsin by comparing different proteins in a hydrogen/deuterium exchange experiment combined with mass spectrometry to reveal their different functional properties.

In the third and last chapter we describe a new therapeutic approach to use alpha-1-antitryspin in lung transplantation. We evaluated whether storage and transplantability of donor lungs can be improved by adding the protease inhibitor to the storage solution during cold ischemia in a murine orthotopic lung transplantation model.

3. Materials and methods

3.1 Materials

3.1.1 Chemicals and Consumables

Chemicals were purchased from the companies BD Biosciences (Franklin Lakes, NJ, USA), Bio-Rad Laboratories (Hercules, CA, USA), Biozym (Hessisch Oldendorf, Germany), Life Technologies (Carlsbad, CA, USA), Merck (Darmstadt, Germany), PAA Laboratories GmbH (Pasching, Austria), GE Healthcare (Little Chalfont, Buckinghamshire, UK), Qiagen (Hilden, Deutschland), Roth (Karlsruhe, Germany), and Sigma-Aldrich (St Louis, MO, USA), unless mentioned otherwise. Restriction enzymes and T4 DNA ligase were purchased from New England Biolabs (Ipswich, MA, USA) and Thermo Fisher Scientific (Waltham, MA, USA). Consumables such as pipette tips, centrifuge tubes, reaction tubes, and microwell plates were procured from Biozym (Hessisch Oldendorf, Germany), Eppendorf (Hamburg, Germany), BD Biosciences and Nunc/Thermo Fisher Scientific (Waltham, MA, USA). Cell culture flasks and dishes were obtained from Corning (Corning, NY, USA) and BD Biosciences.

3.1.2 Laboratory equipment

Autoklave	Varioklav, H+P Labortechnik, Oberschleissheim, Germany
Balances	PM 4800 Delta Range, Mettler-Toledo, Columbus, OH, USA 2001 MP2, Sartorius, Göttingen, Deutschland
Centrifuges	5417R, Eppendorf
	5417C, Eppendorf
	Rotanta 460R, Hettich, Tuttlingen, Germany
	Rotanta/R, Hettich
Film developer	X-Omat M35, Kodak
FPLC	ÄKTAprimeTM, Amersham-Pharmacia
Gel electrophoresis chambers/ power supplies	Bio-Rad, Amersham-Pharmacia, MPI workshop
Incubation shaker	HT Multitron, Infors, Bottmingen, Switzerland
Incubator	BBD6220, Heraeus, Thermo Scientific, Waltham, MA, USA
Incubator	Jouan, Germany
Icemachine	Ziegra, Isernhagen, Germany
Laminar flow	LaminAir HB 2472S, Heraeus, Hanau, Germany
Magnetic stirrer	MR3003, Heidolph, Kelheim, Germany
	KMO2 basic, IKA, Staufen, Germany

Microplate reader	FLUOStar Optima, BMG Labtech, Offenburg, Germany
Microscope	Leica DM IL, Leica Microsystems, Wetzlar, Germany
pH-meter	Inolab pH Level 1, WTW, Weilheim, Germany
PCR cycler	T3 Thermocycler, Biometra, Göttingen, Germany
Semidry blotter	Biometra, Göttingen, Germany
Shakers	130 basic, IKA KS
	260 basic, IKA KS
Spectrophotometer	ND-1000, peqlab, Erlangen, Germany
	Biophotometer, Eppendorf
Thermoblock	Thermomixer 5436, Eppendorf
Ultrasonic bath	Sonorex digital 10P, Bandelin, Berlin, Germany
Water bath incubator	MA6, Lauda, Lauda-Königshofen, Germany
Water preparation	Milli Q Advantage, Millipore, Billerica, MA, USA

3.1.3 Oligonucleotides

Oligonucleotides were synthesized by Eurofins Genomics (Ebersberg, Germany).

Oligonucleotide	Sequence
Serpina2 qPCR	
DJ3701_SerpA2for	5'-TGGAGAAAAGAACTGGAAGA-3'
DJ3702_SerpA2rev	5'-ATGTCAAATCTACCCAGGTG-3'
Serpina2 genotyping	
DJ3754_SA2_ex2f3	5'-GCCTCTGTCTTGCAGGAGAAT-3'
DJ3751_SA2_r3	5'-TCGGTGTCCCTGAAGTTGAT-3'
Cloning pET24c_serpina2_His	
DJ3706_serpa2_f	5'-CGGGGATCCATGCAGAAGATCTCCTATAACGT-3'
DJ3707_serpa2_r	5'-GTGGTGCTCGAGTTTTTGGGTGGGATTCACCAC-3'
Cloning AAT^{mt}	
DJ3708	5'-TCGAGGACCCTGACTCATCG-3'
DJ3709	5'-ATCGATGAGTCAGGGTCC-3'
Cloning pETSUMOSerpina2	
pETSUMOSerpinA2_F	5'-TGGTGGACAGAAGATCTCCTATAACGTCACCG-3'
pETSUMOSerpinA2_R	5'-GAGTACTTTATTTTTGGGTGGGATTC-3'
Cloning PQEserpina2	
F1_PQEserpinA2_F	5'-tccaaGGACAGAAGATCTCCTATAACGTCAC-3'
F1_PQEserpinA2_R	5'-GCTtcattaTTTTTGGGTGGGATTCACC-3'

3.1.4 Plasmids

Plasmid	Construct	Origin
pTT5	-	NRC Biotechnology Research Institute (Ottawa, Ontario, Canada)
pTT5-hAAT	SigIgκ-AAT-H6	Therese Dau, AG Jenne
pTT5-hAAT M1(V213)		Therese Dau, AG Jenne
pTT5-hAAT M1 (A213)		Therese Dau, AG Jenne

Pet24-c(+)	-	69751, Novagen
Pet28_His_SUMO	-	Huntington lab, Cambridge

Vector maps can be found in the Appendix (9).

3.1.5 *E.coli* bacterial strains

Strain	Genotype	Source
DH5α	F– Φ80*lac*ZΔM15 Δ(*lac*ZYA-*arg*F) U169 *rec*A1 *end*A1 *hsd*R17 (rK–, mK+) *pho*A *sup*E44 λ– *thi*-1 *gyr*A96 *rel*A1	18265017, Thermo Fisher Scientific
BL21	*fhuA2 [lon] ompT gal (λ DE3) [dcm] ΔhsdS λ DE3 = λ sBamHIo ΔEcoRI-B int::(lacI::PlacUV5::T7 gene1) i21 Δnin5*	C2527I, NEB
SHuffle® Express	*fhuA2 [lon] ompT ahpC gal* λatt::pNEB3-r1-*cDsbC* (SpecR, *lacI^{q}) ΔtrxB sulA11* R(*mcr-73::miniTn10*--Tet^{S})*2 [dcm] R(zgb-210::Tn10* --Tet^{S}) *endA1 Δgor Δ(mcrC-mrr)114::IS10*	C3028J, NEB
Rosetta™ 2(DE3)pLysS	F^{-} *ompT hsdS*$_{B}$(r_{B}^{-} m_{B}^{-}) *gal dcm* (DE3) pLysSRARE2 (Cam^{R})	71403, Novagen

3.1.6 Recombinant and purified proteins

Protein	Origin
AAT, human	Athens Research & Technology (Athens, GA, USA)
Cathepsin G, human	219373, Calbiochem (Merck, Darmstadt, Germany)
Neutrophil elastase, human	Elastin Products (Owensville, MO, USA)
Neutrophil elastase, mouse	Therese Dau, AG Jenne
Proteinase 3, human	Diarect AG (Freiburg, Germany)
Proteinase 3, mouse	Therese Dau, AG Jenne
Trypsin, bovine	Sigma-Aldrich
Kallekrein 3	AG Jenne
Cathepsin B	Recombinatnly expressed in *Pichia pastoris,* AG Jenne
Cathepsin L	Recombinatnly expressed in *Pichia pastori,* AG Jenne
Cathepsin C	Heike Kittel, AG Jenne
Chymase	230780, Calbiochem (Merck, Darmstadt, Germany)
NSP4	Natascha Perera, AG Jenne

3.1.7 Antibodies

Primary antibodies

Antigen/ isotype control	Species	Clone	Provider	Cat. No.
IgG1 Isotype	Mouse	-	BD Biosciences	349040
serpina2-G12 polyclonal IgG	Goat	-	Santa Cruz	109866
SA2 mAb 6	Rat	4E10	AG Jenne/AG Kremmer IMI	-
SA2 mAb 75	Rat	5H4	AG Jenne/AG Kremmer IMI	-
SA2 mAb 76	Rat	3G6	AG Jenne/AG Kremmer IMI	-
SA2 mAb 77	Rat	2F6	AG Jenne/AG Kremmer IMI	-
SA2 mAb 80	Rat	2D11	AG Jenne/AG Kremmer IMI	-
SA2/AAT mAb 104	Rat	13C7	AG Jenne/AG Kremmer IMI	-
Ly6 mAb	Rat IgG2a, κ	1A8	Biolegend	127601

Secondary antibodies

Antigen	Species	Label	Provider	Cat. No.
Rat IgG+IgM	Goat	HRP	Jackson Immuno Research	112-035-068
Goat	Mouse	HRP	Millipore	

Other

Protein	Species	Label	Provider	Cat. No.
Avidin		HRP	Invitrogen	434423

3.1.8 Synthetic substrates

FRET substrates

Sequence	Cleaving protease	Provider
5-TAMRA-EKAWSKYQ-Dap(CF)	-	EMC Microcollections
5-TAMRA-EKPWSKPQ-Dap(CF)	-	EMC Microcollections
TAMRA-VADnVRDYQ-Dap(CF)	PR3	EMC Microcollections

SBzl substrate

Sequence	Cleaving protease	Provider
Boc-APnV-SBzl	PR3, NE	Bachem

3.1.9 Cell line

The cell line HEK 293 EBNA1 was purchased from the NRC Biotechnology Research Institute (National Research Council in Montreal, Canada).

3.1.10 Mouse strains

We obtained pathogen-free C57BL/6J mice from Charles River.

PR3/NE knockout animals (*Ela2*$^{-/-}$*Prtn3*$^{-/-}$) were established by Pfister *et al.*[25]. Mice were backcrossed for more than ten generations with C57BL/6J mice. All animals were kept under normal housing conditions with constant temperature and humidity, a 12 hour light cycle, and food and water were allowed *ad libitum*.

3.2 Molecular biological methods

3.2.1 Polymerase chain reaction (PCR)

PCR is a fast and easy method to specifically amplify a DNA fragment from very small amounts of template DNA. Two oligonucleotides flanking the two ends of the DNA fragment, which should be amplified, are used as Primers. They contain a free 3´-OH at one end, ensuring the synthesis of the new strand in only one direction. The synthesis is carried out by a Taq polymerase, which is stable at high temperatures. By adding and linking new nucleotides to the primers many copies of the amplicon are generated. PCR is carried out in several subsequent cycles, beginning with a denaturation step in which the strands of the DNA double helix separate from each other, followed by an annealing step in which the primers bind to the ends of the desired DNA fragment. All cycles are completed by a final extension step in which the DNA polymerase extends all DNA fragments to their full length. For all PCRs the HotStarTaq DNA Polymerase from Qiagen was used.

HotStarTaq PCR reaction (25 µl):

Component	Concentration
PCR buffer (Qiagen)	1x
dNTP-mix (10 mM)	0.2 mM
Forward primer (10 µM)	0.2 µM
Reverse primer (10 µM)	0.2 µM
HotStarTaq DNA polymerase	0.25 µl
DNA template (1 ng/µl)	1 µl
H_2O up to 25 µl	

HotStarTaq PCR program:

Pre-heating: 100 °C

[°C]	[s]		
95	30		
95	30	Denaturation	30 x
50 - 65	60	Annealing	
72	75	Elongation	
72	300		
4	∞		

12

3.2.2 Restriction (double) digest of PCR products

Restriction endonucleases are enzymes which cleave DNA at a specific recognition sequence. The DNA obtained from PCR was digested with one or two different restriction enzymes to produce linear fragments with non-complementary ends. To enable DNA ligation into a vector the plasmid is digested with the same enzymes as the PCR product. The reaction mixture consisted of the DNA-fragment, the restriction enzyme(s) and a buffer suitable for the enzymes. 1 µg DNA was digested with 10 U of the restriction enzymes. The mixture was incubated according to the manufacturers' instructions . Restrictionenzymes were purchased from New England Biolabs or Thermo Fisher Scientific.

3.2.1 Agarose gel electrophoresis

DNA fragments are negatively charged due to their sugar-phosphate backbone and can therefore be separated in an agarose gel matrix in an electric field on the basis of their size. Agarose gels were prepared with TAE buffer supplemented with SYBR Safe (Life Technologies, dilution 1: 10000) to visualize DNA by exposure to UV light (254-366 nm). To prepare the gel, agarose (LE agarose, 840004 or Sieve 3:1 agarose, 850091, Biozym) was dissolved in TAE buffer by heating in a microwave for about 2 min. 0.8 – 4 % (w/v) agarose gels were casted depending on the fragment size to be analyzed. After addition of DNA loading buffer the samples were buffer, the samples were loaded into the gel slots and the gel was run in TAE-buffer at 80 V. To determine the size of the DNA fragments, the bands were compared to a molecular weight standard (Gene Ruler 1kb, Fermentas, Thermo Fisher Scientific).

50 x TAE buffer	
Tris	242 g
0.5 M EDTA pH 8.0	100 ml
Acetic acid	57.1 ml
H_2O to 1 L	

10 x DNA Loading buffer	
Bromphenol blue	0.25% (w/v)
Xylenecyanol	0.25% (w/v)
Glycerol	50% (w/v)

3.2.2 Dephosphorylation of vector DNA

To prevent the digested vector from self-ligation, it was dephosphorylated with the Calf Intestinal Alkaline Phosphatase (New England Biolabs). 1 µl of Alkaline Phosphatase was added to up to 5 µg of vector DNA in a restriction digest after 15 min and incubated for another 45 min at 37 °C.

3.2.3 DNA purification

Digested PCR products or vectors were purified by gel extraction (QIAquick GelExtraction Kit, Qiagen) or with the QIAquick PCR Purification Kit (Qiagen) in accordance with the manufacturer's instructions. The final elution volume comprised 30-50 µL elution buffer or ddH_2O, which was heated to 70 °C before elution for higher concentration results.

3.2.4 Determination of DNA concentration

DNA concentrations were measured with the Nanodrop. Then 2 µl of the sample were pipetted onto the Nanodrop. For determination of DNA concentrations I measured the absorption at 260 nm.

The theoretical fundament for this measurement is described by the Beer-Lambert law:

$$A = \lg \frac{I_0}{I} = c \cdot \varepsilon \cdot d$$

A…Absorption
I_0...intensity of incident light
I…intensity of transmitted light
c…concentration of absorbing particles
ε…molar extinction coefficient
d…thickness of sample

3.2.5 Ligation

T4 DNA Ligase or the Quick Ligation Kit (both from New England Biolabs) were used to link the ends of the digested and dephosphorylated vector with the insert according to the manufacturer's manual. Ligation reactions employing T4 DNA Ligase were carried out for 2-4 h at room temperature or at 16 °C for 16 h. When using the Quick Ligation Kit the reaction mixture was incubated between 5-15 min at room temperature. For each reaction we took 50 ng vector DNA and a molar ration of 5 to 10 of vector and insert in a total volume of 20 µl.

Example of T4 DNA Ligase reaction mixture:

Component	**20 µl reaction**
Vector DNA (4 kb)	50 ng
Insert DNA (1 kb)	37.5 ng
T4 DNA Ligase	1 µl
10X T4 DNA Ligase Buffer	2 µl
ddH_2O	Up to 20 µl

3.2.6 Preparation of $CaCl_2$-competent bacteria

5 ml of LB medium (Luria-Bertani-Broth) were inoculated with a single colony of *E.coli* DH5α and grown without the addition of antibodies in a 15 ml tube at 37 °C with shaking (250 rpm) overnight. On the next day 4 ml of the pre-culture were added to 400 ml fresh LB medium. The cells were incubated (37 °C, 250 rpm) until the OD_{600} reached 0.4, which took approximately three hours. Then, the bacterial suspension was pre-cooled on ice in 50 ml tubes for 10 min. Subsequently, the suspensions were pelleted by centrifugation without break (7 minutes, 3000 rpm, 4 °C). For all remaining steps the cells were kept on ice and all flasks, pipette tips and tubes were pre-cooled at 4 °C. Cell pellets of 100 ml culture volume were resuspended in 10 ml ice-cold $CaCl_2$ buffer and centrifuged again (5 min, 2500 rpm, 4 °C, no brakes). Cell pellets were again resuspended in 10 ml ice-cold $CaCl_2$ buffer and incubated on ice for 30 min followed by centrifugation (5 min, 2500 rpm, 4 °C, no brakes). Bacteria pellets were resuspended in 2ml ice-cold $CaCl_2$ buffer and 150 µl aliquots were snap frozen in liquid nitrogen and stored at -80 °C.

$CaCl_2$ buffer	
$CaCl_2$	60 mM
PIPES	10 mM
Glycerol	15% (w/v)
pH 7	

LB medium	
Bacto tryptone	1% (w/v)
Yeast Extract	0.5% (w/v)
NaCl	1% (w/v)
pH 7.5, autoclaved	

LB agar plates	
LB medium	1 L
Bacto agar	1.5% (w/v)
autoclaved	

3.2.7 Transformation of $CaCl_2$-competent bacteria

Competent *E. coli* DH5α were thawed on ice for 10 min. Transformation of plasmid DNA into competent *E.coli* cells was performed by mixing 100 µl of competent bacteria cells with 5 µl of the ligation reaction followed by incubation on ice for 30 min. This allows the plasmid DNA to attach to the cell wall of the bacteria. A heat-shock was performed for 45 sec at 42 °C in a water bath, and then the tube was immediately chilled on ice for about 10 min. The heat-shock permeabilizes the cell membrane for a short duration and the plasmid DNA can enter the bacteria. After that 900 µl of LB medium were added, followed by incubation for 1 h at 37 °C in a shaking thermoblock. 200 µl cell suspension was plated on LB agar plates containing the respective antibiotics and incubated overnight at 37 °C.

3.2.8 DNA Sequencing

In order to check whether plasmids with a positive restriction digest result contain any mutations they were sequenced by Eurofins MWG GmbH (Ebersberg, Germany).

3.2.9 Plasmid DNA purification from bacteria

Purification of Plasmid DNA from 5 ml *E.coli* overnight culture was carried out with the QIAprep Spin Miniprep Kit (Qiagen). After alkaline lysis of the bacterial cells the DNA was bound to a silica membrane in high salt. For the purification of higher amounts of Plasmid DNA out of larger overnight cultures the PureYield™ Plasmid Maxiprep System (Promega) was utilized. Furthermore, this purification procedure included an endotoxin removal step to remove protein, RNA and endotoxin contaminants from the DNA preparation. Both kits were used according to the manufacturer's protocol. The purified and endotoxin free plasmid DNA was used for transfection of mammalian cells (HEK 293EBNA). Removal of endotoxin was necessary to avoid reduced transfection efficiency.

3.2.10 Glycerol cultures

Glycerin cultures were established for permanent stocking of bacteria cultures. For this purpose an overnight culture of bacteria was grown in 3 ml LB in a 15 ml tube at 37 °C with shaking. Then, the bacteria cell suspension was centrifuged (4000 rpm, 10 min). Autoclaved glycerol (87%) and LB was added to the bacteria pellet to get a 15 – 20 % final concentration of glycerol in a cryotube. The tube was snap frozen in liquid nitrogen and stored at – 80 °C.

3.2.11 Quantitative real-time RT-PCR analysis

cDNA of 46 healthy human tissues (Cat. No.: HMRT 102) and a human brain panel (Cat. No. HBRT 101) were obtained from OriGene Technologies and cDNA of a human megakaryoblastic leukemia cell line, MEG-01, was purchased at ECACC (Cat.No.94012401). Quantitative PCR was performed using the SYBR Green LC480 System (Adhesive clear PCR seal: 600208, 96 well plate, white: 712282, Biozym, LC 480 Cycler: Roche Diagnostics, Mannheim, Germany). For detection of serpina2 we used the following primer pair: DJ3701 and DJ3702 (see 3.1.3). GAPDH primers (OriGene Technologies, Cat. No.: HMRT 102, included in kit) were used as intrinsic control for normalization of the results.

3.2.12 Serpina2 genotyping of human blood samples

Whole blood (100 µl) was used to extract DNA with the DNeasy Blood and Tissue Kit (69506, Qiagen). During the isolation procedure 20 µl of proteinase K (20 mg/ml) were added to 100 µl whole blood diluted in 100 µl PBS. DNA was eluted in 100 µl elution buffer. Whether the isolation was successful, was determined by measuring the DNA concentration with the Nanodrop. DNA yield ranged from 10 – 20 ng/µl.

As a first step, a PCR with the KAPA2G Fast Genotyping Mix (KK5121, Roche) was carried out to amplify the serpina2 DNA fragment.

Serpina2 genotyping PCR reaction (25 µl):

Component	[µl]	Final concentration
KAPA Mix	12.5	
DJ3754, forward primer (10 µM)	1.25	0.5 µM
DJ3751, reverse primer (10 µM)	1.25	0.5 µM
DNA template (10 – 20 ng/µl)	1	
H_2O	9	

Serpina2 genotyping PCR program:

Pre-heating: 100 °C

[°C]	[s]		
95	180		
95	15	Denaturation	35 x
58	20	Annealing	
72	30	Elongation	
72	600		
4	∞		

The second step was to digest the PCR product with the two restriction enzymes in separate reactions. Digestion with BsmI (R0134S, NEB) was used to identify serpina2 deletion genotypes and BseLI (ER1201, Thermo Fisher Scientific) was used to identify serpina2 fs108 genotypes. Reaction mixtures were incubated at 60°C for two hours.

Digestion reaction (13 µl):

Component	[µl]
PCR	7
10 x Tango buffer	1.3
BseLI	1
H_2O	4.6

Component	[µl]
PCR	7
10 x Cut smart	1.3
BsmI	1
H_2O	4.6

Subsequently, the digested PCR products were analyzed on a 4 % agarose gel (Sieve 3:1 agarose, 850091, Biozym) by electrophoresis for 2 hours at 85 V.

3.3 Recombinant protein expression

3.3.1 Serpina2 expression in *E.coli*

For the expression of serpina2 we used competent *E.coli* BL21(DE3) (C2527I, NEB). DE3 indicates that the host (lysogen of λDE3) carries a chromosomal copy of the T7 RNA polymerase gene under control of the lacUV5 promoter and can therefore be induced with Isopropyl β-D-1-thiogalactopyranoside (IPTG) for production of protein from target genes cloned in pET vectors. We also utilized two enhanced BL21 derivatives: the SHuffle® Express(C3028J, NEB) strain, engineered to promote disulfide bond formation in the cytoplasm and the Rosetta™ 2(DE3)pLysS (71403, Novagen) designed to enhance the expression of eukaryotic proteins that contain codons rarely used in *E. coli*. pLysS strains express T7 lysozyme, which further suppresses basal expression of T7 RNA polymerase prior to induction, thus stabilizing pET recombinants encoding target proteins that affect cell growth and viability.

For overexpression of recombinant proteins, competent *E.coli* cells were transformed with different serpina2 plasmids (pET_24c_serpina2_His, pET24c_His_SUMO_serpina2, and PQEwa_His_TEV_serpina2). Cells were grown at 37 °C in LB medium in the presence of the appropriate antibiotics until the OD_{600} reached 0.6 – 0.8. Then IPTG was added to a final concentration of 0.5 mM to induce protein expression. After growth for 16 h at 18 °C or 37 °C the cells were harvested by centrifugation.

Supplement	Stock solution	In media diluted to
Ampicillin	100 mg/ml in H_2O	100 µg/ml
Kanamycin	30 mg/ml in H_2O	30 µg/ml
IPTG	234.3 mg/ml (1 M) in H_2O	0.5 mM

3.3.2 Expression of AAT and AAT variants in HEK 293 cells

Before transfection HEK 293 cells were grown to a density of 1 x 10^6 cells/ml. Polyethyleneimine (PEI) a cationic polymer, that binds to negatively charged DNA, was used

for the generation of PEI/DNA complexes.30 µl of PEI were added to 500 µl of Optipro serum free medium (Invitrogen) and 7.5 µg of plasmid DNA were added to 500 µl Optipro in a separate tube. Both mixtures were combined and incubated at room temperature for 20 min. The PEI/DNA mixture was added drop-by-drop to 15 ml (15 million cells) cell suspension to ensure equal distribution of the DNA. The cells were incubated at 37 °C and after 24 hours Bacto TC Lactalbumin Hydrolysate (BD Biosciences), which is the enzymatically hydrolyzed portion of milk whey, was added as an amino acid supplement to 0.5% final concentration. Supernatants were harvested after 4 days by centrifugation (1500 rpm/10 min/ 4 °C).

3.4 Protein analysis

3.4.1 Purification of recombinant proteins by Ni-NTA

First, the cell culture supernatant was filtered through a 0.22 µm membrane (Millipore). For proteins with lower expression rate, the supernatant was concentrated using a ultrafiltration membrane with 10 kDa cut-off (Amicon Ultra centrifugal filter, UFC801024, Merck). Then, the supernatant was dialyzed against Ni-NTA binding buffer. The dialyzed supernatant was again filtered (0.22 µM) and the protein solution was applied to a HisTrap HP column (GE Healthcare) previously equilibrated in binding buffer. The column was washed with binding buffer, and bound proteins were eluted applying a linear imidazole gradient from 50 mM to 1 M imidazole in binding buffer. Fractions were collected and analyzed by SDS-PAGE and coomassie or silver staining. The fractions that contained the protein of interest were pooled and concentrated.

Ni-NTA binding buffer	
Na_2HPO4	20 mM
NaCl	300 mM
Imidazole	10 - 20 mM
pH 7.4	

Ni-NTA elution buffer	
Na_2HPO4	20 mM
NaCl	300 mM
Imidazole	1 M
pH 7.4	

3.4.2 Purification of recombinant protein by anti-His immunoaffinity

After Ni-NTA affinity purification, some recombinant proteins were subjected to a second step of purification to get rid of contaminations by non-specifically binding proteins. An anti-His affinity resin (Cat.No. L00439-1, GenScript) was used according to the manufacturer's protocol. We chose to use an acidic elution procedure.

Anti-His affinity resin binding buffer	
Tris HCl	50 mM
NaCl	150 mM
pH 7.4	

Anti-His affinity resin elution buffer	
Glycine HCl	0.1 M
pH 2.5	

Anti-His affinity resin neutralization buffer	
Tris	1 M
pH 9.0	

3.4.3 Determination of protein concentration

The concentration of protein solutions was either assessed by a bicinchonic acid (BCA) assay carried out according to the manufacturer's instructions, or by spectrophotometrically measurement of absorbance at 280 nm. The concentration can be calculated using the Beer-Lambert law (see 3.4.3).

The extinction coefficient of each protein was determined by using the ProtParam tool (http://us.expasy.org/tools/ protparam.htm) inserting the protein sequence obtained from the UniProt database (http://www.uniprot.org/).

3.4.4 Sodium dodecyl sulfate - polyacrylamide gel electrophoresis (SDS-PAGE)

To separate proteins according to their size we used SDS-PAGE. We use self-made discontinuous gels, which consist of a stacking gel and a resolving gel. In the stacking gel the proteins form thin sharp bands due to the slightly acidic milieu and the low concentration of acrylamide. Then they enter the resolving gel, which has a more basic pH and a higher polyacrylamide concentration that leads to the separation of the proteins according to their size. Both, the samples and the gel/gel running buffer contain the detergent SDS, which denatures the proteins. They unfold into their secondary structure and get negatively charged according to their size. The sample buffer contains also ß-mercaptoethanol which is able to reduce disulfide bonds. Before loading, the protein samples were denatured by incubation in sample buffer at 95°C for 5 min, and then were centrifuged for 1 min at 12 000 rpm. For analysis, up to 20 µl of sample and 10 µl of protein marker (Prestained Protein Marker, Broad Range, New England Biolabs) were loaded.

Sample buffer 4 x, reducing	
Tris	200 mM
Glycine	200 mM
SDS	1 mM
MeOH	20%
pH 6.8	

3.4.5 Protein detection

Coomassie staining

After SDS-PAGE gels were incubated for 1 h in Coomassie staining solution. To remove unspecific staining the gel was incubated Coomassie destaining solution until protein bands were visible. The gels were photographed with a Chemidoc imaging system (Bio-Rad).

Coomassie staining solution	
Coomassie Brilliant Blue	0.25 % (w/v)
Methanol	45 % (v/v)
Acetic acid	10 % (v/v)

Coomassie destaining solution	
Methanol	45 % (v/v)
Acetic acid	10 % (v/v)

Silver nitrate staining

After SDS-PAGE the gel was incubated in fixation solution for 1 h at room temperature while shaking. Subsequently, it was washed three times in 50% ethanol for 20 min, then the gel was incubated in thiosulfate solution for 1 min for sensitization, then rinsed in tap water three times for 20 sec. After incubation in silver nitrate solution for 20 min, the gel was again washed three times for 20 sec in tap water, and then the gel was kept in development solution until protein bands became visible. To stop the staining reaction the gel was quickly rinsed in tap water and then incubated in stopping solution for at least 20 min. After the stopping solution was replaced with tap water, the gels were photographed with a Chemidoc imaging system (Bio-Rad).

Fixation solution	
Methanol	50 % (v/v)
Acetic acid	12 % (v/v)
Formaldehyde 37%	0.5 ml/l

Thiosulfate solution	
$Na_2S_2O_3$ x 5 H_2O	0.2 g/l

Silver nitrate solution	
AgNO3	2 g/l
Formaldehyde 37%	0.75 ml/l

Development solution	
Na2CO3	60 g/l
$Na_2S_2O_3$ x 5 H_2O	4 mg/l
Formaldehyde 37%	0.5 ml/l

Stopping solution	
Methanol	50 % (v/v)
Acetic acid	12 % (v/v)

3.4.6 Measurement of enzymatic activity

3.4.6.1 Förster/Fluorescence resonance energy transfer (FRET)

FRET substrates mimicking the RCL of serpina2 were developed to test cleavage by potential target proteases of the serpin. The TAMRA-FRET substrates (see 3.1.8) were diluted in DMSO to reach a concentration of 100 µM.

Typical reaction:

Component	**[µl]**	**Final concentration**
Activity assay buffer	40	
Protease 1 µM	5	0.1 µM
FRET substrate 100 µM	5	10 µM
Final volume	**50**	

Activity assay buffer	
Tris	50 mM
NaCl	150 mM
Triton X-100	0.01 %
pH 8.0	

The reaction components were combined in a microtiter plate and the hydrolysis rate of the FRET peptides was followed by measuring the fluorescence (λEx = 485 nm and λEm = 520 nm). Specificity was assessed by recording the increasing fluorescence over time for each substrate. Only the slope of the reaction curve was used to define the enzymatic activity in RFUs (relative fluorescent units).

3.4.6.2 Assay for inhibitory activity measurement

The enzymatic activities of the serine proteases, NE and PR3, were determined using thiobenzyl ester substrates and Ellman's reagent (5,5'-dithiobis-(2-nitrobenzoic acid) or DTNB). Free thiobenzylester groups react with DTNB and form yellow 2-nitro-5-thiobenzoate ions. The rate of hydrolysis was measured at 405 nm. Inhibitory activities of 0.5 µM AATwt and AATmt were tested in an activity assay using 0.1 µM recombinant mouse or human NE or PR3. The remaining activity of the proteases was determined using thiobenzyl ester substrate (see 0) at 1 mM substrate concentration and 0.5 mM DTNB in activity assay buffer (see 3.4.6.1).

3.4.7 Deglycosylation of protein with Endo H and PNGase

To monitor protein trafficking and comparison of size of unmodified protein from different species we deglycosylated protein with PNGase F (P0704S, NEB) and Endo H (P0702S, NEB) according to the manufacturer's protocol. PNGase F, an amidase, cleaves off high mannose, hybrid, and complex oligosaccharides of N-linked glycoproteins between the innermost GlcNAc and asparagine residues. Endo H can cleave high mannose and hybrid glycans, but fails to hydrolyse complex glycans, this modification takes place when a protein successfully entered the Golgi apparatus. Proteins containing glycans resistant to Endo H must have entered the Golgi apparatus.

3.4.8 Mass Spectrometry (MS) – Sample preparation and analysis

3.4.8.1 Preparation for immunoprecipitated MS samples

MS has become the method of choice for protein detection. For sample preparation we immunoprecipitated serpina2 in protein lysates (RIPA buffer) using the monoclonal antibodies established in this work (mAb 75 and mAb 80), and Dynabeads™ Protein G for immunoprecipitation (10003D, Thermo Fisher Scientific) according to the manufacturer's protocol. Subsequently, the proteins on the beads were treated with 20 µl lysis buffer. The

buffer contained guanidinium, a strong chaotropic agent, that denatures proteins, and reducing agent TCEP (tris(2-carboxyethyl) phosphine) to hydrolyze disulfide bonds. The free sulfhydryl groups on the cysteine residues are then alkylated with chloroacetamide to prevent reformation of disulfide bonds. Then the reduced and alkylated proteins were diluted 1:10 in digestion buffer and digested with Lys-C (200 ng) and Trypsin (200 ng) overnight at 37 °C. After digestion each sample was acidified to a final concentration of 1% trifluoroacetic acid.

We purified the proteins using stage tips containing SDB-RPS material (poly(styrene-divinylbenzene) copolymer modified with sulfonic acid groups). SDB-RPS material was used to plug 200 µl pipette tips and activated wit 100 µl acetonitrile. Subsequently, it was equilibrated with 100 µl equilibration buffer followed by 100 µl containing 0.2% trifluoroacetic acid. Then the sample (in 1% trifluoroacetic acid) was loaded onto the stage tip, and washed with 100 µl containing 0.2% trifluoroacetic acid. Peptides were eluted with 60 µl elution buffer into a PCR tube. After elution the samples were concentrated with speed-vacuum until no liquid was left and all peptides stuck to the wall of the PCR tube. The peptides were dissolved in measurement buffer and sonicated for 10 min in a water bath. Samples were stored at -20 °C before analysis.

Lysis buffer	
Guanidinium Chloride	6 M
TCEP	10 mM
Chloroacetamide	40 mM
Tris	100 mM
pH 8.5	

Digestion buffer	
Acetonitrile	10%
Tris pH 8.5	25 mM

Equilibration buffer for SDB-RPS tips	
Methanol	30%
Trifluoroacetic acid	1%

Elution buffer for SDB-RPS tips	
Ammonia (25%)	5%
Acetonitrile	80%

Measurement buffer	
Acetonitrile	2%
Trifluoroacetic acid	0.1%

3.4.8.2 Sample preparation for whole tissue lysate analysis:

Samples (10µg each) were subjected to tryptic digest using a modified filter-aided sample preparation (FASP)[26,27]. After centrifugation samples were acidified with 100 % trifluoroacetic acid. (Sample preparation for whole tissue lysate analysis was carried out by the Core Facility Proteomics at the Helmholtz Center Munich.)

3.4.8.3 MS measurement:

Mass spectrometry measurement was either performed in data dependent (DDA) or data independent (DIA) mode by the Core Facility Proteomics at the Helmholtz Center Munich.

MS data were acquired on a QExactive (QE) high field (HF) mass spectrometer (Thermo Fisher Scientific Inc.). Each sample (0.5 µg) was loaded automatically onto the on online coupled RSLC (Ultimate 3000, Thermo Fisher Scientific Inc.) HPLC system. A nano trap column (300 µm inner diameter × 5 mm, column material: Acclaim PepMap100 C18, 5 µm, 100 Å; LC Packings, Sunnyvale, CA) was utilized before separation by reversed phase chromatography (Acquity UPLC M-Class HSS T3 Column 75µm ID x 250mm, 1.8µm; Waters, Eschborn, Germany) at 40°C. Peptides were eluted from the column at 250 nl/min using increasing acetonitrile concentrations (in 0.1% formic acid) from 3% to 41 % over a 105 minutes gradient.

DDA method and analysis:

The high-resolution MS spectrum (60,000 full width at half-maximum) was acquired with a mass range from 300 to 1500 m/z with automatic gain control target set to 3 x 10^6 and a maximum of 50 ms injection time. The 10 most abundant peptide ions from the MS pre-scan were selected for fragmentation (MS/MS) if at least doube-charged, with a dynamic exclusion of 30 seconds. MS/MS spectra were recorded with automatic gain control target set to 1 x 10^5 and a maximum of 100 ms injection time (resolution: 15,000). All spectra were recorded in profile type and the normalized collision energy was set to 28.

Qualitative data analysis for DDA with Scaffold software:

Scaffold software (Proteome software, Version 4.7.2) was used for spectra analysis. We searched against the Swissprot human database (Release 2017.02 containing 553474 sequences) and a few complementary proteins for spiking. Search parameters used were set to 10 ppm peptide mass tolerance, and 20 mmu fragment mass tolerance. Carbamidomethylation of cysteine was set as fixed modification and oxidation of methionine and deamidation of asparagine and glutamine was allowed as variable modification, with only one missed cleavage site. Mascot integrated decoy database search was set to a false discovery rate (FDR) of 1 % with a percolator ion score cut-off of 13 and an appropriate significance threshold p.

Qualitative data analysis for DDA with MaxQuant software:

MaxQuant software (version 1.4.1.12, Cox & Mann, 2008) was used to analyze raw files. Peak lists were searched against the human UniProt FASTA database (version August 2017), and a database of common contaminants (247 entries) by the Andromeda search engine (Cox et al, 2011). Carbamidomethylation of cysteine was set as fixed modification and oxidation of methionine and deamidation of asparagine and glutamine was allowed as variable modification, with only one missed cleavage site. False discovery rate was set to 0.01 for peptides and proteins, which allows a minimum peptide length of seven aa. It was

determined by searching a reverse database. In the database search enzyme specificity was set as C-terminal to arginine and lysine, and we allowed a maximum of two missed cleavages. For peptide identification we accepted a precursor mass deviation up to 4.5 ppm after time-dependent mass calibration and a fragment mass deviation of up to 20 ppm. The minimum ratio count was set to two for label-free quantification in MaxQuant (MaxLFQ[28]). The retention time alignment window was set to 30 min for matching between runs (match time window 1 min).

HRM DIA method and analysis:

We started with a survey scan from 300 to 1650 m/z and an automatic gain control target of 120 ms maximum injection time (resolution: 120,000). Fragmentation was performed via higher energy collisional dissociation with a target value of 3e6 ions determined with predictive automated gain control. Precursor peptides were isolated with 37 variable windows spanning from 300 to 1650 m/z with an automated gain control target of 3e6 and automatic injection time (resoulution: 30,000). The normalized collision energy was 28 and the spectra were recorded in profile type.

Spectral library for DIA measurement:

A special peptide spectral library containing serpina2 with 25 unique peptides equaling a protein coverage of 56% was generated in Spectronaut (Version 10, Biognosys) with default settings using the Proteome Discoverer combined result file. Spectronaut was equipped with the Swissprot human database. The final spectral library generated in Spectronaut contained 151 protein groups and 1261peptide precursors.

Spectronaut analysis of DIA measurement:

The DIA MS data was analyzed using the Spectronaut 10 software applying default settings with the exception: quantification was limited to proteotypic peptides; data filtering was set to Q-value 25% percentile, summing-up peptide abundances.

3.5 Cell biological methods

3.5.1 Determination of cell count and viability

A hemocytometer (Neubauer improved) was used to count the number of viable cells. For this purpose 10 µl of cell suspension were mixed with 10 µl Trypan blue buffer and all viable cell were counted in the four quadrants. Dead cells have perforated membranes; Trypan blue can enter into the cytoplasm and stains these cells blue. The average number of cells in one quadrant (100 nl) was multiplied with the dilution factor and by 10^4 to determine the number of cells/ml.

Trypan blue buffer	
Trypan blue	0.1% (w/v)
PBS	
pH 7.4	

3.5.2 Isolation of PMNs and PBMCs from human blood

To carry out a hypotonic granulocyte lysis 18 ml (2 x 9 ml in EDTA tubes, BD Biosciences) fresh blood was drawn from a healthy volunteer and pipetted into a 50 ml tube. Additionally, PBS was added to a final volume of 35 – 40 ml. To create a density gradient Pancoll (17-0891-01, GE Healthcare) was very carefully added to the bottom of the 50 ml tube with a disposable pipette. The tube was centrifuged (20 min, 20 °C, 500 x g, without brake!) and the forming layers were carefully removed. The plasma was discarded, the lymphocytes – or peripheral blood mononuclear cells (PBMCs) were stored in a separate tube, the Pancoll was discarded and the erythrocytes and granulocytes (polymorphonuclear cells – PMNs) at the bottom of the tube were diluted in PBS to a final volume of 40 ml. To create a dextran gradient 8 ml of 6 % dextran were added to the solution. Erythrocytes pass the dextran gradient, whereas granulocytes stay in solution, after 30 min of sedimentation at room temperature the granulocyte rich supernatant was transferred to a separate tube and centrifuged (5 min, 4 °C, 500 x g).

The supernatant was discarded and the granulocyte pellet was washed with 5 ml 0.2 % NaCl solution for 1 min to lyse the remaining erythrocytes. Then, 5 ml 1.6% NaCl were added for another minute and the solution was filled up to 30 ml with PBS. After a final centrifugation step (5 min, 4 °C, 500 x g) the PMNs were resuspended in PBS and stored at -20 °C.

3.5.3 Preparation of total cell lysates

For the lysis of PMNs or PBMCs, cells were resuspended in cold RIPA (radioimmunoprecipitation assay) buffer (12 µl/10^6 cells). After incubating on ice for 20 min and sonification (four times 5 min, plus 5 min cooling step between sonification steps) the samples were centrifuged (10 min, 4 °C, 20 000 x g). Cell debris and DNA remained in the pellet, while the supernatant was transferred to a new tube.

RIPA buffer	
Tris	50 mM
NaCl	150 mM
EDTA	1 mM
Deoxycholic acid	0.5% (w/v)
SDS	0.1 % (w/v)
Nonidet P-40 (Igepal)	0.5% (w/v)
pH8.0	

3.6 Immunological methods

3.6.1 Immunoblotting

For immunoblotting, proteins were transferred onto a polyvinylidene difluoride (PVDF) membrane, activated in 100% methanol for 20 sec, using a semi-dry transfer machine. The ‘sandwich’ consisted of one layer of Whatman paper followed by the PVDF membrane, the SDS-PAGE gel and another layer of Whatman paper. All components were soaked in transfer buffer and assembled on the transfer machine. The proteins were transferred at 200 mA for 50 min. The membrane was then blocked for 1 h at room temperature, and incubated with the primary antibody diluted in blocking buffer overnight at 4°C with shaking. After

washing the membrane three times for 10 min with PBS-T at room temperature, the membrane was incubated with the appropriate HRP-conjugated secondary antibody at room temperature for at least 1 h, and washed again four times for 5 min with PBS-T. Proteins were detected with the Super Signal® West Pico Chemiluminescent Substrate (#34080, Thermo Scientific). 750 µl of both Solution A (Luminol Enhancer Solution) and Solution B (Stable Peroxide Solution) were mixed and immediately added to the membrane for a two min incubation. The membrane was developed by using the Chemidoc imaging system (Bio-Rad).

Transfer buffer	
Tris	25 mM
Glycine	200 mM
SDS	1 mM
MeOH	20%

PBS-T	
NaCl	140 mM
KCl	3 mM
Na_2HPO_4 x 12 H_2O	8 mM
KH_2PO_4	1 mM
Tween-20	0.05% (v/v)
pH 7.4	

Blocking buffer	
Non-Fat Dry Milk Blocker	5% (w/v)
PBS-T	

3.6.2 Enzyme-linked immunosorbent assay (ELISA)

A sandwich ELISA was established and performed to measure serpina2 in human samples. First, the detection antibody (mAB 75) was coated onto a 96 well plate at a concentration of 1 µg/ml in coating buffer at 4 °C overnight. In between all following steps, the plate was washed with three times 200 µl PBS-T (see 3.6.1) and all incubation steps were carried out at room temperature in a humid chamber. Wells were blocked for one hour in 200 µl blocking buffer to prevent unspecific binding. Subsequently, the samples (diluted 1:10 with blocking

buffer) were incubated for 1.5 h. For detection the biotinylated mAB 80 was added (100µl, 1 µg/µl) and incubated for 1.5 h, and then Avidin-HRP (dilutied 1: 3000 in blocking buffer) for 1 h. For development of the ELISA TMB substrate (Cat.No. T4444, Sigma-Aldrich) was added and incubated up to 20 min. The OD values were measured at λ=370 nm.

Biotinylation of mAb80:

A 20 nM solution of Sulfo-NHS-Biotin (Cat.No. 2322-50, Biovision) in DMSO was added to IgG solution (2 mg/ml) with 20 fold molar excess and incubated for 1 h at room temperature. Then the biotinylated antibody solution was dialyzed against PBS to get rid of excess Biotin.

Coating buffer	
Na_2CO_3	10 mM
$NaHCO_3$	10 mM

Blocking buffer	
NaCl	140 mM
KCl	3 mM
Na_2HPO_4 x 12 H_2O	8 mM
KH_2PO_4	1 mM
Tween-20	0.05% (v/v)
BSA	2% (w/v)
pH 7.4	

3.6.3 Immunohistochemistry

Sections containing lung tissue slices were sequentially incubated for 20 minutes at 65 °C. Then they were sequentially transferred to 100% xylene, then 100%, 90%, 80% and 70% ethanol, followed by tap water for 5 min, and rinsed in distilled water. Antigen retrieval was performed in 0.01 M citric acid pH 6.0 in a cooker chamber for 30 minutes at 125°C. Tissue was rehydrated with PBS-Tween 20 (0,1%) for 10 min. Endogenous peroxidases were quenched by incubation in 3% H_2O_2 (30%, H1009, Sigma Aldrich) in PBS for 10 min. After washing with PBS and PBS-Tween 20 (0,1%) avidin solution (Avidin/Biotin Blocking Kit, SP-2001; Vector Laboratories) was added and incubated for 15 min, followed by washing with

PBS-T (1x PBS-Tween 20 0,1%); biotin solution was added for 15 min, washed with PBS-T; nonspecific antibody-binding sites were blocked with blocking solution, PBSA (BSA 3% in PBS) for 1 h, and sections were incubated for 1.5 h with the specific primary antibody diluted in blocking buffer. Sections were stained with monoclonal rat mouse-specific Ly-6G monoclonal antibody (working dilution 1:200, clone 1A8, Biolegend) for detection of neutrophils. After washing in PBS-T, visualization was performed via incubation with HRP-conjugated secondary antibody with goat rat-specific IgG (H+L), biotin conjugated (working dilution 1:250, Thermofisher) for 30 min at room temperature followed by addition of the corresponding peroxidase substrate (ImmPACT DAB Peroxidase (HRP) Substrate, SK-4105; Vector Laboratories). After counterstaining with hematoxylin, dehydration and mounting, the sections were scanned using the Axio Imager (Imager.M2, Zeiss). High resolution images, which were taken at the same magnification and areas were randomly chosen and microscopically analyzed for neutrophil counting. The mean number of at least ten images was used for quantification.

3.7 Mouse model analysis (AAT in transplantation)

3.7.1 Study approval

All animal experiments were conducted under strict governmental and international guidelines and were approved by the local government for the administrative region of Upper Bavaria (Project 55.2–1-54-2532-120-2015).

3.7.2 Orthotopic lung transplantation model

Orthotopic lung transplantation was performed as described by Krupnick *et al.* with minor modifications[29]. C57BL/6J mice (male, 8-12 weeks old) were utilized as donors, and C57BL/6J and *Ela*$^{-/-}$*Pr3*$^{-/-}$ mice (male, 8-12 weeks old) were utilized as recipients. In brief, donors were anesthetized with a mixture of ketamine/xylazine injected intraperitoneally. The pulmonary artery (PA), bronchus (BR) and pulmonary vein (PV) were separated with blunted

forceps, prior to cuffing with, 24G, 20G and 22G cuffs, respectively. The left lung lobe was perfused intravenously with Perfadex (3 ml). Subsequently, it was perfused with Perfadex supplemented with protein at a concentration of 1 mg/ml (Albumin, AAT^{wt} or AAT^{mt}). The PA and PV were clamped with Biemer micro vessel clips (Bbraun), in order to keep the solution inside the blood vessels, and it was stored for 18 hours at 4°C before implantation. The recipient was anesthetized with a medetomidine/midazolam/fentanyl (1/0.05/0.02 mg/kg), intubated, and connected to a small animal ventilator (Harvard Apparatus), at a respiratory rate of 120 bpm and a tidal volume of 300 µL. The chest was incised on the left side between rib 3 and rib 4 and the native left lobe of the mouse lung retracted with a clamp. The hilar structures were carefully separated with blunted forceps. The donor lung graft, prepared 18 hours earlier, was perfused intravenously with Perfadex to rinse out the storage solution. After arrest of the blood and air flow towards the left lung, the cuffed graft PA, BR and PV were inserted into the recipient counterparts, and the connection was secured with 9-0 sutures. The native left lung was removed and the incision in the chest was closed with a 6-0 suture, after removing all potential air bubbles from the chest. After administration of antagonist the animal was extubated at the first signs of spontaneous breathing. After the operation, the recipients were allowed to recover at 30 °C and received buprenorphine (0.1 mg/kg). The mice were sacrificed four hours after transplantation for PGD assessment.

3.7.3 Allograft tissue sample collection (blood gas, bronchoalveolar lavage)

The recipient was anesthetized with a mixture of medetomidine/midazolam/fentanyl (1/0.05/0.02 mg/kg) four hours after lung surgery. After intubation (300 µl room air/120 strokes/min), a midline abdominal incision was executed, the diaphragm incised and the chest opened to lay bare the lung and heart block. The right bronchus and pulmonary vein were clamped for 5 min (75 µl room air /120 strokes/min) and the oxygenation function of the transplanted left lobe was determined by collection of blood from the left ventricle of the heart and direct measurement of the pO_2 [%] in a blood gas analyzer (ABL80 FLEX CO-OX

analyzer, Radiometer). Subsequently, with the right bronchus still clamped, BAL of the transplanted left lung was collected by instilling cold PBS (three times, 200 µL) into the trachea. The BALF was obtained by centrifugation (400 g, 20 min, 4°C) and protein concentration was measured with the Pierce™ BCA Protein Assay Kit (catalog no. 23225, Thermofisher). 30.000 cells from the BAL cell pellet were used for a cytospin (200 x g, 6 min, 4°C) and stained with May Grünwald (1424, Merck) and Giemsa (Merck, 9204) solution in order to perform a differential cell count. The lower part of the lung was kept separately for protein analysis (snap freezing, storage at -80 °C) and the remaining upper part was utilized for histology (inflation with and storage in 4% PFA).

3.7.4 Western blot analysis of transplanted lung lysates

Whole lung tissues were subjected to a tissue disrupter in liquid nitrogen to form fine tissue powders of each lung. Subsequently, the powder was dissolved in cold RIPA buffer (see 3.5.3) and left on ice for 15 min, followed by sonification (four times, 5 min). Cell debris and DNA were pelleted and removed by centrifugation (10 min, 20000 x, 4 °C). The Pierce™ BCA Protein Assay Kit (23225, Thermofisher) was used to measure the total protein concentration of the lysate (absorption at 562nm). 40 µg per lane were separated by reducing SDS-PAGE and transferred to a polyvinylidene difluoride (PVDF) membrane. AAT was detected using a human AAT specific monoclonal antibody from a rat hybridoma (13C7, 1:10 in PBS-T and 5 % milk, Götzfried *et al.*, unpublished) and peroxidase-conjugated goat rat-specific IgG+IgM antibodies 1:10,000 (Jackson Immuno Research Laboratories).

3.7.5 Lung tissue preparation for staining of lung sections

Left mouse lungs were inflated with 4% PFA through an intratracheal cannula at the time of sacrifice, the trachea was ligated, and the lungs were fixed in 4% PFA, at 4°C overnight, and transferred to 70% ethanol before paraffin-embedding. The grafts were subsequently embedded in agarose, and cut into 3 pieces, and then separated 3 mm from each other. The

pieces were embedded in paraffin, and then sliced into 3 µm-thin sections with a microtome (Hyrax M55, Zeiss).

3.7.6 Hematoxylin and eosin staining of lung tissue sections

Sections were placed in a 65°C oven for 20 minutes to melt the paraffin for deparaffinization. Then they were transferred sequentially to 100% xylene, 100%, 90%, 80% and 70% ethanol, and rinsed in tap water for 5 min, followed by distilled water. First, sections were stained with Hematoxylin (Hematoxylin solution, GHS-232, Sigma Aldrich) for 6 min, rinsed in distilled water, and tap water for 15 min, followed by distilled water. Then they were stained with eosin for 10 min and washed in tap water for 5 min. Subsequently, sections were dehydrated with ethanol 100% and xylene, and mounted with glue (Entellan, Merck). For visualization the slides were were scanned with Myrax Desk.

3.8 Statistics (AAT in lung transplantation)

All results are reported as mean ± SEM. A Mann-Whitney U-test was performed using GraphPad Prism version 5.00 for Windows, GraphPad Software, and www.graphpad.com. P-values of less than or equal to 0.05 were considered significant.

4. More than just a pseudogene: serpina2 in the epididymis

4.1 Serpina2 - Introduction

4.1.1 Serpina2 – a clade A serpin very similar to serpina1 (alpha-1-antitrypsin)

A large set of extracellular serpins prevent organ damage by inhibiting excessive proteases in inflammatory diseases. One poorly characterized member of this family is serpina2, which was originally annotated and regarded as a pseudogene.

By definition, pseudogenes are DNA segments, which are composed like a gene, but they do not function as template for a functional protein[30,31]. A gene without function is not exposed to selection pressure and usually gains mutations over time. However, serpina2 is widely conserved, which implies that it is under natural selection pressure like a functional gene. In more recent studies it has been shown that some declared pseudogenes do have functions, after all, and that the boundary between 'living' and 'dead' genes is more ambiguous than initially assumed[32]. While several pseudogenes are definitively 'dying' and non-functional, many cases have been reported, in which the RNAs of declared pseudogenes are transcribed and processed to interfere with paralogous genes[33,34].

Originally serpina2 was declared to be a polymorphic pseudogene, due to a missing promotor region and an alteration in the start codon, in which ATG was mutated to ATA. So far, two major null allele variants of serpina2 are known: A 2 kb deletion affecting exon IV and part of exon V, and a frameshift mutation (fs108) in exon II, which leads to a premature stop codon[35]. An analysis of the 1000 Genomes Project data (http://www.internationalgenome.org/) performed by our collaboration partner Dr. Susana Seixas revealed that the fs108 mutation is most frequent in the South and Middle American population, but also occurs in the Middle East region and to a much lower extent in Europe. The deletion allele is most common in the African population, but can also be found in Europe (**Figure 4.1**).

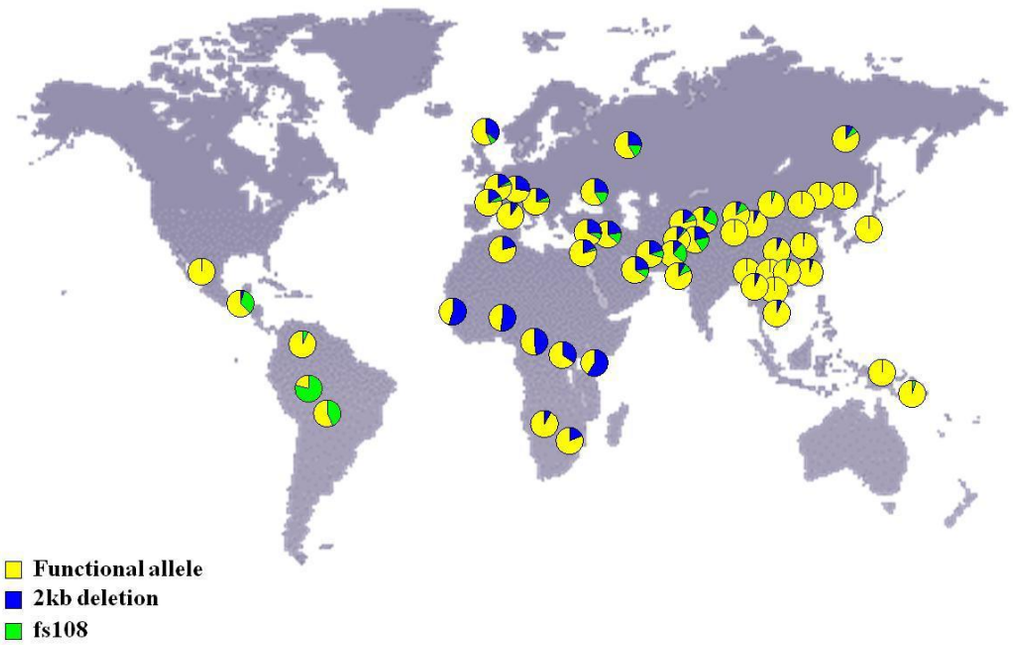

Figure 4.1 Distribution of the two non-functional alleles of serpina2 (Seixas *et al.,* unpublished).

There are several mechanisms of how pseudogenes can be generated. One of them is the phenomenon of gene duplication caused by homologous recombination. Subsequently, the new gene can acquire mutations that lead to the exaptation of novel functions or they are on the path towards loss of function of the original gene and removal from the genome. Gene duplication is thought to be the most important driving force in evolution, since it represents the starting point of evolutionary innovation[36]. Extensive nucleotide sequence homology with the AAT gene suggests that serpina2 arose from a recent gene duplication event occurring about 90 million years ago[37]. Serpina2 is closely linked and highly homologues to alpha-1-antitrypsin (serpina1), however, extremely polymorphic in human populations. Both genes are found next to the other nine clade A serpins on chromosome 14, and serpina2 is located within 12 kb downstream of the authentic human alpha-1-antitrypsin gene (**Figure 4.2**).

Figure 4.2 Organization of clade A serpins on chromosome 14q32.1. (KAL: kallikrein-like inhibitor, data was derived from the publicly available human genome database, http://www.ensembl.org/)

Serpina1 and serpina2 share a protein sequence identity of 60.3% (254/421 aa), and a nucleotide sequence similarity of 73.2% (308/421 aa). There are only 1% gaps (4/421 aa) within the sequence. Though interestingly, the active sites of the proteins are quite divergent, which implies altered substrate specificity (marked in turquoise in **Figure 4.3**). Interestingly, serpina2 is the only known serpin carrying a tryptophan (W) residue in P1 position.

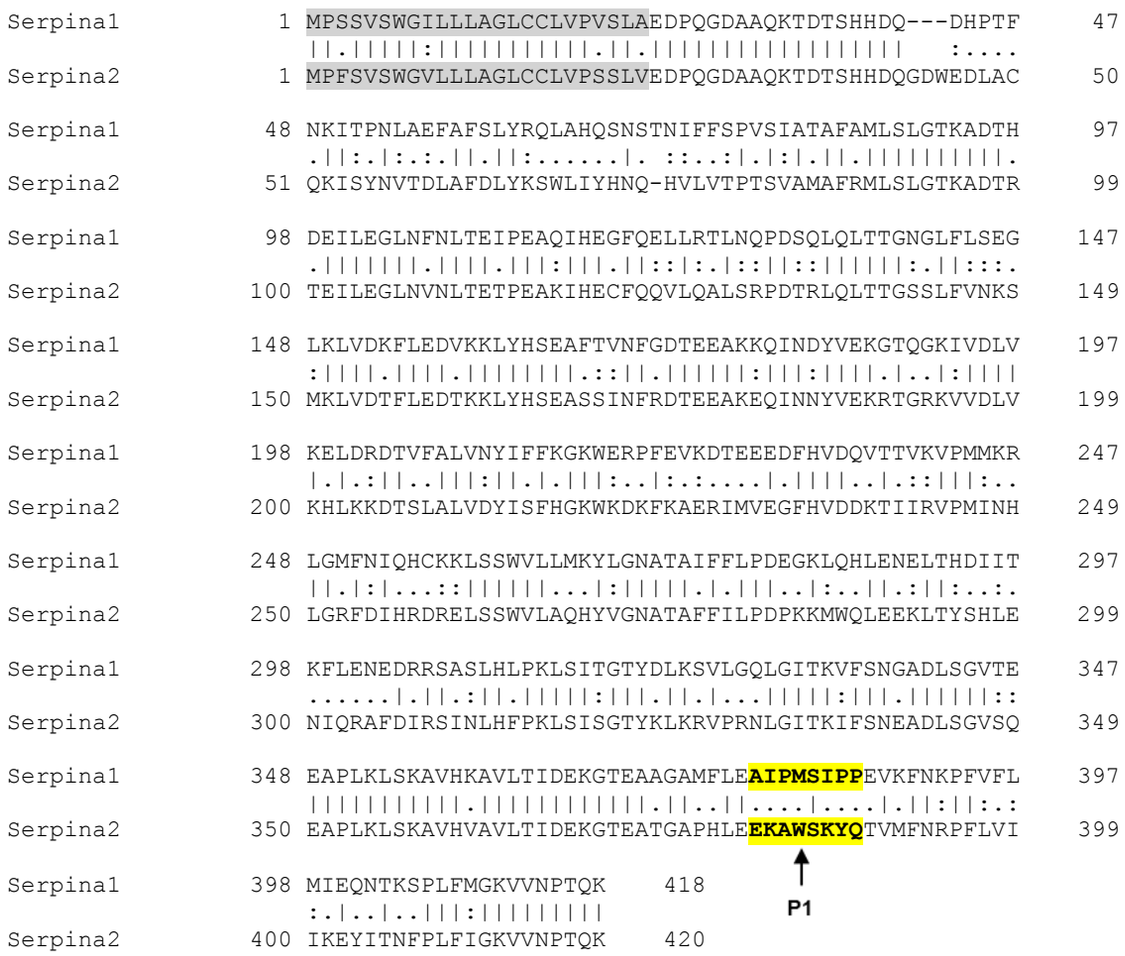

Figure 4.3 Comparison of serpina1 (AAT) and serpina2 sequence homology. Signal peptides are marked in grey, and the reactive center loop sequences are marked in yellow (P4 – P4'). Pairwise sequence alignment was carried out using the EMBOSS Needle tool (http://www.ebi.ac.uk/Tools/psa/emboss_needle/). Protein sequences were obtained from the Uniprot website (http://www.uniprot.org, serpina1 - P01009 (A1AT_HUMAN) , serpina2 - P20848 (A1ATR_HUMAN)).

The first literature specifically mentioning serpina2 was published in the 80's. Serpina2, or alpha-1-antitrypsin-related gene (ATR), was suggested as a marker for prenatal diagnosis of AAT deficiency in 1987 (Lancet)[38]. One year later another study investigated the expression of serpina2 using a RNA protection assay against human RNA (liver, lung, spleen, skeletal muscle and brain) and concluded that it seemed to be a pseudogene[39]. However, another

study suggested that it might not be a classical pseudogene due to the fact that all RNA splice sites are conserved and the lack of internal termination codons in the exonic regions[40]. Twenty years later a research group in Portugal became interested in serpina2 and proposed in a genetic analysis that it is in the ongoing process of becoming a pseudogene but could encode a functional serpin and currently be expressed in some humans[35]. Additionally, they found that serpina2 is completely deleted in chimpanzees, but present in most great apes, and that serpina2 mRNA might be differentially expressed in testes and leukocytes. In a second publication they propose that serpina2 is an intracellular glycoprotein located in the endoplasmic reticulum, and that it is not degraded by the proteasome through unfolded protein response and therefore seems to be folding correctly. They suggest that serpina2 is a chymotrypsin-like protease inhibitor, because it was shown in *in vitro* studies that the M358W substitution in the RCL of AAT, which is also present in serpina2, changes the affinity of the inhibitor towards chymotrypsin[41]. Furthermore, they show that based on mRNA detection serpina2 is expressed in several human tissues[42].

4.1.2 Hints for serpina2 expression in databases

Until recently, serpina2 was regarded as a pseudogene. However, there is evidence in several databases for the expression of serpina2.

GTEx (https://www.gtexportal.org/ home/gene/SERPINA2) detects a signal for serpina2 gene expression in whole blood, and to a lower extent in the kidney, but not in testis and many other organs. In the EMBL-EBI gene expression atlas serpina2 is found in testis (http://www.ebi.ac.uk/gxa/genes/ENSG00000258597?bs=%7B%22homo%20sapiens%22%3A%5B%22ORGANISM_PART%22%5D%7D#baseline).

There are 67 reports for serpina2 protein identification in the Pride Archive (http://www.ebi.ac.uk/pride/archive/simpleSearch?q=P20848&show=10&page=4&sort=score&order=ddes). Among them are several human plasma proteome analyses.

In the proteomics database (https://www.proteomicsdb.org/proteomicsdb/#human/

proteinDetails/53815/expression) serpina2 was found in the kidney and platelets. Six unique peptides were identified, with sequence coverage of 20.24%.

To sum it up, there are multiple hints for serpina2 expression at the mRNA and protein level. Most of these refer to testis and blood, in particular to platelets.

4.1.3 Objectives

In previous work the tissue distribution and protease inhibiting function of serpina2 remained unclear as appropriate analytical tools were not available. The goal of this study was to develop such tools and determine the potential role of serpina2.

We hypothesized that serpina2, being very homologous to alpha-1-antitrypsin, could have a similar role as genetic modifier of inflammatory diseases.

So far, only polyclonal serpina2 antibodies (Santa Cruz) were available. Therefore, we recombinantly produced the protein for analysis and monoclonal antibodies to it for detection. With these new antibodies we explored protein expression in human tissue positive for serpina2 mRNA. In addition, we verified the expression of serpina2 with mass spectrometry methods to make a clear statement whether serpina2 exists as a protein. Furthermore, we designed experiments to analyze the functional properties of the putative protease inhibitor.

4.2 Serpina2 – Results

4.2.1 Serpina2 mRNA expression

In June 2013 it was published, that serpina2 is expressed at the mRNA level in several healthy human tissues including lung, liver, leukocytes and testes[42]. However, we discovered that forward and reverse primers located on the same exon and not spaced from one another by an intron, were used for the underlying experiment. This does not exclude the amplification of contaminating genomic DNA in a cDNA preparation and can lead to false positive results. To reexamine mRNA expression we tested a cDNA panel of 46 healthy human tissues, a panel of 24 different brain tissues and a megakaryocytic cell line (MEG-01). We found that serpina2 was exclusively expressed in the epididymis (**Figure 4.4**), all other tissues and the megakaryocytic cell line were tested negative.

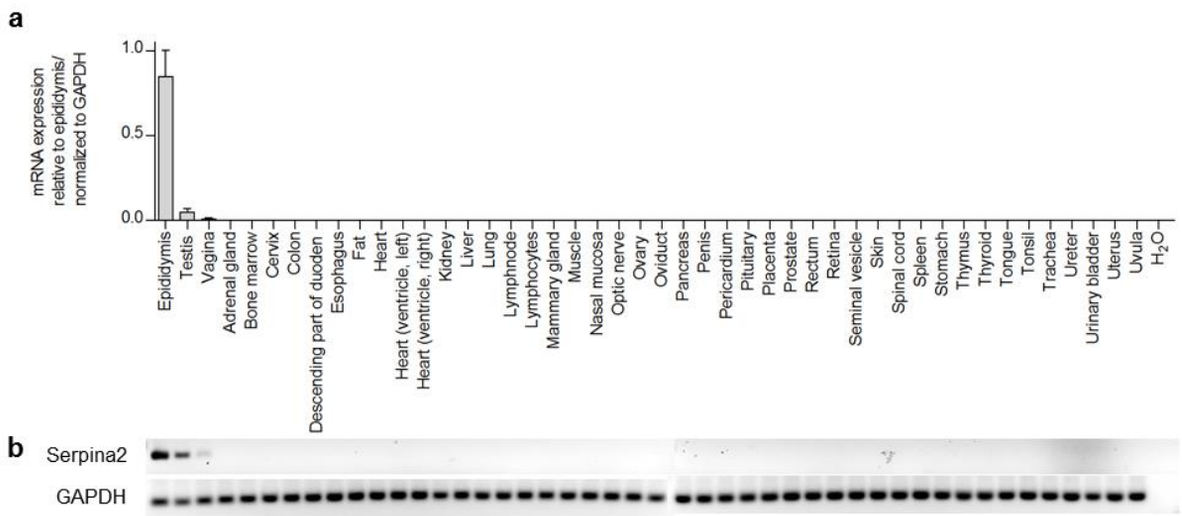

Figure 4.4 mRNA expression of serpina2 in 46 human tissues. (**a**) Quantitative RT-PCR analysis of a cDNA panel from human healthy organs. Transcript levels of serpina2 are shown relative to the expression in the epididymis. Glyceraldehyde 3-phosphate dehydrogenase (GAPDH) was used as endogenous control and data are based on three independent experiments (n=3, ±SD) (**b**) Amplified cDNA products were analyzed on an agarose gel to verify qPCR data.

4.2.2 Expression and purification of recombinant serpina2

In order to study serpina2, our goal was to produce enough pure recombinant protein for the production of monoclonal antibodies, crystallization and biochemical assays.

4.2.2.1 Expression of serpina2 in HEK 293 cells

When HEK 293 cells were transfected with serpina2 plasmid and incubated for 4 days we observed that the vast majority of the plasmid remained intracellular and only small amounts could be detected in the supernatant. Therefore, we decided to purify the protein from total cell lysates under denaturing conditions in 8 M Urea (**Figure 4.5**). This technique allowed us to purify approximately 0.5 mg per 10 ml cell suspension. We used the early eluting fraction of serpina2 (E1) for the production of monoclonal antibodies.

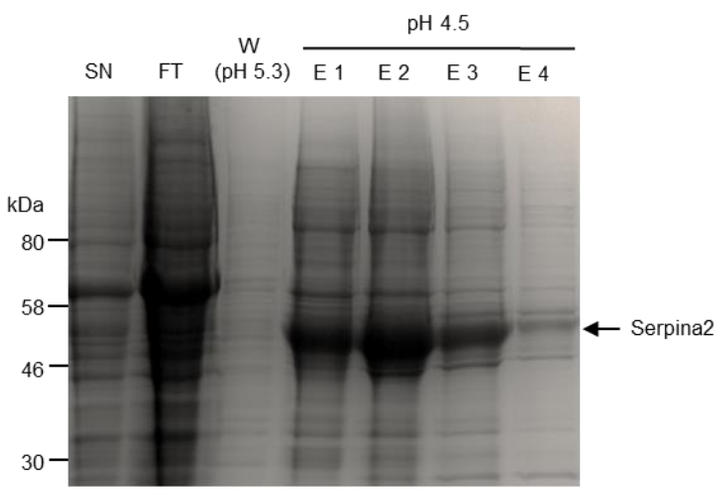

Figure 4.5 Expression of serpina2 in HEK 293 cells. Coomassie stained gel showing the purification of serpina2 under denaturing conditions (8 M Urea). The arrow points to the serpina2 band in the elution fraction. The supernatant (pH 7.4) was loaded onto a Ni-NTA column, washed at pH 5.3, and eluted at pH 4.5. (SN = supernatant, FT = flow through, W = wash, E1 - 4 = elution 1 - 4)

4.2.2.2 Expression of serpina2 in Schneider 2 cells

Schneider 2 (S2) cells were transfected with a pIEx-serpina2 plasmid by our collaboration partner Prof. Dr. Wurm (Laboratory of Cellular Biotechnology, Institute of Bioengineering, École Polytechnique Fédérale de Lausanne, Switzerland), who sent us the supernatant. We used a Ni-NTA column to purify serpina2 under native conditions by liquid chromatography, followed by a second step of affinity purification using immobilized anti-His monoclonal antibody (**Figure 4.6**). However, with this technique we could generate only small amounts of recombinant serpina2.

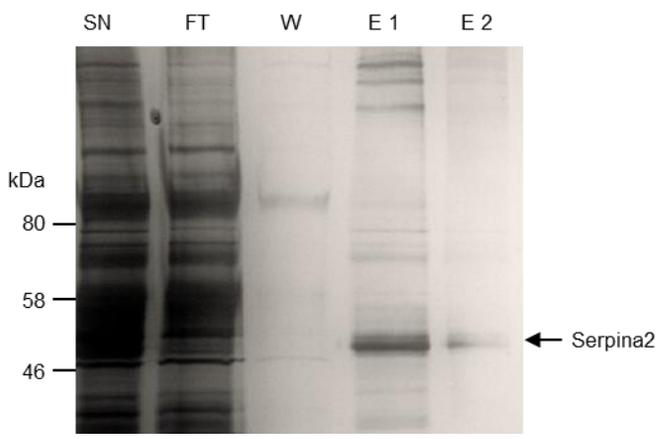

Figure 4.6 Expression of serpina2 in S2 cells. Silver stained gel showing the purification of serpina2 under native conditions. The arrow points to the serpina2 band in the elution fraction. (SN = supernatant, FT = flow through, W = wash, E1 = elution 1, E2 = elution 2)

4.2.2.3 Expression of serpina2 in *E. coli*

We also tried to express and purify serpina2 in the *E. coli* strain BL21. Again, after purification with a Ni-NTA column and anti-His immunoaffinity resin, we were able to obtain small amounts of the soluble protein (**Figure 4.7**).

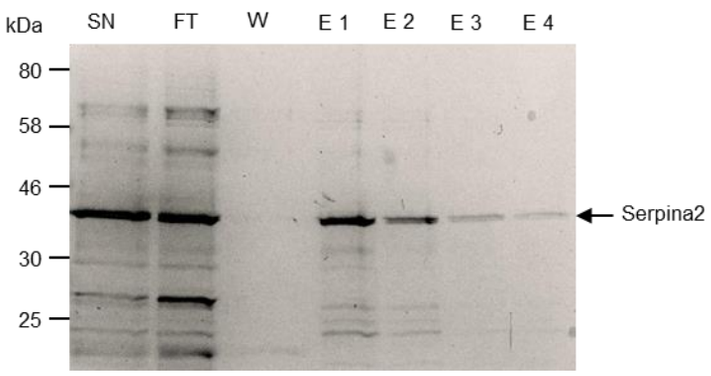

Figure 4.7 Expression of serpina2 in BL21 *E.coli*. Silver stained gel showing the purification of serpina2 under native conditions. The arrow points to the serpina2 band in the elution fraction. (SN = supernatant, FT = flow through, W = wash, E1 - 4 = elution 1 - 4)

With the help of our cooperation partner Jim Huntington (Cambridge Institute for Medical Research, University of Cambridge) and his postdoc Stéphanie Polderdijk, who are leading experts in the purification and crystallization of serpins, we tried to express serpina2 in different *E.coli* strains (BL21(DE3), SHuffle® Express, Rosetta™ 2(DE3)pLysS) and the plasmids pET24c_serpina2_His, pET28_His_SUMO_serpina2, and PQEwa_His_TEV_serpina2. We managed to produce several milligrams of His_SUMO_serpina2 by refolding the inclusion body material from BL21(DE3) cells transformed with the pET28_His_SUMO_serpina2 plasmid in Pipes buffer. However, when we cleaved off the SUMO-tag with the Sumo3 protease the protein precipitated and could not be used in further experiments.

4.2.3 Generation of several monoclonal antibodies against serpina2

We were able to produce enough serpina2 protein in HEK 293 cells under denaturing conditions (8 M Urea) to immunize one rat for the production of monoclonal antibodies against serpina2. Hybridoma supernatants were generated in cooperation with Dr. Elisabeth Kremmer (Helmholtz Center Munich). From a large collection (119) of rat monoclonal antibodies we selected the most sensitive and specific antibodies against serpina2, that did not cross-react with AAT (serpina1). All hybridoma supernatants containing monoclonal antibodies were tested for their binding to native and denatured serpina2, as well as native and denatured AAT in an ELISA and by Western blotting (**Figure 4.8**). To make sure that a positive signal was not generated by a contaminating protein of HEK 293 cells, which was contained in our preparation of the immunogen, we secured with serpina2 purified from *E. coli*. Out of the 119 supernatants, 7 reacted only with native AAT, 3 reacted with both, native and denatured AAT and 17 antibodies reacted only with native and denatured serpina2 (results of all 119 hybridoma supernatants are shown in Appendix 9.2). One antibody (mAb 104) gave a particularly strong signal with both, AAT and serpina2 (native and denatured) and was used as a control in the test experiments. We picked five serpina2 specific antibodies yielding the highest signal in the ELISA for a large scale production of antibodies and used them for further experiments.

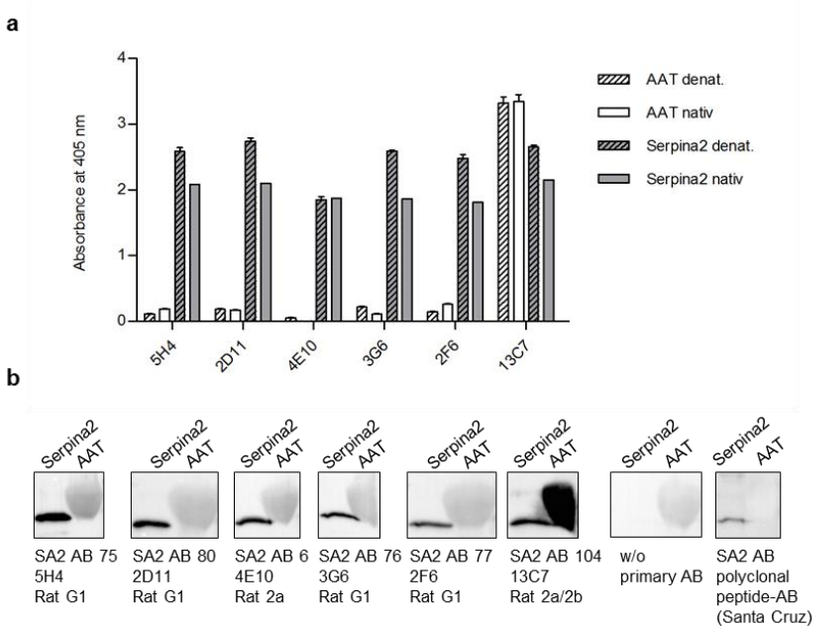

Figure 4.8 Selection of the most specific and sensitive monoclonal antibodies against serpina2. (**a**) ELISA showing the reactivity of several antibodies with either denatured or native AAT or serpina2. The recombinant proteins were coated, then hybridoma supernatant was added and the ELISA was developed using a HRP conjugated anti-rat secondary antibody and ABTS substrate. Absorbance was measured at 405 nm (n = 3, ± SD). (**b**) Western blot analysis of selected antibodies showing a strong reaction with serpina2 but not AAT, except for mAb 104, which strongly reacts with both proteins.

4.2.4 Serpina2 genotyping of human samples

We developed a genotyping strategy to detect the two known null alleles in human DNA samples to search for serpina2 null individuals. After isolation of DNA from whole blood or epididymis tissue and PCR amplification of serpina2 (primer pair DJ3754/3751), we used the restriction enzymes Bse LI to detect the frameshift 108 mutation (fs108) and BsmI for detection of the start codon deletion. We found that out of 66 tested individuals, 11 (16.67%) carried the fs108 mutation, and 27 (40.91%) the mutation of the start codon (ATG -> ATA). Only one individual, P-2107, carried both the fs108 and the start codon deletion allele, and represents therefore a natural serpina2 deficient individual. Data is summarized in **Figure 4.9**.

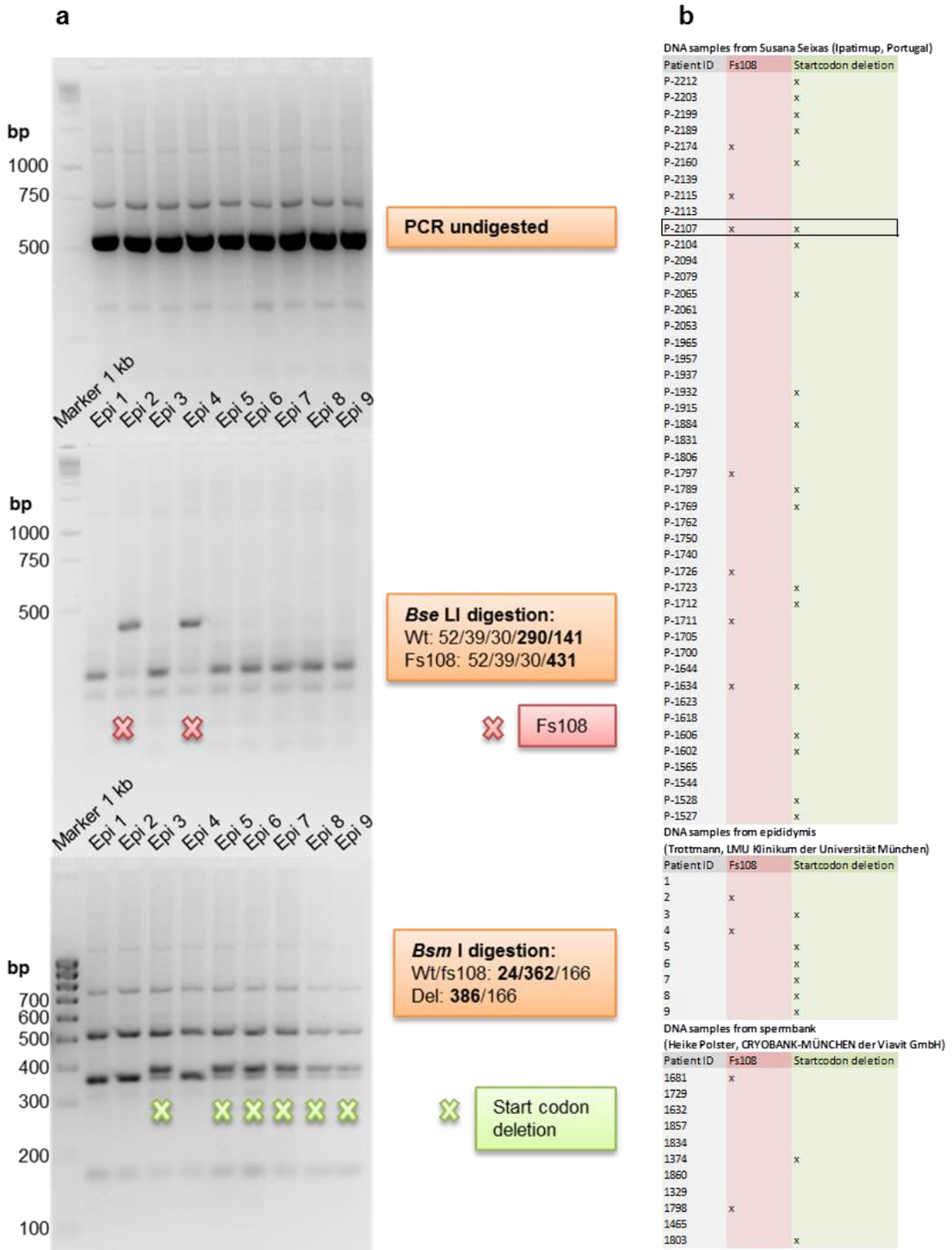

Figure 4.9 Genotyping of serpina2 deletion alleles in human samples. (**a**) DNA gel showing the PCR products with primer pair DJ3754/3751 at the top, followed by the PCR product digested with *Bse* LI or *Bsm* I.(Epi1-9: DNA extracted from epididymis tissue donor 1-9; orange boxes describe the expected length of the fragments in bp after digestion) (**b**) Summary of all genotyped human DNA samples. Individual P-2107 carries both mutations and is therefore a serpina2 null individual.

4.2.5 Serpina2 protein expression in human tissue samples

We found serpina2 mRNA exclusively in the epididymis. Therefore, we tested whether serpina2 is expressed at the protein level by Western blot. Epididymis donor tissue from male-to-female transsexuals (n = 9) was kindly provided by Dr. med. Matthias Trottmann (Funktionsoberarzt, Urologischen Klinik Großhadern, LMU Klinikum der Universität München). The age range of these donors was 26 – 52 years, and each patient received estradiol treatment for up to six years before patient samples were collected post-orchiectomy[43].

As shown in Figure 4.9 all nine epididymis donors carry at least one functional serpina2 allele and were therefore expected to express the protein. With our monoclonal antibodies we were able to detect serpina2 in epididymal tissue lysates (**Figure 4.10**). Both, serpina2 mAb 75 and mAb 80 detected a similar signal pattern. ß-actin was used as an internal loading control. Serpina2 was detected in all nine epididymis protein lysates from individual donors.

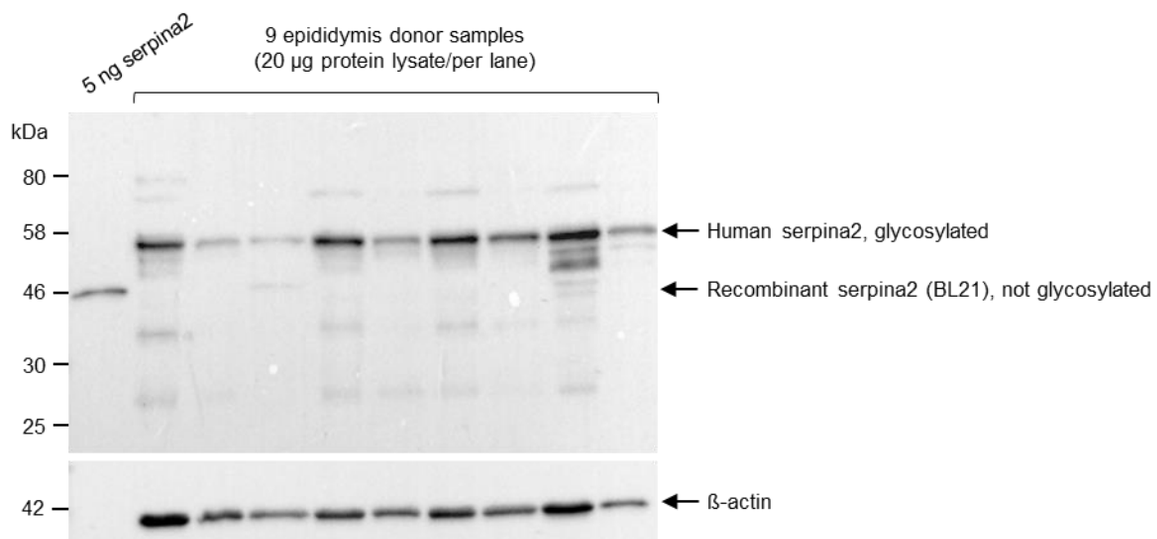

Figure 4.10 Serpina2 protein was detected in epididymal tissue lysates. Western blot analysis using mAb 80 and secondary HRP-conjugated anti-rat AB.

Additionally, we stained paraffin embedded epididymis tissue sections to find out more about the tissue distribution of serpina2 (**Figure 4.11**). On some tissue slices the efferent ductuli, which connect the rete testis with the caput epididymis, were visible. Granula on the apical pole of (ciliated) epithelial cells in the efferent ductuli stained positive for serpina2. While we detected a very specific staining in the ductuli efferenti, the signal in the epididymis ducts varied much more. In one donor we detected a signal in smooth muscle cells and in another one in the basal nuclei of the epithelial cells.

We were curious, whether the potentially secreted serpina2 can be found in seminal plasma or semen itself. We performed Western blots using samples kindly provided and genetically analyzed by Susana Seixas using our mAb 75. We tested semen and seminal fluid of five individuals carrying at least one functional serpina2 allele and one individual with two deletion alleles, and no signal was detected.

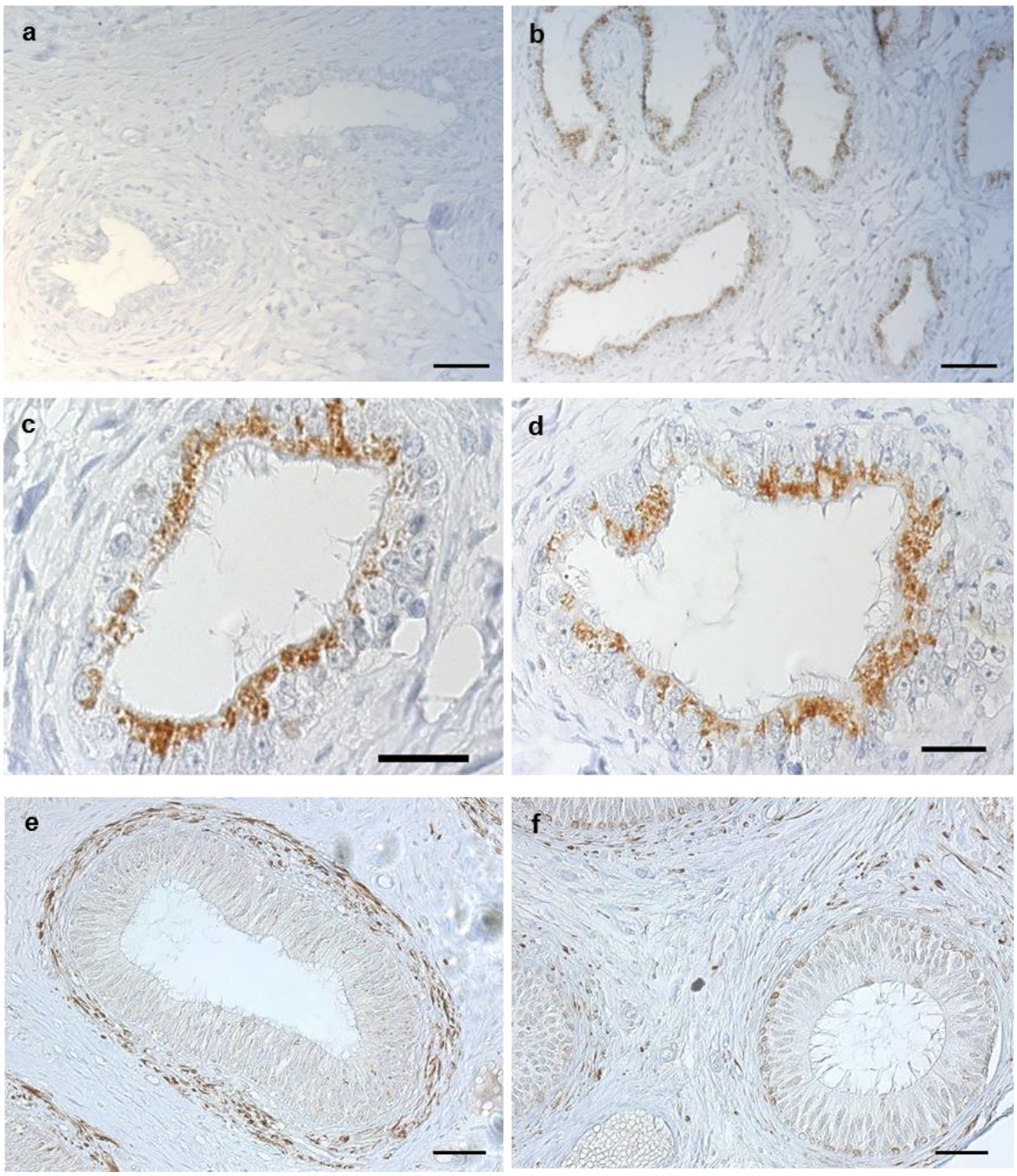

Figure 4.11 Serpina2 staining of human efferent ductules and epididymis using anti-serpina2 mAb 75. (**a**) Negative control (**b**) Serpina2 was detected in granula on the apical pole of (ciliated) epithelial cells in the efferent ductules of the epididymis. (**c**) and (**d**) show a magnification of serpina2 staining of the efferent ductules. Serpina2 was also detected in the epididymis of two different donors: (**e**) smooth muscle cells and (**f**) basal nuclei of the epithelial cells. (Scale bars, a,b and e,f 50 µM, c and d 20 µM**).**

4.2.6 Serpina2 protein expression in different blood components

To identify serpina2 protein in cell populations and plasma of human blood we did Western blot experiments using our mAb 75 and mAb 80, and the commercially available polyclonal peptide antibody from Santa Cruz.

We analyzed eight different plasma samples, one of them (P2107) carried an allele for the frameshift mutation as well as for the start codon deletion, and is therefore used as negative control in a Western Blot experiment (**Figure 4.12 a**). For all plasma samples from donors carrying at least one functional serpina2 allele we detected a band at 75 kDa, but the lower band at approximately 47 kDa is not visible in the P2107 (null allele) sample, which strongly suggests that this lower is a specific signal for serpina2. In **Figure 4.12 b** we analyzed 50 µg of MEG-01 (a megakaryocytic cell line) whole cell lysate, and found that only the lower band (47 kDa) is visible, however we were not able to detect serpina2 in a qPCR experiment with MEG-01 cDNA.

Additionally we analyzed human platelet lysate (HPL) with two of our serpina2 monoclonal antibodies (**Figure 4.12 c and d**) and compared it to the signal in plasma and serum. We again detected two different bands (80 and 47 kDa), the lower band was even stronger in HPL. Interestingly, the 47 kDa signal in HPL could also be detected with a polyclonal peptide antibody G12 (Santa Cruz) (**Figure 4.12 e**). The most dominant band in these samples are visible in the Coomassie stained gel, but it can be excluded that they are responsible for the signals in the Western blot, otherwise they should be visible in all lanes.

An ortholog of serpina2 can be found in most great apes, but not in bonobos or chimpanzees[35]. Serum samples of several great apes, including the two species deficient for serpina2, were kindly provided by Dr. Andreas Bernhard (Zoo veterinarian, Zoo Leipzig, Germany) and our analysis revealed that our mAbs seem to react unspecifically. Bonobo and chimpanzee serum was supposed to serve as negative control. However, we detected a 47 kDa band in their plasma samples as we did in gorilla, orang-utan, sacred baboon and

rhesus macaque. We tested the great apes sera with two different monoclonal antibodies and detected a signal with both of them (**Figure 4.12 f and g**).

Since it was reported, that serpina2 might be expressed in leukocytes (staining with polyclonal serpina2 Santa Cruz antibody K12)[42], we isolated PMNs and PBMCs from whole human blood of several donors and found that there was no protein band detectable in total cell lysates.

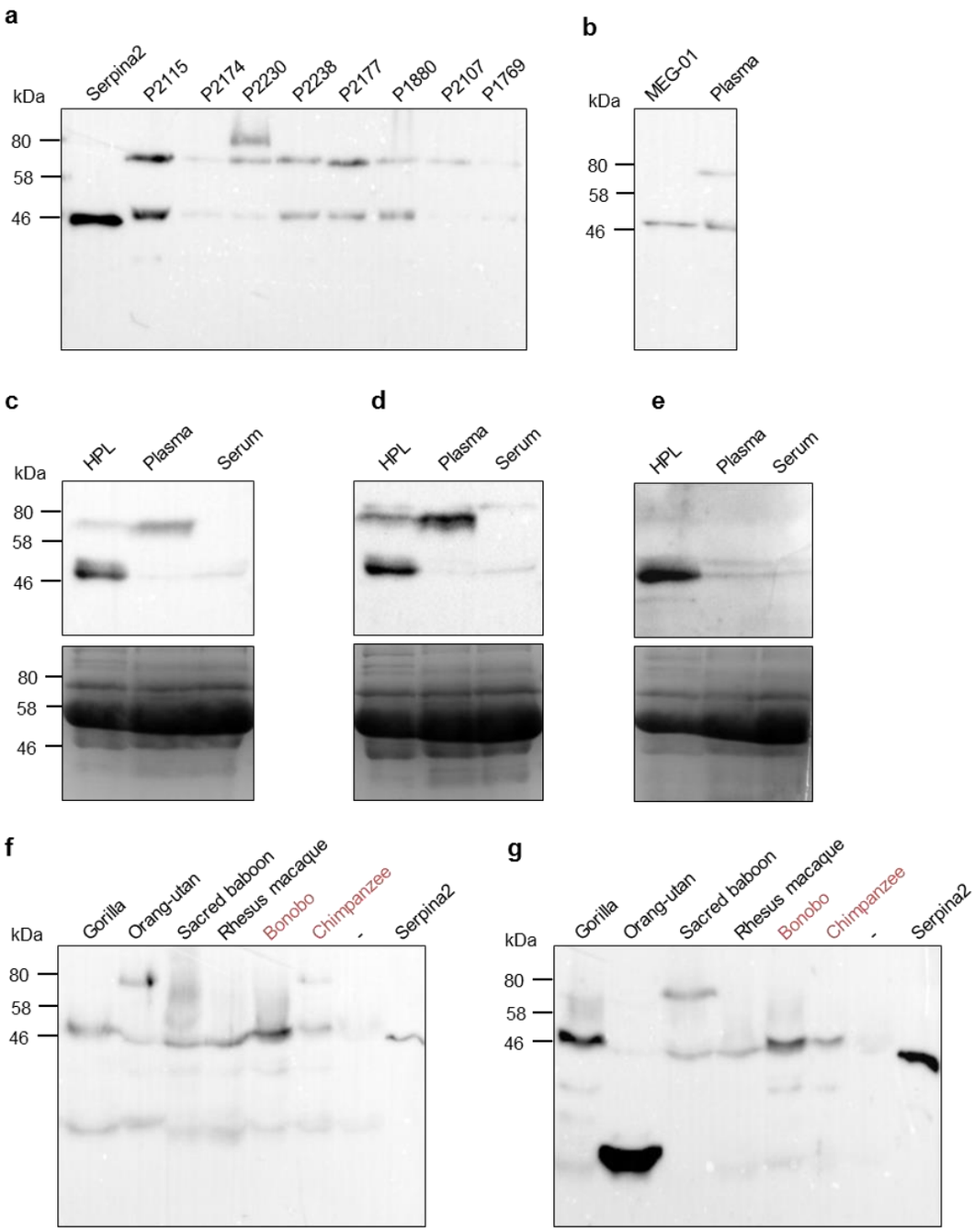

Figure 4.12 Western blot analysis of serpina2 in human blood. (**a**) Western Blot of eight different plasma samples, P2107 is a serpina2 null individual using mAb 75. (**b**) MEG-01 cell line lysate was analyzed and compared to a plasma sample using mAb 75.(**c-e**) Western blot of human platelet lysate (HPL), plasma and serum using three different serpina2 antibodies: (**c**) Serpina2 mAb 80, (**d**) Serpina2 mAb 75 and (**e**) Polyclonal peptide antibody (Santa Cruz), and secondary HRP-conjugated polyclonal anti-rat Ab. The gels on the bottom represent the Coomassie stained gels after Western blot transfer. **(f** and **g**) Serum samples of six great apes were analyzed with mAb 75 (**f**) and mAb80 (**g**); bonobo and chimpanzee (red) lost the serpina2 gene. For all blots we used a HRP-conjugated anti-rat secondary Ab and deglycosylated (PNGase F) serpina2 derived from S2 cells served as positive control.

Several plasma samples (also kindly provided by Susana Seixas, Portugal) were analyzed in a sandwich ELISA using two different mAb against serpina2 detecting different epitopes for capture and detection (**Figure 4.13 a**). As anticipated the P2107 (serpina2 deletion, see Figure 4.9, and no signal in Western blot, see figure 4.12) sample was negative, whereas we detected a very high signal for P1713 and P1847 (**Figure 4.13 b**).

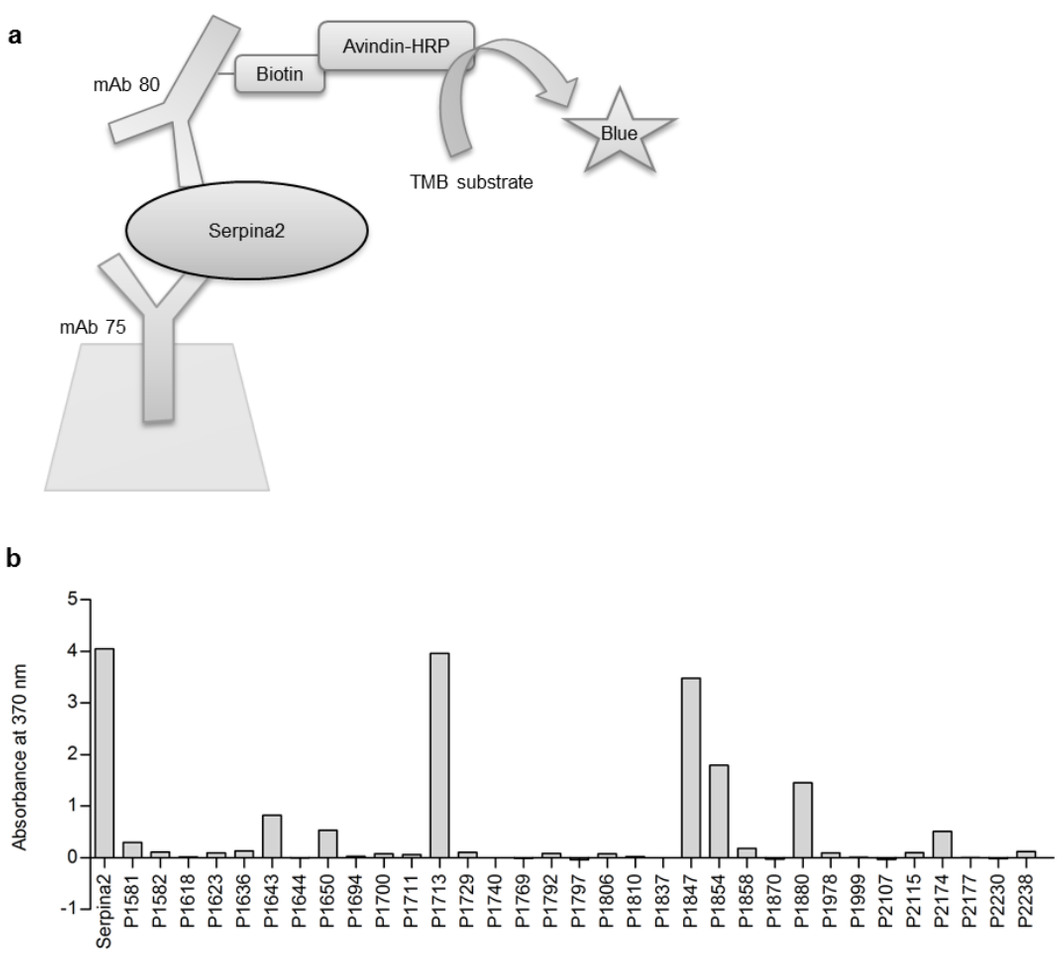

Figure 4.13 Sandwich ELISA to measure serpina2 in plasma. (**a**) Experimental setup: Anit-serpina2 mAb 75 was coated, then incubated with available plasma samples. For detection of potentially bound serpina2 biotinylated mAb 80, Avidin-HRP and TMB substrate were added. (**b**) Plasma sample P1713 and P1847 gave very strong signals in the sandwich ELISA. Serpina2 from S2 cells was used as a positive control. Absorbance at λ=370 nm was measured after 15 min incubation.

4.2.7 Glycosylation of recombinant and natural serpina2

To find out more about the glycosylation state of recombinantly expressed and natural serpina2 in epididymis tissue lysate and HPL, we performed deglycosylation experiments using PNGase F and Endo H (Endo-ß-N-acetylglucosaminidase H). While PNGase F is able to cleave off almost all N-linked glycans, Endo H is unable to cleave N-linked complex type glycans. Serpina2 contains four theoretical N-linked glycosylation sites. We could show that serpina2, overexpressed in HEK 293 cells, can be deglycosylated by PNGase F and Endo H meaning that it never entered the Golgi apparatus and no complex sugars were attached to the protein. The Western blot signal in cell culture supernatants is most likely due to proteins released by dead cells (**Figure 4.14 a**). On the contrary, serpina2 in human epididymis lysate can be deglycosylated with PNGase F but not Endo H treatment. A signal for natural glycosylated serpina2 can be detected at about 50 kDa, whereas a deglycosylated sample appears at about 47 kDa. Since Endo H is unable to deglycosylate the protein it must have passed the Golgi apparatus and contained complex sugars. Also a higher band of about 80 kDa was detected in Western blot; this signal reacts in the same manner to deglycosylation as the lower serpina2 band. The higher band could represent a serpina2-protease-complex or our antibody cross-reacts with another protein (**Figure 4.14 b**). In **Figure 4.14 c** we deglycosylated HPL and compared it to deglycosylated recombinant serpina2 (S2). For HPL we only detect a slight shift of the 47 kDa band when treated with PNGase F, and the higher band in HPL follows the same pattern as the 80 kDa band in the epididymis lysates.

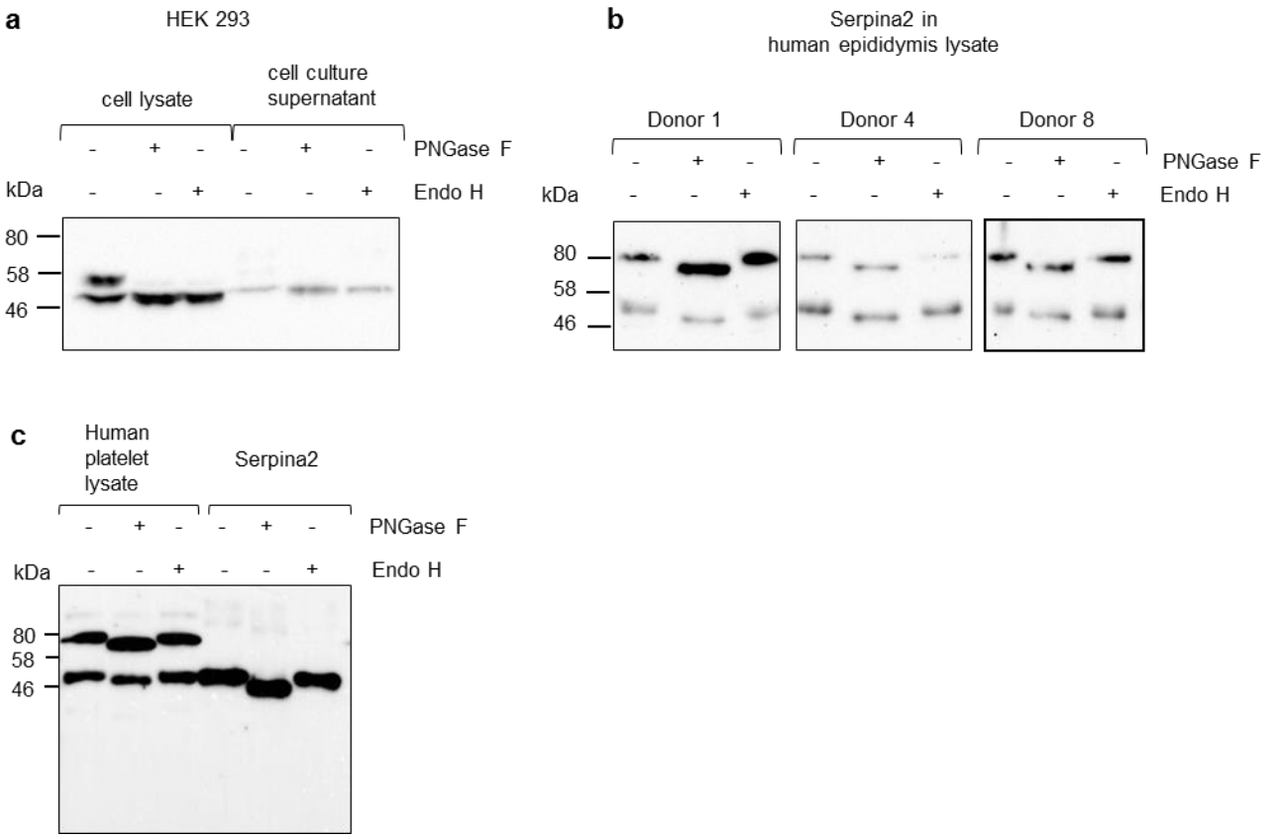

Figure 4.14 Deglycosylation of recombinant and natural serpina2. (**a**) Western blot analysis of cell lysate and cell culture supernatant of HEK 293 cells transfected with serpina2 plasmids. (**b**) Western Blot analysis of human epididymis lysate from three different donors. (**c**) Western Blot analysis of human platelet lysate and recombinant serpina2 derived from S2 cells. All samples were treated with PNGase F and Endo H to monitor protein trafficking. Western blots analyses were carried out using mAb 75 and secondary HRP-conjugated polyclonal anti-rat Ab.

4.2.8 Mass spectrometry analysis of human tissue lysates

Particularly, as we also found a few hints for serpina2 expression in whole blood and platelets in databases, we tried to verify these results and also our own Western blot results for epididymis tissue lysate pointing to serpina2 expression.

In a mass spectrometry analysis of samples that we immunoprecipitated with our newly established monoclonal antibodies (SA2 mAb 80 and 75, see Figure 4.8), we found up to two unique peptides in human platelet lysate (pool originated from more than 100 donors), in the serum of one man, and up to six unique peptides in epididymis total cell lysate from two individual donors (p=0.01).

Interestingly, when we tried to analyze total cell lysates (DDA and DIA mode, see 3.4.8.3) without immunoprecipitation we were not able to identify any peptides.

4.2.9 Finding potential target proteases of serpina2

We designed and evaluated FRET substrates that mimic the reactive center loop of serpina2 with the goal to find target proteases of potential inhibitor. Serpins are pseudo-substrates (decoy substrates) which entrap proteases by virtue of an exposed reactive center loop. Once the peptide loop is bound to the target protease, the serpin undergoes a drastic conformational change causing an irreversible inhibition of the protease.

One substrate, designed to equal the reactive center loop of serpina2 completely, was best cleaved by chymotrypsin, but also cathepsin G (CTSG), neutrophil elastase (NE), proteinase 3 (PR3), and trypsin (TR). The second substrate also mimicked the reactive center loop, but contained two additional prolines, which prevent cleavage before and after this position. This substrate was only cleaved by CHTR, and not by any other tested protease (**Figure 4.15**).

a

Protease cleavage site

	P15	P14	P13	P12	P11	P10	P9	P8	P7	P6	P5	P4	P3	P2	P1		P1‘	P2‘	P3‘	P4‘
serpina1	C	T	E	A	A	G	A	M	F	L	E	A	I	P	M		S	I	P	P
serpina2	G	T	E	A	T	G	A	P	H	L	E	E	K	A	W		S	K	Y	Q

b

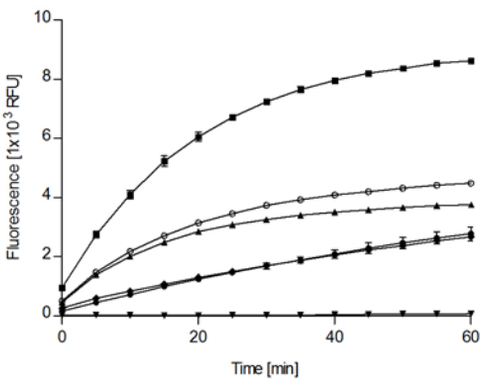

c

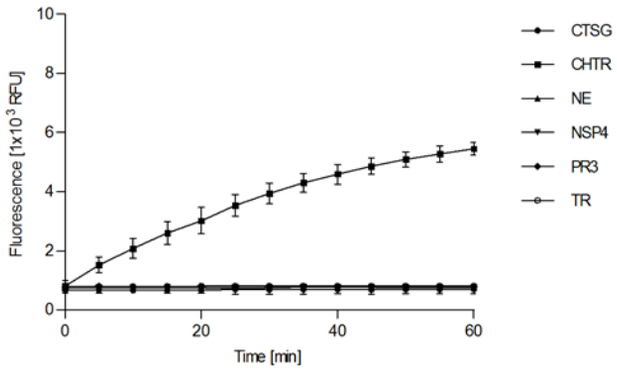

Figure 4.15 Specificity of FRET substrates mimicking the RCL of serpina2 towards serine proteases, trypsin and chymotrypsin. (**a**) Table showing the reactive center loop sequence of serpina1 and serpina2 (P15 – P4'). (**b**) Cleavage of a FRET substrate (5-TAMRA-EKAWSKYQ-Dap(CF)) that exactly mimics the RCL of serpina2. (**c**) Cleavage of a FRET substrate with two proline substitutions (5-TAMRA-EKPWSKPQ-Dap(CF)) that is very similar to the RCL of serpina2. Fluorescent signals were obtained at λEx = 485 nm and λEm = 520 nm. Data represent the mean of three independent experiments (n=3, ±SD).

Moreover, we investigated whether a serpina1 chimera, carrying the reactive center loop of serpina2 can be cleaved by proteases. For this purpose we cloned the reactive center loop of serpina2 into the AAT sequence (pTT5 vector), produced the serpina1 chimera in HEK 293 cells and purified it by Ni-NTA affinity chromatography. After incubation with several proteases we found, that the protein was cleaved by cathepsin G, chymotrypsin and trypsin suggesting again that chymotrypsin-like proteases are putative targets of serpina2. However, we observed that the serpina1 chimera did not form covalent complexes with any of the tested proteases. We also tested additional proteases in silver gels and found that cathepsin L and to a lesser extent cathepsin B were able to cleave the serpina1 chimera (no complexes), but not kallikrein 3, cathepsin C and mast cell chymase. In activity assays the most promising protease candidates, chymotrypsin and trypsin, were not inhibited when incubated with the serpina2 chimera.

a

Protease cleavage site

	P15	P14	P13	P12	P11	P10	P9	P8	P7	P6	P5	P4	P3	P2	P1		P1‘	P2‘	P3‘	P4‘
serpina1	C	T	E	A	A	G	A	M	F	L	E	A	I	P	M		S	I	P	P
serpina2	G	T	E	A	T	G	A	P	H	L	E	E	K	A	W		S	K	Y	Q
serpina1 chimera	C	T	E	A	A	G	A	M	F	L	E	E	K	A	W		S	I	P	P

b

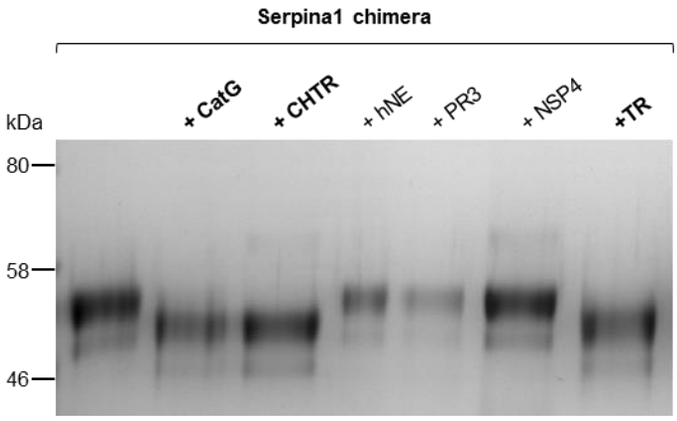

Figure 4.16 Protease cleavage of a serpina1 chimera carrying the reactive center loop of serpina2. (**a**) Table showing the reactive center loop sequence of serpina1, serpina2 and the serpina1 chimera (P15 – P4’).(**b**) Serpina1 chimera incubated with several proteases (10 min, 37 °C) on a silver stained SDS-PAGE gel.

4.3 Serpina2 – Discussion

4.3.1 Serpina2 tends to precipitate when recombinantly expressed

We managed to purify enough serpina2 expressed in HEK 293 cells under denaturing conditions to establish rat monoclonal antibodies. And we obtained small amounts of soluble serpina2 from S2 cells and *E. coli* cells.

In general, serpina2 folds poorly when overexpressed and forms intracellular aggregates. The karyotype of HEK293 cells is very complex and shows many abnormalities. It contains two or more copies of each chromosome with a chromosome number of 64. One variation is the presence of three copies of the X chromosome and it lacks any trace of a Y chromosome[44]. This suggests that the source fetus was female and we cannot exclude that the serpina2 gene was epigenetically silenced or affected in another way by this cell line, since it seems to be specific for male individuals.

We were able to produce several milligrams of SUMO-tagged serpina2 in *E.coli* BL21 cells with the pET24c_His_SUMO_serpina2 plasmid. Small ubiquitin-related modifier (SUMO) fusions are known to enhance the solubility of expressed fusion proteins[45]. To prevent precipitation of the protein, we chose a refold buffer containing Pipes, pH 6.5, to make sure that neither His_SUMO_serpina2 (pI 7.07) nor serpina2 with cleaved His-SUMO tag (pI 8.82) are in a solution at a pH that corresponds to their isoelectric point, because at this point a protein exists as an ampholyte and shows the least solubility. Nevertheless, cleaving off the SUMO-tag resulted in complete precipitation of the protein, which is another indication, that serpina2 tends to form aggregates very strongly.

4.3.2 Serpina2 mRNA and protein expression in human tissues

In our studies we could reveal, that serpina2 mRNA transcripts can only be found in the epididymis. Our results disprove the previously published data on serpina2[42], because of inappropriate primers used in these PCR experiments.

Our genetic analysis revealed that the ortholog of serpina2 in the mouse is called serpina1f (**Figure 4.17**).

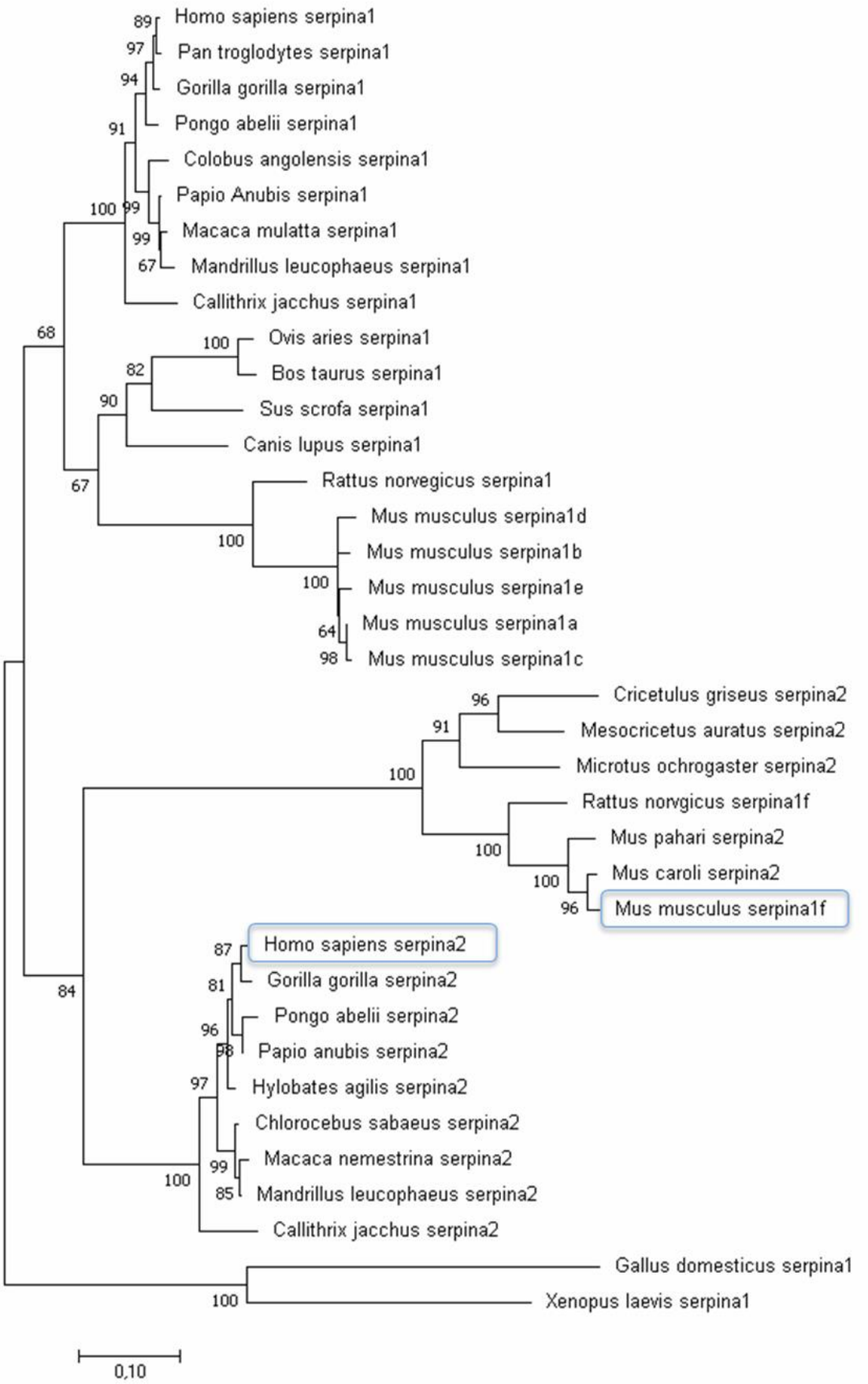
Homo sapiens serpina1
Pan troglodytes serpina1
Gorilla gorilla serpina1
Pongo abelii serpina1
Colobus angolensis serpina1
Papio Anubis serpina1
Macaca mulatta serpina1
Mandrillus leucophaeus serpina1
Callithrix jacchus serpina1
Ovis aries serpina1
Bos taurus serpina1
Sus scrofa serpina1
Canis lupus serpina1
Rattus norvegicus serpina1
Mus musculus serpina1d
Mus musculus serpina1b
Mus musculus serpina1e
Mus musculus serpina1a
Mus musculus serpina1c
Cricetulus griseus serpina2
Mesocricetus auratus serpina2
Microtus ochrogaster serpina2
Rattus norvgicus serpina1f
Mus pahari serpina2
Mus caroli serpina2
Mus musculus serpina1f
Homo sapiens serpina2
Gorilla gorilla serpina2
Pongo abelii serpina2
Papio anubis serpina2
Hylobates agilis serpina2
Chlorocebus sabaeus serpina2
Macaca nemestrina serpina2
Mandrillus leucophaeus serpina2
Callithrix jacchus serpina2
Gallus domesticus serpina1
Xenopus laevis serpina1
0,10

Figure 4.17 Phylogenetic tree showing the relationship of human serpina2 and murine serpina1f. The evolutionary history was inferred by using the Maximum Likelihood method based on the Jukes-Cantor model. The tree with the highest log likelihood (-8636,11) is shown. The percentage of trees in which the associated taxa clustered together is shown next to the branches. Initial tree(s) for the heuristic search were obtained automatically by applying Neighbor-Join and BioNJ algorithms to a matrix of pairwise distances estimated using the Maximum Composite Likelihood (MCL) approach, and then selecting the topology with superior log likelihood value. The tree is drawn to scale, with branch lengths measured in the number of substitutions per site. The analysis involved 37 nucleotide sequences. Codon positions included were 1st+2nd+3rd+Noncoding. All positions containing gaps and missing data were eliminated. There were a total of 646 positions in the final dataset. Phylogenetic and molecular evolutionary analyses were conducted using MEGA version 7[46].

Compared to other serpin orthologs in the mouse (serpina1a –serpina1e) serpina1f shares little homology with the human serpina2 (38% amino acid identity)[47]. However, serpina1f has also been reported to be highly expressed in the mouse epididymis[48]. This data strongly supports our result, that serpina2 is as well predominantly expressed in this organ. Additionally, serpina1f mRNA expression has been shown to increase significantly around puberty when the testosterone level in plasma increases indicating androgen-dependence[48].

In general, human and mouse genes are highly conserved. The serpin gene families in both species represent a result of multiple gene duplication events, though the murine serpin clusters show an even higher degree of divergence. It has been discussed, that the driving force behind that could be the potential exposure to a higher number of pathogen-associated proteases[49]. One could speculate that the function of serpina2 could also be associated to a defense mechanism against harmful proteases released by bacteria. Several examples of genes containing the serpin domain have been reported to play important roles in antimicrobial actions[50-52] and the fertility process[53-55].

The epididymis is an elongated cord-like structure along the posterior border of the testis (**Figure 4.18**). Its elongated coiled duct system serves the maturation, transit, and storage of

spermatozoa. Prior studies reported transcriptomics data of the different regions of the epididymis: caput, corpus and cauda. In these studies serpina2 was not identified[56]. It is possible that serpina2 mRNA can only be found in the efferent ductules and that our commercial mRNA sample also contained epididymis material and efferent ductules, while in the published study these parts were carefully separated as they were interested in the three distinctive parts of the epididymis.

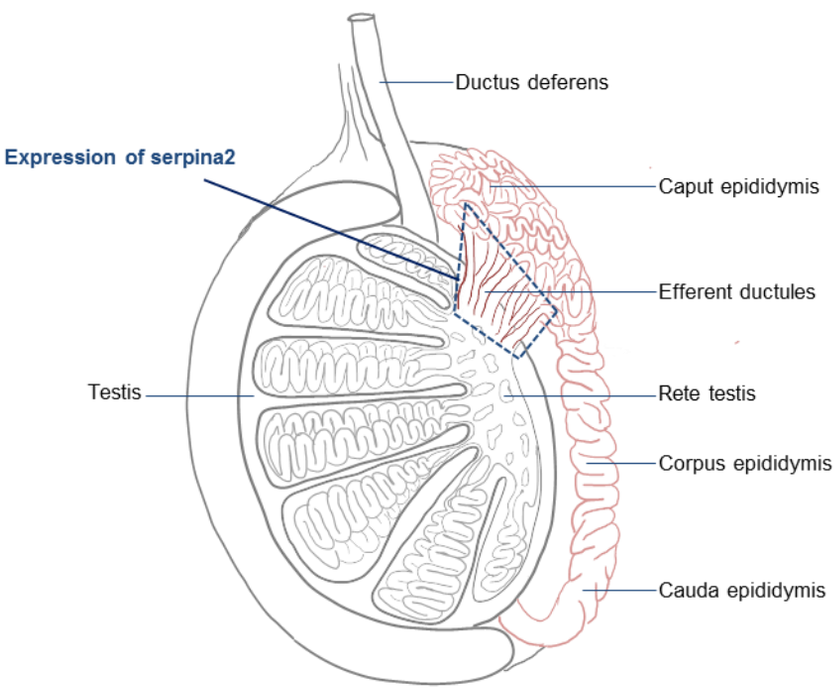

Figure 4.18 Vertical section of a human testicle to show the location of the epididymis and the efferent ductules. The efferent ductules and the epididymis structure are depicted in red. Fully matured spermatozoa are transported from the testis to the epididymis and then the ductus deferens (vas deferens) transports sperm to the ejaculatory ducts. Our immunoprecipitation results demonstrate that serpina2 is most likely expressed in the efferent ductules (marked in dark blue).

With our newly established serpina2 monoclonal antibodies we were able to detect protein in human tissues. The variable band intensities we detected in the Western blot experiment with epididymis tissue (see 4.2.5) are probably due to incomplete tissue disruption of some

samples, and to variation in the tissue samples themselves, the epididymis is divided in substructures (Caput, corpus, and cauda epididymis) that show in general different protein expression patterns. Since we found strong, specific protein signals in the efferent ductuli by immunohistochemistry, which are directly connected to the caput epididymis, tissue from this region is more likely to show a positive signal for serpina2 in Western blot. However, we have no information from which section of the epididymis the tissue was derived from. We also have to take into account, that the analyzed epididymis donor tissue from male-to-female transsexuals was quite heterogeneous: patients were not equally pre-treated with estradiol, most of them received additional medication (Gonadotropin-releasing hormone analogues (GnRH), progestins, progesterone, anti-androgens), and they were different in age[43].

Another study using these same tissue samples revealed that long-term estradiol treatment significantly reduced the diameter of seminiferous tubules in the testis, it increased collagen synthesis in the extracellular matrix and spermatogenesis was severely impaired[43]. Therefore, no mature spermatids could be observed in the stained tissue sections and the limitations of our results are that the pretreatment of the male-to-female transsexuals could also have an effect on serpina2. We cannot formally exclude that serpina2 protein expression was induced by hormone treatment, and our data might not represent serpina2 protein expression in normal testis tissue.

We also have to take the inconsistent treatment of donors into consideration for evaluation of serpina2 signal on the epididymis tissue sections. We detected the strongest signal of serpina2 in the ductuli efferenti (Figure 4.18). In large mammals, like humans, multiple entries connect the rete testis and the epididymis, approximately 6 - 15 efferent ductuli connect the rete testis with the caput epididymis. In smaller animals, for example in rodents only 3 – 8 ductules merge into a single duct that enters the epididymis[57]. The ductuli efferenti are covered by a stratified epithelium consisting of highly prismatic cells often carrying motile cilia (kinocilia). The ciliated cells serve to stir the luminal fluids, to increase the concentration

of luminal sperm. The epithelium is surrounded by a band of smooth muscle cells that helps to propel spermatids toward the epididymis. It could be speculated that serpina2 interacts with a protein related to the epididymis cilia. Several serpins are known, that do not exhibit classical inhibitory activity, but carry out other important functions. One well known member of the serpin family, which acts as chaperone and is found in the endoplasmic reticulum, is serpinh1. It is responsible for monitoring the collagen integrity in ER\Golgi boundary[58]. Perhaps serpina2 has a chaperone-like function, which would also fit to the fact that it is poorly or not at all secreted. The serpina2 positive granula on the apical pole of (ciliated) epithelial cells could either be a result of actually expressed and correctly folded serpina2 that has a function in sperm maturation, or the positive signal is due to aggregated serpina2 accumulation in granula or lysosomes, straining the health of epithelial cells. However, if that is the case, the question remains why serpina2 is not degraded by the unfolded protein response or autophagy in these epithelial cells. There are various protein quality control pathways available by mammalian cells, but there are also cases in which protein degradation is circumvented and misfolded proteins are deposited inside the cells. At the point where cells can no longer withstand the pressure of misfolded proteins, the organism is usually negatively affected. It is well known, that polymerization is a consequence of some natural serpin mutants. The most popular example of an aggregation prone serpin is the Z-mutant of serpina1 (introduced in 2.3 Alpha-1-antitrypsin deficiency), which is associated with lung emphysema and liver cirrhosis[24].

The phenomenon of disease development due to failing protein homeostasis has also been extensively studied in devastating neurodegenerative diseases like Alzheimer's or Parkinson's disease. The proteins that cause these diseases have a very high propensity to misfold or aggregate and therefore represent a potential threat for the survival of cells and the well-being of an organism[59].

These examples of deposition of misfolded proteins share common features – they exhibit a propensity to misfold/aggregate, but are usually soluble and they seem to build up later in life suggesting a gradually fail with age of protein quality control pathways[59].

Just like individuals expressing the Z-mutant of serpina1, those expressing serpina2 could have a disadvantage due to misfolded protein in their epithelial cells of the epididymis presumably later in life.

Predominantly in human platelet lysate, but also in serum and plasma we detected a positive signal in Western blots with our newly established serpina2 antibodies. Remarkably, in human platelet lysates the same band was detected by a commercially available serpina2 peptide antibody. The serpin superfamily includes serine protease inhibitors essential for the cascade of blood coagulation. Therefore, it is conceivable that serpina2 could also play a role in fine tuning of this mechanism. We also tested sera from grate apes and detected not only a positive Western blot signal in the ones known to express serpina2, but also in those with serpina2 deletion (bonobo and chimpanzee), which were supposed to serve as negative control. The limitations of our study are that we cannot exclude that our antibodies cross react to some extent with abundant serpins existing in human samples, because this family shares a very similar structure. However, we ruled out their reaction with serpina1.

Additionally, we analyzed seminal fluid by Western blotting and could not detect any signal. Seminal plasma is known to contain a large number of proteases and protease inhibitors, including many serine protease inhibitors like serpina1 or serpina5[60]. That our antibodies do not cross react with any of these serpins supports the assumption that we detect a real positive serpina2 signal in other samples.

Intrigued by this positive signal, in particular in human platelet lysate, we performed deglycosylation experiments and revealed that serpina2 overexpressed in HEK 293 cells does not enter the Golgi apparatus, whereas natural serpina2 could not be deglycosylated by

Endo H, which means that it must have been processed in the Golgi like a normally folded protein.

In addition, we developed a sandwich ELISA to check whether we can detect serpina2 in human plasma samples. Our analysis revealed that two out of 33 samples exhibited very strong positive signals (P1713 and P1847), whereas the plasma sample from the serpina2 deficient individual (P2107) was tested negative for serpina2 in Western blot (Figure 4.12). The positive ELISA signals again support the assumption that serpina2 is present in human plasma. Unfortunately, the genotype of P1713 and P1748 is unknown, however, as a next step we will try to verify whether serpina2 peptides can be found in those plasma samples after immunoprecipitation with our serpina2 mAbs.

4.3.3 Serpina2 peptides are found in blood and epididymis samples

The result of our mass spectrometry experiments further revealed that serpina2 might not be a pseudogene after all. The protein was identified in human platelet lysate, serum and the epididymis. It was, however, expressed at very low level, and could only be identified after immunoprecipitation using our newly established serpina2 mAbs.

4.3.4 Genotyping of serpina2

In order to find a human negative control blood sample we analyzed 66 human DNA samples and found that 16.67% carried the fs108 mutation, and 40.91% the start codon deletion mutation. Only one individual turned out to be a serpina2 null individual (P2107). In P2107 plasma we could not detect a positive band around 47 kDa like in the other human samples, indicating that the western blot signal might be genuine (Figure 4.12)..

4.3.5 Chymotrypsin-like proteases could be targets of serpina2

CHTR was able to cleave both FRET substrates mimicking the RCL of serpina2, suggesting that chymotrypsin-like proteases could be potential candidates for target proteases.

In experiments with serpina1 chimera carrying part of the RCL of serpina2 we noticed that the protein did not show any signs of misfolding. Although the chimera did not form complexes with proteases, it was cleaved by chymotrypsin, trypsin and cathepsin G, proving that the loop was in principle accessible.

Serpina2 is the only known serpin with a tryptophan in the P1 position. Interestingly, according to the ensemble database (serpina2, LOC103158570) the Chinese hamster also carries a serpina2 gene with tryptophan in P1 position, but unfortunately there is also no additional information on hamster serpina2.

In search of a possible target protease of serpina2, the serine protease *Prss40* attracted our attention. Speaking in terms of evolution, the loss of *Prss40* preceded the loss or inactivation of serpina2. Interestingly, pseudogenes of serpina2 are found in species that lack a functional *Prss40*. In line with this observation, a functional Prss40 gene can only be found in species with a functional serpina2 gene. It seems quite possible that pseudogenization of the protease *Prss40* resulted in the disappearance of the corresponding protease inhibitor.

In 1998 *Prss40* was first described as a novel serine protease in the acrosome of mouse sperm, where proteolytic enzymes are important for the limited hydrolysis of the zona pellucida. This is the barrier, which sperm cells have to traverse in order to successfully fertilize a mammalian egg. The *Prss40* gene product is predicted to have chymotrypsin-like activity because it shares sequence similarities and active site features (Ser-189; chymotrypsinogen numbering) with chymotrypsin-like enzymes[61].

Several indications for a role of proteases and inhibitors in fertility can be found in the literature[62,63]. For example disruption of the protein C inhibitor (serpina5) results in male infertility in mice[64]. Serpina5 and serpina2 are close neighbors, located on the same chromosome (see Figure 4.2). Another example is Prss37, a protease that has been shown to be required for sperm migration. Prss37 knockout resulted in male infertility[65]. Moreover, it has been reported that chymotrypsin treatment of sperm cells improves intra-uterine

insemination and pregnancy rates after in vitro fertilization[66-69]. It is conceivable that sperm cells could be pretreated with Prss40 in a much more targeted manner than it is being done with chymotrypsin.

To explore, whether serine protease 40 is a real target of serpina2 we aim to produce active recombinant Prss40 for functional analysis. This approach will provide further insight into the function and relevance of serpina2.

4.3.6 Concluding remarks on serpina2

This work has unambiguously demonstrated that serpina2 is not a classical pseudogene but rather a lowly expressed gene that can be found in the epididymis at the mRNA and protein level. We are not completely convinced that serpina2 expressed in human blood. On the one hand, we were not able to find a mRNA source and we have to consider unspecific binding of the newly established serpina2 antibodies. On the other hand, we found a serpina2 signal even with the commercially available peptide antibody, too, and finding peptides in mass spectrometry experiments is an indication for the presence of serpina2.

We could not conclusively characterize a possible function of serpina2, however, we assume, when folded correctly, it is most likely able to inhibit chymotrypsin-like proteases.

It is conceivable that possibly misfolded or aggregated serpina2 is disadvantageous in humans, and that it is preferable not to have it. In this case, however, it seems odd to find an intact serpina2 in most primate species and it is difficult to explain why it has been kept for so long, and why there are not more cases of gene inactivation in other species.

In an ongoing study we are examining blood and sperm quality of semen donors with the help of the Cryobank München (Viavit GmbH) to identify serpina2 deficient individuals at the genetic and biochemical level. We hope to find more negative control samples to verify the specificity of our antibodies and ideally to identify a difference of sperm quality and overall fertility in presence or absence of serpina2.

In conclusion, serpina2 is not a pseudogene; it is an epididymis specific potential inhibitor of chymotrypsin-like proteases and may improve sperm maturation.

For a better understanding of male fertility and reproductive success it is important to understand the mechanism of all ongoing protease – inhibitor interactions, and to identify potentially harmful proteins like serpina2.

5. Characterization of two common coding variants of serpina1 (M1(V213) and M1(A213))

5.1 Serpina1 coding variants- Introduction

Several major alleles of AAT (serpina1) can be found in human populations: the normal M alleles (M1, M2, M3, M4) and the rare S and Z variants. The M alleles result in normal levels of AAT, the S allele in reduced levels and the Z variant leads to very low levels of AAT in blood. The M allele is considered as normal type resulting in a normal phenotype (MM) with functional activity to inhibit neutrophil elastase efficiently[70]. In this study we investigated the properties of two different variations of the M1 allele: M1(V213) and M1(A213). A213 represents the minor allele, whereas V213 is the prevailing M1 allele in Caucasians. Both variants have been shown to be functionally equivalent plasma isoforms leading to very similar plasma levels of AAT[71]. In order to provide evidence for the differential properties of the two M1 alleles the corresponding proteins were stably expressed in HEK 293 cells, purified and functionally characterized in a hydrogen/deuterium exchange measurement experiment combined with mass spectrometry.

5.2 Serpina1 coding variants – Results

5.2.1 Expression of two AAT variants: M1(V213) and M1(A213)

HEK 293 cells were transfected with pTT5-hAAT_ M1V213 or pTT5-hAAT_ M1A213 plasmid and incubated for 4 days. The protein was very efficiently produced and secreted, and high amounts of the two proteins were purified by Ni-NTA chromatography (**Figure 5.1 a**). The approximately 47 kDa proteins were dialyzed in buffer containing 300 mM NaCl, 20 mM Tris, and 10% glycerol (pH 7.4) before they were analyzed in a hydrogen/deuterium exchange measurement experiment by our collaboration partner Patrick Wintrode (University of Maryland, School of Pharmacy)[72].

5.2.2 Hydrogen/deuterium exchange measurement

To find out more about the impact of the amino acid at positon 213 of the AAT molecule, the hydrogen/deuterium exchange rates of the M1(V213) and M1(A213) variant were determined. As depicted in **Figure 5.1 b**, the hydrogen/deuterium exchange rates between the two AAT variants demonstrated significant differences for multiple peptides. In general the alanine variant was more susceptible to deuterium uptake in several surface regions when compared to the valine variant. Especially the M1(A213) substitution resulted in significantly less rigidity of the C-terminal end of the serpins' RCL. Additionally, the strand one of the C ß-sheet (s1c) and strand five of the A-sheet in the shutter region (s5A) exhibited a higher flexibility. In general, we can state that the AAT M1(A213) variant features increased dynamics.

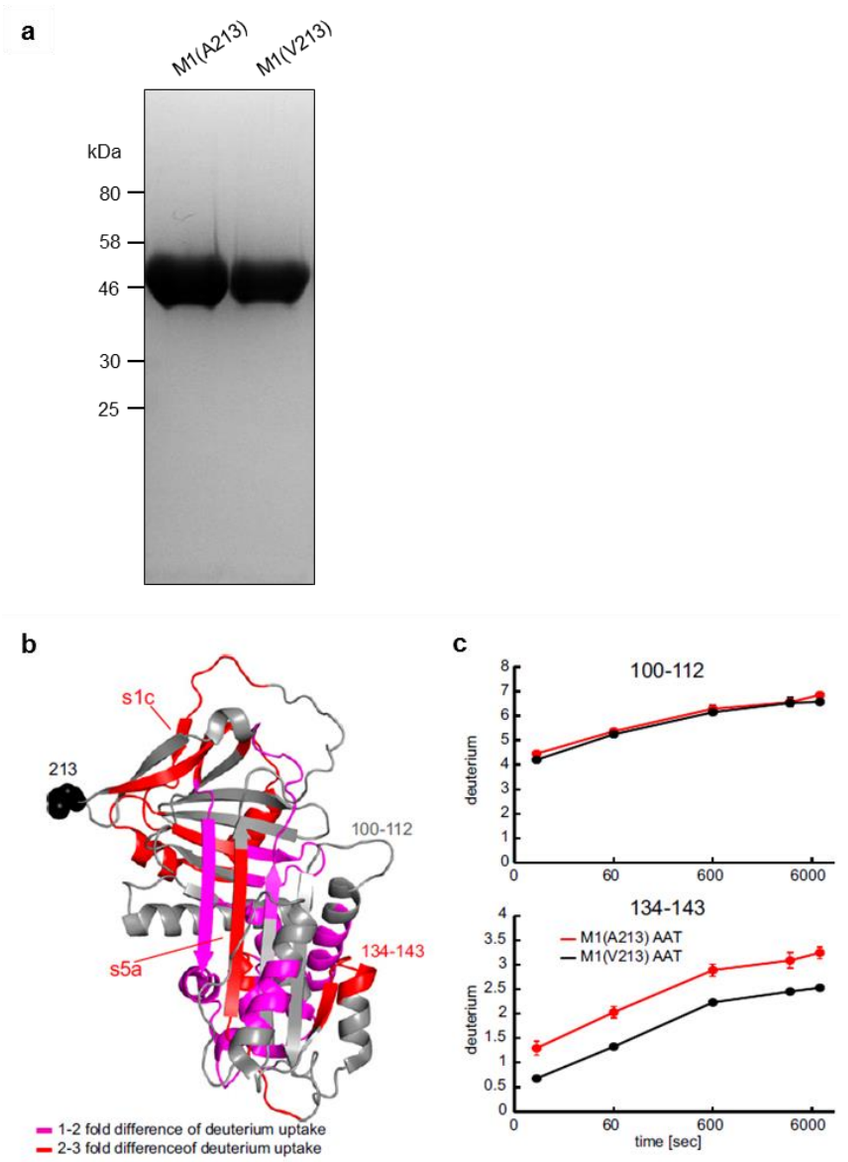

Figure 5.1 Expression of M1(V213) and M1(A213) and hydrogen/deuterium exchange measurement. (**a**) Coomassie gel of AAT M1(V213) and M1(A213) protein after Ni-NTA purification. (**b** and **c**) Differential dynamics of hydrogen/deuterium exchange between AAT variant M1(A213) and M1 (V213). (**b**) The increasing difference in deuterium uptake across five time points (10 sec – 7200 sec) is compared between the two AAT variants. The results are mapped onto the crystal structure of AAT (PDB: 1QLP). A two- to threefold increase of deuterium uptake is labeled in red and a one- to twofold increase is marked in pink. For the grey areas there was no significant difference detected. (**c**) Exemplary kinetic curves for the hydrogen/deuterium exchange measurement. For peptide 100 – 112 there was no difference detected, whereas peptide 134 – 143 showed a significant difference between the two AAT variants at all time points (N=3).

5.3 Serpina1 coding variants - Discussion

Analyzing the two purified serpina1 variants, M1(V213) and M1(A213), in a hydrogen/deuterium exchange experiment revealed differences in the global flexibility of the two proteins. In addition, it has been shown in thermophoresis experiments that the M1(V213) variant interacts stronger with plasma lipoproteins[72].

In former studies performed with the two purified AAT variants in protein- and lipid-free solution no differences between the two proteins were detected. The microscale thermophoresis, which allows to measure AAT – NE interaction in complex solutions like plasma under equilibrium conditions, revealed that M1(V213) exhibits a lower affinity to NE than the M1(A213) variant. The hydrogen-deuterium exchange experiment showed that M1(V213) exhibited a reduced flexibility which favors the interaction with other plasma proteins. M1(V213) also displays higher hydrophobicity. Therefore, its interaction with plasma lipoproteins (HDL (high density lipoprotein), LDL (low density lipoprotein) is increased and, in turn, the interaction with NE is reduced. This would reduce proteolytic inactivation, and most likely improves its local availability by co-transport with lipoproteins.

These findings were published together with a transethnic (Europe, Australia, South Asia), exome-wide association study which revealed the M1(A213) variant to be associated with large artery atherosclerotic stroke[72]. The exact mechanism by which M1(V213) reduces the risk for large artery stroke is not yet fully understood, however, binding to lipoproteins may enhance the local availability of M1(V213) in atherosclerotic plaques compared to the M1(A213) variant. Moreover, M1(A213) being more dynamic and flexible is more prone to proteolytic inactivation by other proteases.

This study illustrates an example of a functionally relevant coding sequence variation in which a single-residue variation outside the inhibitory reactive center loop of the protease inhibitor AAT leads to an alteration that affects its overall structural flexibility and binding properties.

6. Preservation with alpha-1-antitrypsin improves primary graft function of murine lung transplants

6.1 AAT in lung transplantation - Introduction

Optimal preservation of post-ischemic graft function is essential in lung transplantation. When a lung is transplanted it faces two major challenges: The first one is the ischemic storage at 4 °C in which the lung is not supplied with blood. The second challenge is reperfusion, which causes lung injury when blood returns back to the grafted tissue. Both can contribute to primary graft dysfunction (PGD), which is defined as severe form of acute lung injury induced by ischemia/reperfusion and occurs within the first 72 hours after transplantation. PGD is the major cause of early mortality and morbidity after lung transplantation, it affects up to 25% of all patients[73]. To date there are no proven therapies that prevent PGD. Therefore, it is very important to find new strategies to avoid the early onset of inflammation in transplanted lungs.

Additionally, primary graft dysfunction as well as vascular damage increases with prolonged preservation times. Therefore, storage and conservation of donated lungs in protein-free, dextran-containing electrolyte solutions is limited to about six hours. A more sophisticated preservation technique could make it possible to increase the donor pool by allowing longer storage times.

In order to improve the conventional storage solution we hypothesized that proteases released by activated neutrophils in primary graft dysfunction can be neutralized by the natural protease inhibitor AAT, when added to the perfusion solution (Perfadex) during cold ischemic storage (**Figure 6.1**).

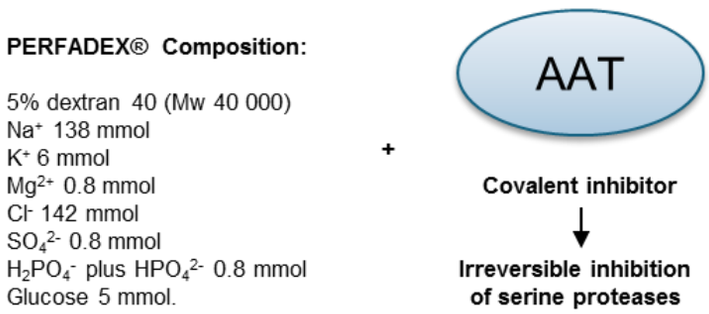

Figure 6.1 Composition of ordinary Perfadex and the addition of AAT.

Advantageous effects of protease inhibitors, in particular of alpha-1-antitrypsin (AAT), have been noticed in certain models of ischemia-reperfusion injury[74-77] at 37 °C[75,77]. These experimental setups, however, do not appropriately mimic the challenges of *ex vivo* organ storage in a cold cell- and protein-free electrolyte solution like Perfadex[78]. Positive results from these previous studies cannot be extrapolated to reperfusion injury after preservation of organs in the cold. Primarily infiltrating neutrophils[79,80] and the duration of oxygen deprivation [81,82] are responsible for the irreversible damage of the transplanted lung tissue. Since activated neutrophils release large amounts of serine proteases, like elastase and proteinase 3, protease inhibitors like bovine aprotinin[83,84], Lex032[76,85], and AAT[74,75,77,86] have been explored experimentally in animal models for treatment of lung transplant recipients. To increase the protease inhibitor concentration in the circulation, they have been administered intravenously or intraperitoneally in these studies[21]. We hypothesized that the inhibitors examined in these studies did not efficiently protect the transplanted graft against infiltrating activated neutrophils, because some applied inhibitors did not have the appropriate inhibitory profile, and they reached the inhibitor-depleted graft in the course of reperfusion too late.

To initiate proof of concept experiments, we developed a new clinically appropriate lung preservation protocol for lung transplant patients. We used a murine orthotopic lung transplantation model (see **Figure 6.2**, established by Krupnick *et al*.[29]), and stored the lung graft in Perfadex containing AAT (1 mg/ml) for an extended time period of 18 hours at 4 °C.

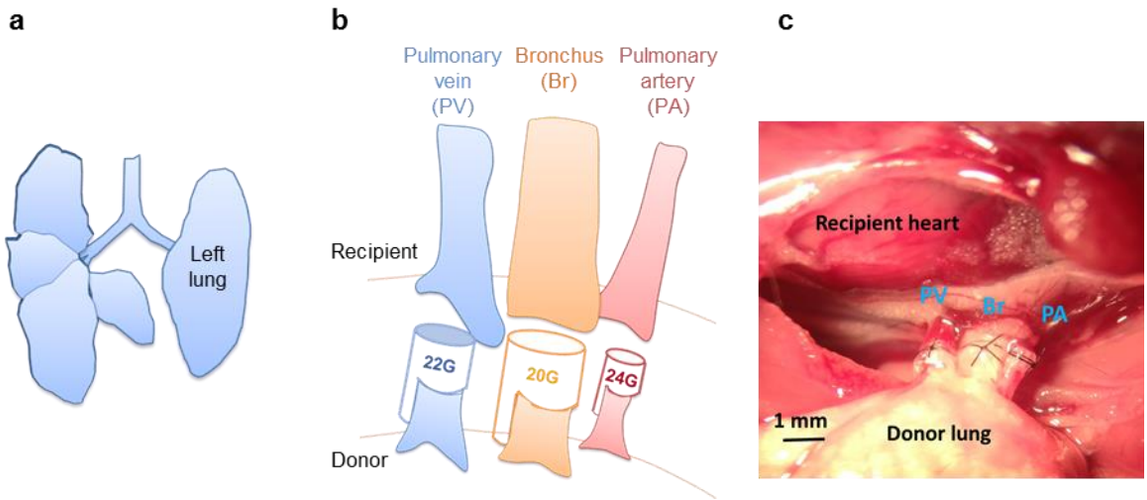

Figure 6.2 Mouse model of orthotopic lung transplantation. (**a**) Model of a murine lung: the right lung consists of four lobes and the left lung only of one lobe. (**b**) Principle of left lung transplantation in the mouse: first the pulmonary artery (PA, red) is attached to the recipient, then the pulmonary vein (PV, blue), and finally the bronchus (Br, orange). (**c**) Picture of left donor lung attached to the recipient during surgery (taken by Natalia Smirnova).

The aim of this preclinical study was to test if vascular leakage and immediate onset of neutrophil-mediated inflammation after reperfusion can be circumvented or soothed by adding AAT to the Perfadex perfusion solution during cold ischemia. Further, we wanted to find out whether the anticipated enhancement of lung graft function can directly be deduced from AAT's protease inhibiting or from other anti-inflammatory, tissue protective or immune modulatory properties. Our results reveal that AAT affects neutrophil-derived elastase and proteinase 3 and mostly prevents immediate reperfusion damage by protease inhibition in the tissue of lung transplants.

6.2 AAT in lung transplantation – Results

6.2.1 Production of AAT^{wt} and AAT^{mt}

The cDNA modification of the human AAT^{mt} (A355D/I356P/P357D/M358S) was introduced by amplifying the cDNA of human AAT with the primer pair DJ3608/DJ3609[87] (see 3.1.3). Acc I and Abs I restriction enzymes (NEB) were used to digest the PCR product. Subsequently, it was cloned into the respective sites of the previously modified wild type pTT5_AAT plasmid.

The AAT^{wt} (human M1(V213)) and AAT^{mt} plasmids were utilized for transient expression in HEK293 cells[72]. We successfully purified large amounts of the proteins and dialyzed them in Perfadex solution for later administration in the orthotopic mouse transplantation experiments.

6.2.2 Treating lung grafts with AAT during storage is more efficient than AAT injection of transplant recipients prior to surgery

We injected mice with 60 µg/g AAT[86] and determined the AAT content in their lungs after one and four hours (**Figure 6.3 a**). We also analyzed the levels of AAT four hours after orthotopic lung transplantation in mice whose graft had been stored under cold ischemia conditions in AAT (1 mg/ml in Perfadex) by Western blotting (**Figure 6.3 b**). We found that the local deposition of AAT was much better achieved in the latter procedure, in which plasma proteins were absent (**Figure 6.3 c**).

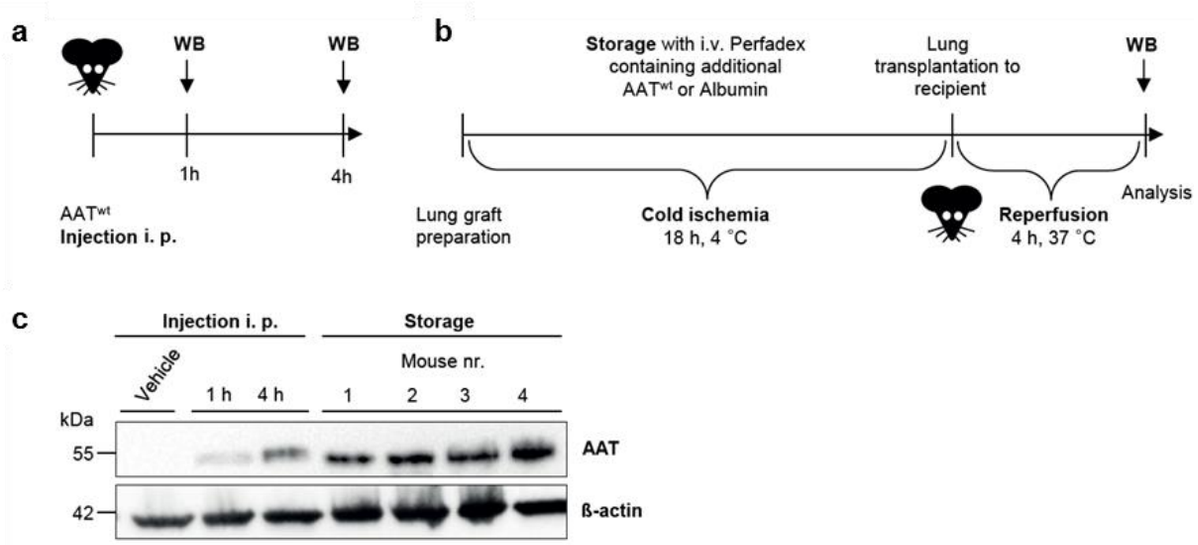

Figure 6.3 Storage in AAT^{wt} containing Perfadex leads to increased AAT levels after reperfusion (4 h) compared to intraperitoneal AAT injection of the recipient mouse. (**a**) Experimental outline of i.p. injection of AAT^{wt}. (**b**) Experimental outline for storage in AAT^{wt} during cold ischemia (18 h, 4 °C) followed by implantation and reperfusion (4 h, 37 °C). (**c**) Western Blot analysis of total left lung tissue lysate. Lane 1: vehicle i. p. injection, lane 2: 1 h after AAT^{wt} injection, lane3: 4 h after AAT^{wt} injection, lane 4 -7: transplanted left lungs of four C57BL/6J recipient mice after 4 h of reperfusion. A specific monoclonal antibody was used for detection of AAT^{wt} and detection of β-actin served as a loading control (see lower panel).

6.2.3 Vascular integrity after cold ischemia

To check whether the lung vasculature is better preserved when AAT is added to the storage solution, we perfused lungs with Evans Blue either before or after storage of 18 hours. Without storage we were able remove the blue stain by flushing with PBS (**Figure 6.4 a)**. After storage for 18 hours at 4°C the vasculature was damaged and we were not able to remove Evans Blue by flushing with PBS, irrespective of whether the graft was stored in Perfadex alone or in Perfadex supplemented with Albumin or AAT (**Figure 6.4 b**).

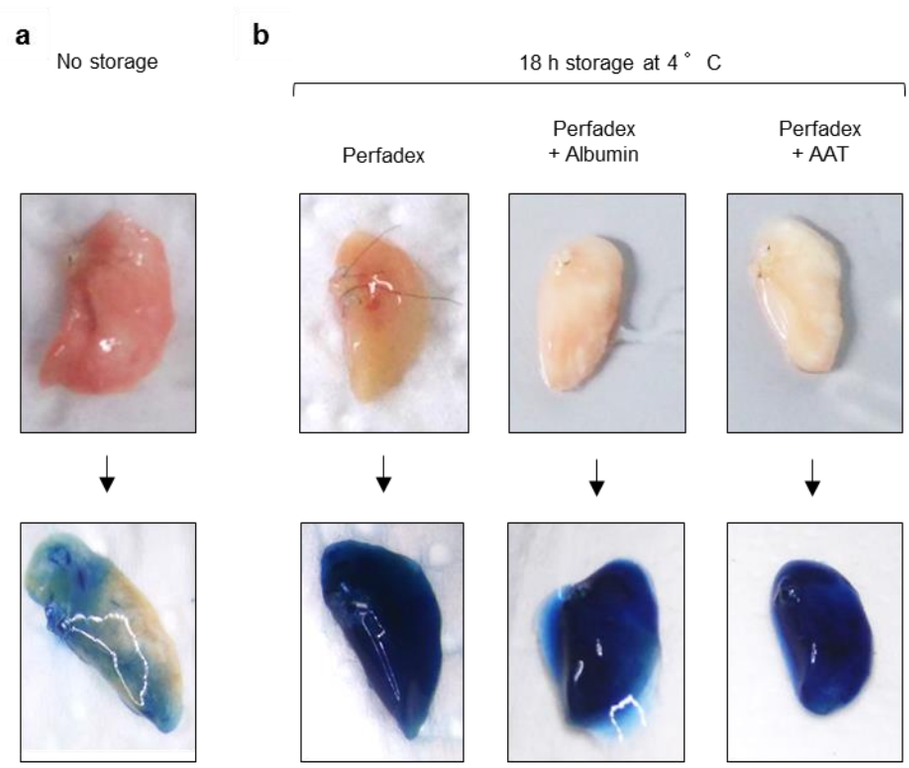

Figure 6.4 Visualization of the loss of vascular integrity after cold ischemia. (**a**) Left mouse lung before (top) and after perfusion with Evans Blue (without storage) followed by perfusion with PBS (bottom). (**b**) Left mouse lung before (top) and after perfusion with Evans Blue followed by perfusion with PBS (bottom) after 18 h storage at 4 °C. The lungs were either stored in Perfadex alone (left), Perfadex supplemented with albumin (1 mg/ml) (middle), or Perfadex supplemented with AAT (1 mg/ml). (Pictures were taken by Natalia Smirnova.)

6.2.4 Storage in AAT improves PGD

A murine orthotopic left lung transplantation model was used to assess PGD after prolonged cold ischemia storage of the left lung in Perfadex (**Figure 6.3 b**). We clearly noticed cellular infiltrates in the transplanted left lobe and neutrophils in the bronchoalveolar lavage fluid. After stopping the air and blood flow from the non-transplanted right lung by clamping the right bronchus, the partial oxygen pressure (pO_2) in the left heart ventricle decreased indicating graft dysfunctions after prolonged cold ischemic storage. With the goal to improve preservation of the lung graft, we explored the potential beneficial effect of AAT by perfusing and storing the lung graft at 4 °C in Perfadex supplemented with AAT. We directly compared AAT with albumin at the same concentration in our mouse transplantation model (**Figure 6.5**). As envisioned, we found a highly significant protective effect on graft preservation both at the histopathological (**Figure 6.5 a**) and functional level (**Figure 6.5 b to e**). Addition of AAT resulted in an almost 40% higher blood oxygenation (**Figure 6.5 b**) in the transplanted left lung. The protein (**Figure 6.5 c**) and neutrophil content of the bronchoalveolar lavage fluid (**Figure 6.5 d**) and the neutrophil infiltration of the transplanted lung (**Figure 6.5 e**) were much lower in the AAT-treated lungs in comparison to the albumin-treated lungs after four hours of reperfusion.

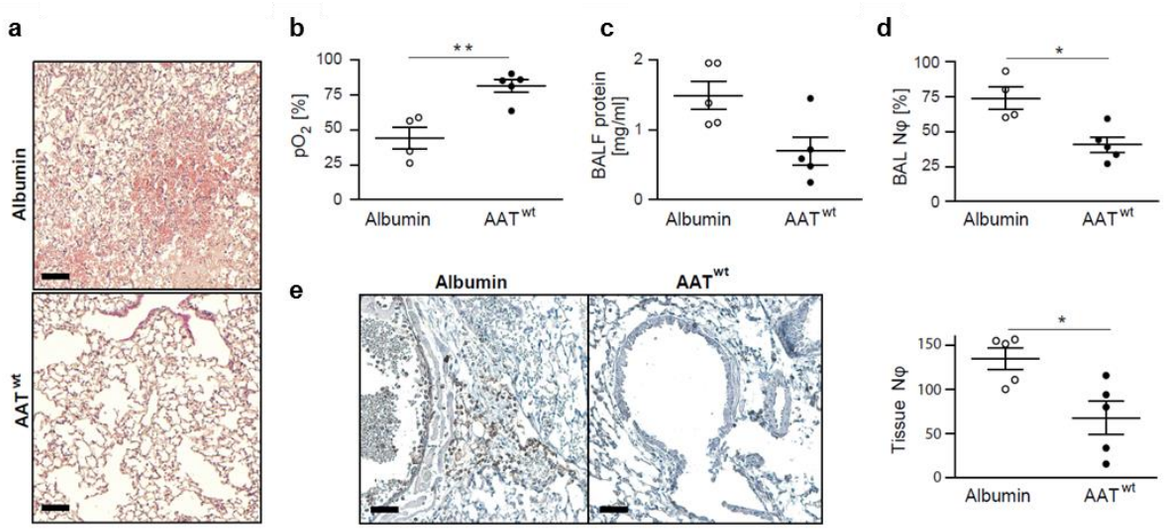

Figure 6.5 Primary graft dysfunction is reduced by AAT. Left lungs of C57BL/6J donor mice were either stored in Perfadex supplemented with wild type AAT (AAT^{wt}) or albumin at 4°C for 18 hours cold ischemia time. Four hours after orthotopic lung transplantation, C57BL/6J recipient mice were sacrificed and the outcome of the two treatment groups were compared (*n*=4-5 per group). (**a**) H&E staining depicting the tissue morphology of a transplanted left lung (scale bars: 200 µm). (**b**) pO_2 (partial oxygen pressure) of the oxygenated blood in the left heart ventricle was determined after clamping the right bronchus for five minutes. During measurement of the oxygen exchange function only the transplanted left lung was mechanically ventilated. (**c**) Total protein concentration in the bronchoalveolar lavage fluid and (**d**) bronchoalveolar lavage neutrophil count for the two different treatment groups. (**e**) Immunohistochemistry (scale bars, 200 µm) and quantification of neutrophils in the transplanted left lungs from 10 randomly chosen visual microscopic fields. Data are represented as mean ± SEM and compared with a Mann-Whitney test (**p=0.0159, *p<0.05).

6.2.5 Lung grafts are not preserved by a non-inhibitory AAT variant

To explore potential pleiotropic effects of AAT in graft protection, we separated the anti-proteolytic functions of the RCL from other AAT-associated modulatory functions on the remaining surface of the molecule. We eliminated trypsin-, chymotrypsin- or elastase-targeting specificity by substituting two residues in the RCL by aspartate residues (position P4 and P2) and two residues by a proline and serine residue (P3 and P1, respectively) (**Figure 6.6 a**). Changing the P4 Ala-355 and the P2 Pro-357 to a negatively charged Asp alters the hydrophobic nature of the RCL and reduces the interactions of AAT with phospholipid bilayers[88]. Shifting the Pro-357 to position 356 (P3) and replacing the methionine-358 conservatively by a serine alters the canonical inhibitory conformation and ß-pleated strand extension of the RCL (P4 to P3')[89] and its specificity which are both required for the inhibition of serine proteases.

In accordance with our assumptions, the RCL mutant of AAT (AAT^{mt}) produced in HEK 293 cells[72] was no longer able to inhibit murine and human neutrophil elastase (NE) and proteinase 3 (PR3) (**Figure 6.6 b**). However, the purified recombinant wild type AAT (AAT^{wt}) inhibited human and mouse NE and PR3 effectively. We intentionally designed the sequence modifications in the RCL of AAT to abolish cleavage by various mammalian proteases (assessed with the programs Prosper, Cascleave2.0 and PeptideCutter).

In the lung transplantation experiments with AAT^{mt} in direct comparison to albumin, acute lung inflammation as judged from histology sections (**Figure 6.6 c**), the oxygenation of blood in the transplanted left lobe (**Figure 6.6 d**), and the protein content in the bronchoalveolar lavage fluid (**Figure 6.6 e**) was indistinguishable between the two treatment groups. Also the amount of infiltrating neutrophils in the BAL was not significantly different between the two treatment groups (**Figure 6.6 f**).

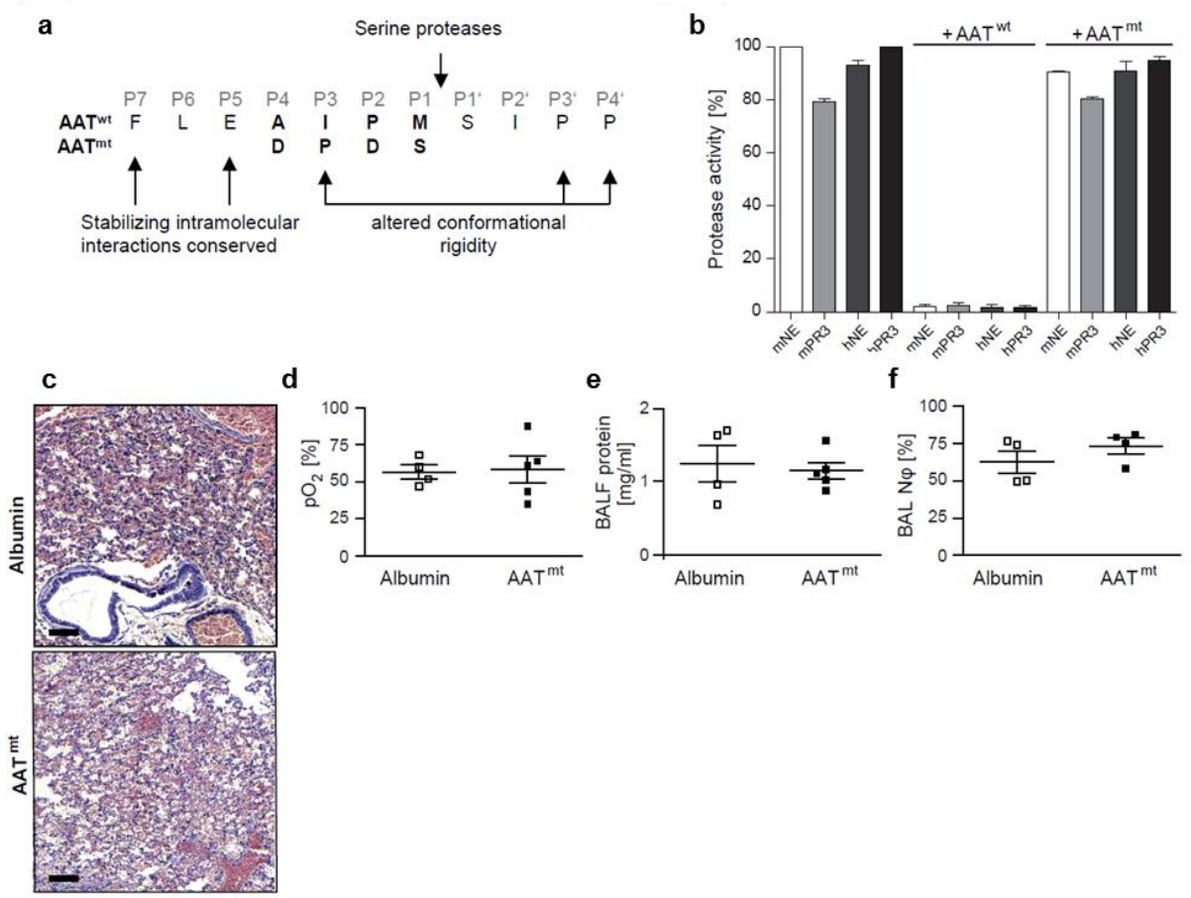

Figure 6.6 A reactive center loop variant of AAT (AAT^{mt}), unable to inhibit proteases, added to the preservation solution is ineffective. (**a**) Structure of the non-inhibitory reactive center loop variant (mutant AAT, AAT^{mt}) with replaced residues at P4 (A→D) and P2 (P→D) and P1 (M→S) with a more polar residue and shifting the P2 proline to the P3 (I→P) position. The new design contains conserved hydrophobic intramolecular interactions in the extended loop, however, the conformation and flexibility of the loop was altered by the proline at P3. (**b**) Proteolytic activities of human (h) and murine (m) neutrophil elastase (NE) and proteinase 3 (PR3) with or without the addition of AAT^{wt} or AAT^{mt}. Data represent three independent experiments (*n*=3, ± SEM). (c to f) Left donor lungs from C57BL/6J mice were stored in either AAT^{mt} or albumin supplemented Perfadex at 4°C for 18 hours. Recipient mice (C57BL/6J) were sacrificed 4 h after transplantation (*n*=4-5 per group). (**c**) H&E staining illustrating the tissue morphology of a left lung after orthotopic transplantation (scale bars, 200 µm). (**d**) pO_2 (partial oxygen pressure) measured in blood collected from the left ventricles of the heart, five minutes after clamping the right bronchus. (**e**) Total protein concentration in the bronchoalveolar lavage fluid and (**f**) bronchoalveolar lavage neutrophil count. Data are represented as mean ± SEM.

6.2.6 PR3 and NE double deficient mice exhibit enhanced primary graft function

To corroborate the detrimental impact of neutrophil serine proteases in PGD further, we compared wild type and PR3/NE double deficient mice as graft recipients. For these experiments we used donor mice with the same genetic background as the recipients (C57BL/6J). The alveoli structure of the transplanted lobe of the double knockout mice appeared much healthier than that of wild type mice after 4 hours of reperfusion as assessed by hematoxylin and eosin staining (**Figure 6.7 a**). After four hours of reperfusion the gas exchange function of the transplanted lobe was clearly preserved in PR3 and NE deficient mice. However, the lung graft in wild type recipient mice performed poorly (**Figure 6.7 b**). The mean partial oxygen pressure was 80% in the arterial blood of the left ventricle of knockout mice compared to only 50% in wild type recipient group after clamping the bronchus of the non-transplanted right lung. The degree of protein exudation (**Figure 6.7 c**) and cellular content of neutrophils in the bronchoalveolar lavage fluid (**Figure 6.7 d**) were not significantly different in the knockout group than in the wild type recipients.

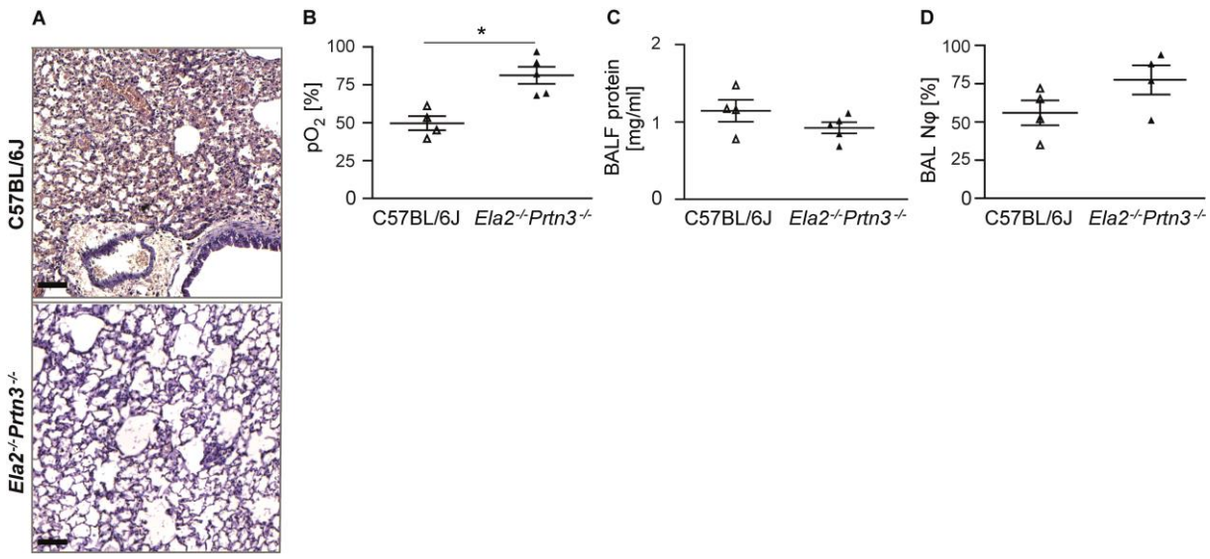

Figure 6.7 Graft dysfunction is mainly triggered by neutrophil elastase and proteinase 3. Donor lungs were taken from wild type mice (C57BL/6J) and perfused with and stored in Perfadex supplemented with albumin (1 mg/ml) for 18 hours at 4°C (cold ischemia). Afterwards, the lungs were orthotopically either transplanted into wild type C57BL/6J mice or into *Ela2*$^{-/-}$*Prtn3*$^{-/-}$ deficient mice with the same genetic background. Mice were sacrificed after 4 h of reperfusion (*n*=4-5 per group). (**a**) H&E staining illustrating the tissue morphology of a transplanted left lung (scale bars, 200 µm). (**b**) pO_2 (partial oxygen pressure) measured in blood collected from the left ventricles of the heart, five minutes after clamping the right bronchus. (**c**) Protein concentration in bronchoalveolar lavage fluid and (**d**) bronchoalveolar lavage neutrophil count in the transplanted mice. Data are represented as mean ± SEM and compared with a Mann-Whitney test (**p*<0.05).

6.3 AAT in lung transplantation – Discussion

Donor lungs transported and stored for more than 6 hours are discarded by transplant surgeons because of an unacceptably high risk of graft dysfunctions. This short preservation time restricts the availability of donor lungs and limits the area of an organ sharing geographic region. Extended hypothermic ischemia times increase the extent of metabolic and structural changes in the transplant and, consequently, the intensity of the early innate immune response in the transplanted organ after the onset of reperfusion, and therefore the risk of PGD after transplantation. The greatest lung tissue damage is thought to be caused by the return of blood plasma and cellular blood components at 37°C after transplantation[81]. Intrigued by the multiple facets of AAT and as it is available for long term augmentation therapy in adults with emphysema due to severe AAT deficiency, we explored its clinical potential in organ conservation during cold ischemic storage and in graft protection from reperfusion injury after lung transplantation in a demanding, clinically relevant mouse model. We discussed that AAT in the preservation solution diffused into the perivascular and interstitial space throughout perfusion and storage of the transplant and was, therefore, optimally deposited in advance to protect the lung against the influx of adhering and extravasating neutrophils around the blood vessels. The anti-protease shield of AAT represented the most pivotal mechanism of lung preservation in this clinical setting. More precisely, our results indicate that the inhibition of neutrophil serine proteases, such as proteinase 3 and neutrophil elastase plays the most pivotal role in protecting the donor organ during reperfusion.

However, several alternative mechanisms of tissue protection and AAT's anti-inflammatory function unrelated to its anti-protease functions have been presented in several studies [90-97]. To clarify the paramount therapeutic mechanism of AAT in lung graft protection during reperfusion, we separated the anti-proteolytic functions of the RCL from other potential functions of the AAT molecule. AAT primarily inhibits NE and PR3 and also other proteases like cathepsin G and trypsin-like enzymes, but to a much lesser extent[21,98-101]. Serine

proteases are active in an environment of neutral pH after regulated secretion or activation of zymogens. They occur in the oxidizing extra- and pericellular environment or within the secretory route including storage granules. Therefore, it was unlikely that these proteases were inhibited in the cytosol after membrane binding[88], endocytosis[102] and translocation into the cytosol[103,104]. Inhibition of caspases[90,105], and calpain I [106] in the cytosol have been inferred to be responsible for additional anti-inflammatory properties of the wild type AAT[106-108]. Our results strongly indicate that non-protease mediated functions of AAT do not significantly account for organ protection during the early phase of reperfusion after transplantation.

In accordance with our results using the non-inhibitory AAT variant we found that PR3 and NE double deficient mice exhibited enhanced primary graft functions compared to wild type mice. The homologs of human PR3 and NE in the mouse are only expressed in the myelomonocyte lineage and constitutively deposited in the neutrophils' primary granules[100]. Mice, deficient of these two proteases in the germline, do not exhibit any biological or developmental change in peripheral tissues and organs and no divergent phenotype can be detected under normal housing and living conditions[25]. Therefore, these mice were optimally suited to clarify the role of neutrophil serine proteases after initiating reperfusion of the lung graft. In summary, these findings in PR3/NE knockout mice were in agreement with recent observations in macaques after prolonged inhibition of cathepsin C, which resulted in the depletion of serine proteases in neutrophils[109]. The neutrophil migration and recruitment to the lungs and bronchi was not different in response to tracheal instillation of LPS with these experimental pharmacological conditions.

The preservation technique in our preclinical study reflects very closely how grafts are handled in a routine thoracosurgical setting. The addition of AAT to Perfadex at a final concentration of 1 mg/ml is a safe and easily acceptable modification of the most frequently used preservation solution. This natural human plasma protein has already been approved

for long term substitution therapy in patients with constitutively low levels of AAT, who developed emphysema.

When AAT does not have to compete with other plasma proteins endocytosis and transcytosis by the lung endothelium[102,110] is expected to be more efficient than its uptake from whole blood, even when additional AAT is administered intravenously prior to transplantation surgery. Hence, flushing and perfusion with 15 µM (1 mg/ml) AAT in Perfadex solution is sufficient to deliver the inhibitor to endothelial cells and interstitial lung space after removal of the donor lung from a brain-dead donor.

When a single dose of 60 µg/g AAT was intraperitoneally injected, the tissue levels of AAT in the murine lungs were clearly lower than in the transplanted AAT-perfused lungs after four hours. *Ex vivo* perfusion of the graft with AAT has a great benefit over its systemic delivery to the recipient, and in addition this procedure complies with existent ethical standards. With this protocol, we achieved maximum tissue levels of AAT in the transplanted tissue, before the first activated neutrophils reach it together with other soluble plasma components after the lungs are reconnected to the recipient's circulation.

Our experiments with an AAT RCL mutant and with PR3/NE deficient mice proved our hypothesis that the protease inhibiting functions of AAT on neutrophils in the early phase of blood reperfusion were most important and sufficient to guard the lung graft from immediate inflammatory damage after prolonged storage times. Possibly, other specific inhibitors of NE would be equally effective. Target specificity and very low toxicity of the utilized inhibitors, however, are crucial for drug safety. For instance, a previous clinical study with the inhibitor aprotinin to reduce PGD had to be canceled prematurely as renal toxicity of aprotinin was discerned[111].

In contrast, the organ conservation procedure presented in this thesis on the basis of an appropriately designed animal study, would be ethically acceptable, technically feasible in a clinical trial, well corroborated by long-standing research on AAT and its clinical application.

Moreover, the proposed protocol would be applicable to organ transplantation surgery in general. Improved graft protection by inhibiting PR3 and NE locally in the transplant, can be directly translated into clinical practice. It is expected to improve transplantation outcome and to help solve the organ shortage problem. The study we performed is a prerequisite for clinical trials to utilize AAT not only for diseased AAT-deficiency patients, but also for the preservation and protection of organ viability, especially after prolonged cold ischemia.

7. Bibliography

1 Carrell, R. W. & Travis, J. α1-Antitrypsin and the serpins. Variation and countervariation. *Trends in Biological Sciences* **10:20–24** (1985).

2 Mala, J. G. & Rose, C. Interactions of heat shock protein 47 with collagen and the stress response: an unconventional chaperone model? *Life Sci* **87**, 579-586, doi:10.1016/j.lfs.2010.09.024 (2010).

3 Zhou, A., Wei, Z., Read, R. J. & Carrell, R. W. Structural mechanism for the carriage and release of thyroxine in the blood. *Proc Natl Acad Sci U S A* **103**, 13321-13326, doi:10.1073/pnas.0604080103 (2006).

4 Silverman, G. A. *et al.* The serpins are an expanding superfamily of structurally similar but functionally diverse proteins. Evolution, mechanism of inhibition, novel functions, and a revised nomenclature. *J Biol Chem* **276**, 33293-33296, doi:10.1074/jbc.R100016200 (2001).

5 Irving, J. A., Pike, R. N., Lesk, A. M. & Whisstock, J. C. Phylogeny of the serpin superfamily: implications of patterns of amino acid conservation for structure and function. *Genome Res* **10**, 1845-1864 (2000).

6 Irving, J. A. *et al.* Serpins in prokaryotes. *Mol Biol Evol* **19**, 1881-1890 (2002).

7 Steenbakkers, P. J. *et al.* A serpin in the cellulosome of the anaerobic fungus Piromyces sp. strain E2. *Mycol Res* **112**, 999-1006, doi:10.1016/j.mycres.2008.01.021 (2008).

8 Law, R. H. *et al.* An overview of the serpin superfamily. *Genome Biol* **7**, 216, doi:10.1186/gb-2006-7-5-216 (2006).

9 Heit, C. *et al.* Update of the human and mouse SERPIN gene superfamily. *Hum Genomics* **7**, 22, doi:10.1186/1479-7364-7-22 (2013).

10 Gettins, P. G. & Olson, S. T. Inhibitory serpins. New insights into their folding, polymerization, regulation and clearance. *Biochem J* **473**, 2273-2293, doi:10.1042/BCJ20160014 (2016).

11 Gettins, P. G. Serpin structure, mechanism, and function. *Chem Rev* **102**, 4751-4804 (2002).

12 Huntington, J. A. Serpin structure, function and dysfunction. *J Thromb Haemost* **9 Suppl 1**, 26-34, doi:10.1111/j.1538-7836.2011.04360.x (2011).

13 Stratikos, E. & Gettins, P. G. Formation of the covalent serpin-proteinase complex involves translocation of the proteinase by more than 70 A and full insertion of the reactive center loop into beta-sheet A. *Proc Natl Acad Sci U S A* **96**, 4808-4813 (1999).

14 Schechter, I. & Berger, A. On the size of the active site in proteases. I. Papain. *Biochem Biophys Res Commun* **27**, 157-162 (1967).

15 Owen, M. C., Brennan, S. O., Lewis, J. H. & Carrell, R. W. Mutation of antitrypsin to antithrombin. alpha 1-antitrypsin Pittsburgh (358 Met leads to Arg), a fatal bleeding disorder. *N Engl J Med* **309**, 694-698, doi:10.1056/NEJM198309223091203 (1983).

16 Heeb, M. J., Espana, F. & Griffin, J. H. Inhibition and complexation of activated protein C by two major inhibitors in plasma. *Blood* **73**, 446-454 (1989).

17 Sherman, P. M. *et al.* Saturation mutagenesis of the plasminogen activator inhibitor-1 reactive center. *J Biol Chem* **267**, 7588-7595 (1992).

18 Hortin, G. L., Sviridov, D. & Anderson, N. L. High-abundance polypeptides of the human plasma proteome comprising the top 4 logs of polypeptide abundance. *Clin Chem* **54**, 1608-1616, doi:10.1373/clinchem.2008.108175 (2008).

19 Travis, J. Structure, function, and control of neutrophil proteinases. *Am J Med* **84**, 37-42 (1988).

20 Stoller, J. K. & Aboussouan, L. S. A review of alpha1-antitrypsin deficiency. *Am J Respir Crit Care Med* **185**, 246-259, doi:10.1164/rccm.201108-1428CI (2012).

21 Travis, J. & Salvesen, G. S. Human plasma proteinase inhibitors. *Annu Rev Biochem* **52**, 655-709, doi:10.1146/annurev.bi.52.070183.003255 (1983).

22 Carrell, R. W., Whisstock, J. & Lomas, D. A. Conformational changes in serpins and the mechanism of alpha 1-antitrypsin deficiency. *Am J Respir Crit Care Med* **150**, S171-175, doi:10.1164/ajrccm/150.6_Pt_2.S171 (1994).

23 Gooptu, B. & Lomas, D. A. Conformational pathology of the serpins: themes, variations, and therapeutic strategies. *Annu Rev Biochem* **78**, 147-176, doi:10.1146/annurev.biochem.78.082107.133320 (2009).

24 Mahadeva, R. & Lomas, D. A. Genetics and respiratory disease. 2. Alpha 1-antitrypsin deficiency, cirrhosis and emphysema. *Thorax* **53**, 501-505 (1998).

25 Pfister, H. *et al.* Antineutrophil cytoplasmic autoantibodies against the murine homolog of proteinase 3 (Wegener autoantigen) are pathogenic in vivo. *Blood* **104**, 1411-1418, doi:10.1182/blood-2004-01-0267 (2004).

26 Wisniewski, J. R., Zougman, A., Nagaraj, N. & Mann, M. Universal sample preparation method for proteome analysis. *Nat Methods* **6**, 359-362, doi:10.1038/nmeth.1322 (2009).

27 Grosche, A. *et al.* The Proteome of Native Adult Muller Glial Cells From Murine Retina. *Mol Cell Proteomics* **15**, 462-480, doi:10.1074/mcp.M115.052183 (2016).

28 Tyanova, S., Mann, M. & Cox, J. MaxQuant for in-depth analysis of large SILAC datasets. *Methods Mol Biol* **1188**, 351-364, doi:10.1007/978-1-4939-1142-4_24 (2014).

29 Krupnick, A. S. *et al.* Orthotopic mouse lung transplantation as experimental methodology to study transplant and tumor biology. *Nat Protoc* **4**, 86-93, doi:10.1038/nprot.2008.218 (2009).

30 Vanin, E. F. Processed pseudogenes: characteristics and evolution. *Annu Rev Genet* **19**, 253-272, doi:10.1146/annurev.ge.19.120185.001345 (1985).

31 Mighell, A. J., Smith, N. R., Robinson, P. A. & Markham, A. F. Vertebrate pseudogenes. *FEBS Lett* **468**, 109-114 (2000).

32 Zheng, D. & Gerstein, M. B. The ambiguous boundary between genes and pseudogenes: the dead rise up, or do they? *Trends Genet* **23**, 219-224, doi:10.1016/j.tig.2007.03.003 (2007).

33 Kong, Y. *et al.* Pseudogene PDIA3P1 promotes cell proliferation, migration and invasion, and suppresses apoptosis in hepatocellular carcinoma by regulating the p53 pathway. *Cancer Lett* **407**, 76-83, doi:10.1016/j.canlet.2017.07.031 (2017).

34 Roberts, T. C. & Morris, K. V. Not so pseudo anymore: pseudogenes as therapeutic targets. *Pharmacogenomics* **14**, 2023-2034, doi:10.2217/pgs.13.172 (2013).

35 Seixas, S. *et al.* Sequence diversity at the proximal 14q32.1 SERPIN subcluster: evidence for natural selection favoring the pseudogenization of SERPINA2. *Mol Biol Evol* **24**, 587-598, doi:10.1093/molbev/msl187 (2007).

36 Ohno, S. *Evolution by Gene Duplication*. (1970).

37 Hedges, S. B., Dudley, J. & Kumar, S. TimeTree: a public knowledge-base of divergence times among organisms. *Bioinformatics* **22**, 2971-2972, doi:10.1093/bioinformatics/btl505 (2006).

38 Abbott, C. M. *et al.* Alpha 1-antitrypsin-related gene (ATR) for prenatal diagnosis. *Lancet* **1**, 1425-1426 (1987).

39 Kelsey, G. D., Parkar, M. & Povey, S. The human alpha-1-antitrypsin-related sequence gene: isolation and investigation of its expression. *Ann Hum Genet* **52**, 151-160 (1988).

40 Bao, J. J., Reed-Fourquet, L., Sifers, R. N., Kidd, V. J. & Woo, S. L. Molecular structure and sequence homology of a gene related to alpha 1-antitrypsin in the human genome. *Genomics* **2**, 165-173 (1988).

41 Futamura, A., Stratikos, E., Olson, S. T. & Gettins, P. G. Change in environment of the P1 side chain upon progression from the Michaelis complex to the covalent serpin-proteinase complex. *Biochemistry* **37**, 13110-13119, doi:10.1021/bi981234m (1998).

42 Marques, P. I. *et al.* SERPINA2 is a novel gene with a divergent function from SERPINA1. *PLoS One* **8**, e66889, doi:10.1371/journal.pone.0066889 (2013).

43 Leavy, M. *et al.* Effects of Elevated beta-Estradiol Levels on the Functional Morphology of the Testis - New Insights. *Sci Rep* **7**, 39931, doi:10.1038/srep39931 (2017).

44 Lin, Y. C. *et al.* Genome dynamics of the human embryonic kidney 293 lineage in response to cell biology manipulations. *Nat Commun* **5**, 4767, doi:10.1038/ncomms5767 (2014).

45 Peroutka Iii, R. J., Orcutt, S. J., Strickler, J. E. & Butt, T. R. SUMO fusion technology for enhanced protein expression and purification in prokaryotes and eukaryotes. *Methods Mol Biol* **705**, 15-30, doi:10.1007/978-1-61737-967-3_2 (2011).

46 Kumar, S., Stecher, G. & Tamura, K. MEGA7: Molecular Evolutionary Genetics Analysis Version 7.0 for Bigger Datasets. *Mol Biol Evol* **33**, 1870-1874, doi:10.1093/molbev/msw054 (2016).

47 Forsyth, S., Horvath, A. & Coughlin, P. A review and comparison of the murine alpha1-antitrypsin and alpha1-antichymotrypsin multigene clusters with the human clade A serpins. *Genomics* **81**, 336-345 (2003).

48 Yamazaki, K. *et al.* Identification and characterization of novel and unknown mouse epididymis-specific genes by complementary DNA microarray technology. *Biol Reprod* **75**, 462-468, doi:10.1095/biolreprod.105.048058 (2006).

49 Hill, R. E. & Hastie, N. D. Accelerated evolution in the reactive centre regions of serine protease inhibitors. *Nature* **326**, 96-99, doi:10.1038/326096a0 (1987).

50 Yenugu, S., Hamil, K. G., French, F. S. & Hall, S. H. Antimicrobial actions of the human epididymis 2 (HE2) protein isoforms, HE2alpha, HE2beta1 and HE2beta2. *Reprod Biol Endocrinol* **2**, 61, doi:10.1186/1477-7827-2-61 (2004).

51 Hiemstra, P. S. *et al.* Antibacterial activity of antileukoprotease. *Infect Immun* **64**, 4520-4524 (1996).

52 Simpson, A. J., Maxwell, A. I., Govan, J. R., Haslett, C. & Sallenave, J. M. Elafin (elastase-specific inhibitor) has anti-microbial activity against gram-positive and gram-negative respiratory pathogens. *FEBS Lett* **452**, 309-313 (1999).

53 Richardson, R. T. *et al.* Cloning and sequencing of human Eppin: a novel family of protease inhibitors expressed in the epididymis and testis. *Gene* **270**, 93-102 (2001).

54 Miska, W., Fehl, P. & Henkel, R. Biochemical and immunological characterization of the acrosome reaction-inducing substance (ARIS) of hFF. *Biochem Biophys Res Commun* **199**, 125-129, doi:10.1006/bbrc.1994.1203 (1994).

55 Moore, A., Penfold, L. M., Johnson, J. L., Latchman, D. S. & Moore, H. D. Human sperm-egg binding is inhibited by peptides corresponding to core region of an acrosomal serine protease inhibitor. *Mol Reprod Dev* **34**, 280-291, doi:10.1002/mrd.1080340308 (1993).

56 Browne, J. A., Yang, R., Leir, S. H., Eggener, S. E. & Harris, A. Expression profiles of human epididymis epithelial cells reveal the functional diversity of caput, corpus and cauda regions. *Mol Hum Reprod* **22**, 69-82, doi:10.1093/molehr/gav066 (2016).

57 Ilio, K. Y. & Hess, R. A. Structure and function of the ductuli efferentes: a review. *Microsc Res Tech* **29**, 432-467, doi:10.1002/jemt.1070290604 (1994).

58 Razzaque, M. S. & Taguchi, T. The possible role of colligin/HSP47, a collagen-binding protein, in the pathogenesis of human and experimental fibrotic diseases. *Histol Histopathol* **14**, 1199-1212 (1999).

59 Schneider, K. & Bertolotti, A. Surviving protein quality control catastrophes--from cells to organisms. *J Cell Sci* **128**, 3861-3869, doi:10.1242/jcs.173047 (2015).

60 Laflamme, B. A. & Wolfner, M. F. Identification and function of proteolysis regulators in seminal fluid. *Mol Reprod Dev* **80**, 80-101, doi:10.1002/mrd.22130 (2013).

61 Kohno, N. *et al.* Two novel testicular serine proteases, TESP1 and TESP2, are present in the mouse sperm acrosome. *Biochem Biophys Res Commun* **245**, 658-665 (1998).

62 Murer, V. *et al.* Male fertility defects in mice lacking the serine protease inhibitor protease nexin-1. *Proc Natl Acad Sci U S A* **98**, 3029-3033, doi:10.1073/pnas.051630698 (2001).

63 Zhou, Y. *et al.* An epididymis-specific secretory protein HongrES1 critically regulates sperm capacitation and male fertility. *PLoS One* **3**, e4106, doi:10.1371/journal.pone.0004106 (2008).

64 Uhrin, P. *et al.* Disruption of the protein C inhibitor gene results in impaired spermatogenesis and male infertility. *J Clin Invest* **106**, 1531-1539, doi:10.1172/JCI10768 (2000).

65 Shen, C. *et al.* Prss37 is required for male fertility in the mouse. *Biol Reprod* **88**, 123, doi:10.1095/biolreprod.112.107086 (2013).

66 Citrino, G., Check, J. H., Diantonio, A., Bollendorf, A. & Katsoff, D. Pretreatment of sperm with low hypo-osmotic swelling tests with chymotrypsin prior to intrauterine insemination (IUI) and avoidance of unprotectected intercourse results in pregnancy rates comparable to IUI for other male factor problems. *Clin Exp Obstet Gynecol* **37**, 187-189 (2010).

67 Bollendorf, A., Check, D., Check, J. H., Hourani, W. & McMonagle, K. Comparison of the efficacy of treating sperm with low hypoosmotic swelling test scores with chymotrypsin followed by intrauterine insemination vs in vitro fertilization with intracytoplasmic sperm injection. *Clin Exp Obstet Gynecol* **38**, 24-25 (2011).

68 Check, M. L., Katsoff, D., Check, J. H. & Summers-Chase, D. Effect of treating sperm with low hypo-osmotic swelling test scores with chymotrypsin on pregnancy rates after conventional in vitro fertilization-embryo transfer. *Fertil Steril* **82**, 741-742, doi:10.1016/j.fertnstert.2004.05.066 (2004).

69 Bollendorf, A., Check, J. H., Katsoff, D. & Fedele, A. The use of chymotrypsin/galactose to treat spermatozoa bound with anti-sperm antibodies prior to intra-uterine insemination. *Hum Reprod* **9**, 484-488 (1994).

70 Topic, A. *et al.* Alpha-1-antitrypsin deficiency in Serbian adults with lung diseases. *Genet Test Mol Biomarkers* **16**, 1282-1286, doi:10.1089/gtmb.2012.0152 (2012).

71 Nukiwa, T. *et al.* Characterization of the M1(Ala213) type of alpha 1-antitrypsin, a newly recognized, common "normal" alpha 1-antitrypsin haplotype. *Biochemistry* **26**, 5259-5267 (1987).

72 Malik, R. *et al.* Common coding variant in SERPINA1 increases the risk for large artery stroke. *Proc Natl Acad Sci U S A* **114**, 3613-3618, doi:10.1073/pnas.1616301114 (2017).

73 Lee, J. C. & Christie, J. D. Primary graft dysfunction. *Clin Chest Med* **32**, 279-293, doi:10.1016/j.ccm.2011.02.007 (2011).

74 Daemen, M. A. *et al.* Functional protection by acute phase proteins alpha(1)-acid glycoprotein and alpha(1)-antitrypsin against ischemia/reperfusion injury by preventing apoptosis and inflammation. *Circulation* **102**, 1420-1426 (2000).

75 Rong Yang, Q. L., Margaret H. Collins, Jay L. Grosfeld, and Mark D. Pescovitz. Alpha-1-Proteinase Inhibitor Prolongs Small Intestinal Graft Preservation and Survival. *Journal of Pediatric Surgery* **31**, 1052-1055 (1996).

76 von Dobschuetz, E., Hoffmann, T. & Messmer, K. Inhibition of neutrophil proteinases by recombinant serpin Lex032 reduces capillary no-reflow in ischemia/reperfusion-induced acute pancreatitis. *J Pharmacol Exp Ther* **290**, 782-788 (1999).

77 Gao, W. *et al.* alpha1-Antitrypsin inhibits ischemia reperfusion-induced lung injury by reducing inflammatory response and cell death. *J of Heart Lung Transplantation* **33**, 309-315, doi:10.1016/j.healun.2013.10.031 (2014).

78 de Perrot, M., Liu, M., Waddell, T. K. & Keshavjee, S. Ischemia-reperfusion-induced lung injury. *Am J Respir Crit Care Med* **167**, 490-511, doi:10.1164/rccm.200207-670SO (2003).

79 Meyer, K. C. *et al.* Neutrophils, unopposed neutrophil elastase, and alpha1-antiprotease defenses following human lung transplantation. *Am J Respir Crit Care Med* **164**, 97-102, doi:10.1164/ajrccm.164.1.2006096 (2001).

80 Schofield, Z. V., Woodruff, T. M., Halai, R., Wu, M. C. & Cooper, M. A. Neutrophils--a key component of ischemia-reperfusion injury. *Shock* **40**, 463-470, doi:10.1097/SHK.0000000000000044 (2013).

81 Chen, F. & Date, H. Update on ischemia-reperfusion injury in lung transplantation. *Curr Opin Organ Transplant* **20**, 515-520, doi:10.1097/MOT.0000000000000234 (2015).

82 Laubach, V. E. & Sharma, A. K. Mechanisms of lung ischemia-reperfusion injury. *Curr Opin Organ Transplant* **21**, 246-252, doi:10.1097/MOT.0000000000000304 (2016).

83 Khan, T. A. *et al.* Aprotinin preserves cellular junctions and reduces myocardial edema after regional ischemia and cardioplegic arrest. *Circulation* **112**, I196-201, doi:10.1161/CIRCULATIONAHA.104.526053 (2005).

84 Bittner, H. B. *et al.* Aprotinin decreases reperfusion injury and allograft dysfunction in clinical lung transplantation. *Eur J Cardiothorac Surg* **29**, 210-215, doi:10.1016/j.ejcts.2005.12.001 (2006).

85 Sands, H. & Tuma, R. F. LEX 032: a novel recombinant human protein for the treatment of ischaemic reperfusion injury. *Expert Opin Investig Drugs* **8**, 1907-1916, doi:10.1517/13543784.8.11.1907 (1999).

86 Iskender, I. *et al.* Human alpha1-antitrypsin improves early post-transplant lung function: Pre-clinical studies in a pig lung transplant model. *J Heart Lung Transplant* **35**, 913-921, doi:10.1016/j.healun.2016.03.006 (2016).

87 Perera, N. C. *et al.* NSP4 is stored in azurophil granules and released by activated neutrophils as active endoprotease with restricted specificity. *J Immunol* **191**, 2700-2707, doi:10.4049/jimmunol.1301293 (2013).

88 Gordon, S. M. *et al.* Rosuvastatin Alters the Proteome of High Density Lipoproteins: Generation of alpha-1-antitrypsin Enriched Particles with Anti-inflammatory Properties. *Mol Cell Proteomics* **14**, 3247-3257, doi:10.1074/mcp.M115.054031 (2015).

89 Elliott, P. R., Lomas, D. A., Carrell, R. W. & Abrahams, J. P. Inhibitory conformation of the reactive loop of alpha 1-antitrypsin. *Nat Struct Biol* **3**, 676-681 (1996).

90 Toldo, S. *et al.* Alpha-1 antitrypsin inhibits caspase-1 and protects from acute myocardial ischemia-reperfusion injury. *J Mol Cell Cardiol* **51**, 244-251, doi:10.1016/j.yjmcc.2011.05.003 (2011).

91 Brantly, M. Alpha1-antitrypsin: not just an antiprotease: extending the half-life of a natural anti-inflammatory molecule by conjugation with polyethylene glycol. *Am J Respir Cell Mol Biol* **27**, 652-654, doi:10.1165/rcmb.F250 (2002).

92 Reddy, P. alpha-1 antitrysin DAMPens GVHD. *Blood* **120**, 2780-2781, doi:10.1182/blood-2012-08-442764 (2012).

93 Lewis, E. C. Expanding the clinical indications for alpha(1)-antitrypsin therapy. *Mol Med* **18**, 957-970, doi:10.2119/molmed.2011.00196 (2012).

94 Jenne, D. E. Off-target rewards of augmentation therapy with alpha1-antitrypsin. *Am J Respir Crit Care Med* **190**, 1203-1204, doi:10.1164/rccm.201410-1809ED (2014).

95 Stockley, R. A. alpha1-antitrypsin: a polyfunctional protein? *Lancet Respir Med* **3**, 341-343, doi:10.1016/S2213-2600(15)00094-6 (2015).

96 Baraldo, S. *et al.* Alpha-1 Antitrypsin Deficiency Today: New Insights in the Immunological Pathways. *Respiration* **91**, 380-385, doi:10.1159/000445692 (2016).

97 Guttman, O. *et al.* alpha1-Antitrypsin modifies general NK cell interactions with dendritic cells and specific interactions with islet beta-cells in favor of protection from autoimmune diabetes. *Immunology*, doi:10.1111/imm.12403 (2014).

98 Reid, P. T. & Sallenave, J. M. Neutrophil-derived elastases and their inhibitors: potential role in the pathogenesis of lung disease. *Curr Opin Investig Drugs* **2**, 59-67 (2001).

99 Pham, C. T. Neutrophil serine proteases fine-tune the inflammatory response. *Int J Biochem Cell Biol* **40**, 1317-1333, doi:10.1016/j.biocel.2007.11.008 (2008).

100 Korkmaz, B., Horwitz, M. S., Jenne, D. E. & Gauthier, F. Neutrophil elastase, proteinase 3, and cathepsin G as therapeutic targets in human diseases. *Pharmacol Rev* **62**, 726-759, doi:10.1124/pr.110.002733 (2010).

101 Kessenbrock, K., Dau, T. & Jenne, D. E. Tailor-made inflammation: how neutrophil serine proteases modulate the inflammatory response. *J Mol Med (Berl)* **89**, 23-28, doi:10.1007/s00109-010-0677-3 (2011).

102 Lockett, A. D. *et al.* Scavenger receptor class B, type I-mediated uptake of A1AT by pulmonary endothelial cells. *Am J Physiol Lung Cell Mol Physiol* **309**, L425-434, doi:10.1152/ajplung.00376.2014 (2015).

103 Wang, Y. *et al.* Cytosolic, autocrine alpha-1 proteinase inhibitor (A1PI) inhibits caspase-1 and blocks IL-1beta dependent cytokine release in monocytes. *PLoS One* **7**, e51078, doi:10.1371/journal.pone.0051078 (2012).

104 Serban, K. A. & Petrache, I. Alpha-1 Antitrypsin and Lung Cell Apoptosis. *Ann Am Thorac Soc* **13 Suppl 2**, S146-149, doi:10.1513/AnnalsATS.201505-312KV (2016).

105 Petrache, I. *et al.* alpha-1 antitrypsin inhibits caspase-3 activity, preventing lung endothelial cell apoptosis. *Am J Pathol* **169**, 1155-1166 (2006).

106 Al-Omari, M. *et al.* Acute-phase protein alpha1-antitrypsin inhibits neutrophil calpain I and induces random migration. *Mol Med* **17**, 865-874, doi:10.2119/molmed.2011.00089 (2011).

107 Ehlers, M. R. Immune-modulating effects of alpha-1 antitrypsin. *Biol Chem* **395**, 1187-1193, doi:10.1515/hsz-2014-0161 (2014).

108 Lazrak, A. *et al.* Alpha(1)-antitrypsin inhibits epithelial Na+ transport in vitro and in vivo. *Am J Respir Cell Mol Biol* **41**, 261-270, doi:10.1165/rcmb.2008-0384OC (2009).

109 Guarino, C. *et al.* Prolonged pharmacological inhibition of cathepsin C results in elimination of neutrophil serine proteases. *Biochem Pharmacol* **131**, 52-67, doi:10.1016/j.bcp.2017.02.009 (2017).

110 Sohrab, S. *et al.* Mechanism of alpha-1 antitrypsin endocytosis by lung endothelium. *FASEB J* **23**, 3149-3158, doi:10.1096/fj.09-129304 (2009).

111 Herrington, C. S. *et al.* A randomized, placebo-controlled trial of aprotinin to reduce primary graft dysfunction following lung transplantation. *Clin Transplant* **25**, 90-96, doi:10.1111/j.1399-0012.2010.01319.x (2011).

8. Abbreviations

µl	Microliter
aa	Amino acid
AAT	α-1-antitrypsin proteinase inhibitor
APS	Ammonium persulfate
Asp	Aspartic acid
BAL	Bronchoalveolar lavage
BALF	Bronchoalveolar lavage fluid
bp	Base pair
Cat. No.	Catalog number
CATG	Cathepsin G
CHTR	Chymotrypsin
Cys	Cysteine
Da	Dalton
ddH_2O	Double destilled water
DNA	Deoxyribonucleic acid
ELISA	Enzyme-linked immunosorbent assay
Endo H	Endo-ß-N-acetylglucosaminidase H
FRET	Förster/Fluorescence resonance energy transfer
HDL	High density lipoprotein
HEK	Human embryonic kidney cell line
His	Histidine
HPL	Human platelet lysate
HRP	Horseradish peroxidase
i. p.	Intra peritoneal
IPTG	Isopropyl β-D-1-thiogalactopyranoside
KLK3	Kallikrein 3
LDL	Low density lipoprotein
mAb	Monoclonal antibody

min	Minutes
mRNA	Messenger ribonucleic acid
MS	Mass spectrometry
NE	Neutrophil elastase
NEB	New England Biolabs
NSP4	Neutrophil serine protease 4
OD	Optic density
PBMC	Peripheral blood mononuclear cell
PBS	Phosphate buffered saline
PDB	Protein databasePEI Polyethyleneimine
PGD	Primary graft dysfunction
pI	Isoelectric point
PIPES	Piperazine-N,N’-bis(2-ethanesulfonic acid)
PMN	Polymorphonuclear cells
PNGase F	Peptide -N-Glycosidase F
PR3	Proteinase 3
PVDF	Polyvinylidene difluoride
RCL	Reactive center loop
RIPA	Radioimmunoprecipitation assay buffer
rpm	Rounds per minute
S2	Schneider 2
SBzI	Thiobenzyl ester
sec	Seconds
Ser	Serine
Serpin	Serine protease inhibitor
Sulfo-NHS-Biotin	Biotin 3-sulfo-N-hydroxycuccinimide ester sodium salt
SUMO	Small ubiquitin-related modifier
TCEP	Tris(2-carboxyethyl) phosphine
TEMED	Tetramethylethylenediamine
TR	Trypsin

9. Appendix

9.1 Vector Maps

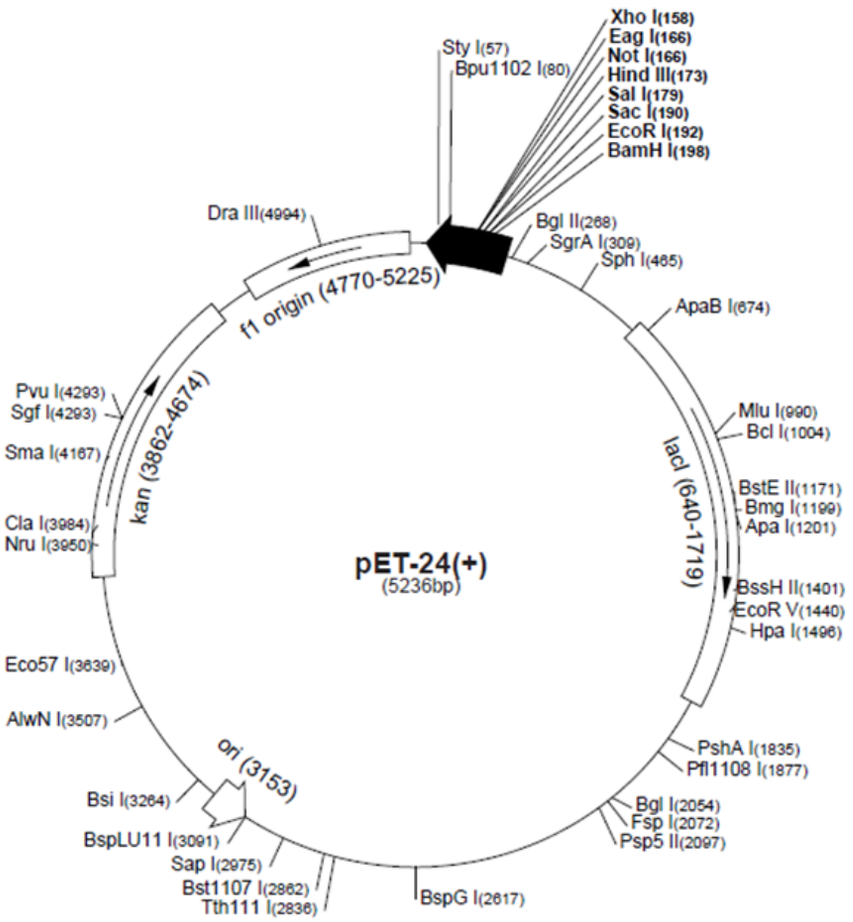

Figure 9.1 Vector map of the pET-24(+) plasmid. Cloing of serpina2 into pET-24 was carried out by digesting the vector with the restriction enzymes BamHI and XhoI to express serpina2 in *E. coli* cell lines. The vector carries a gene for kanamycin resistance.

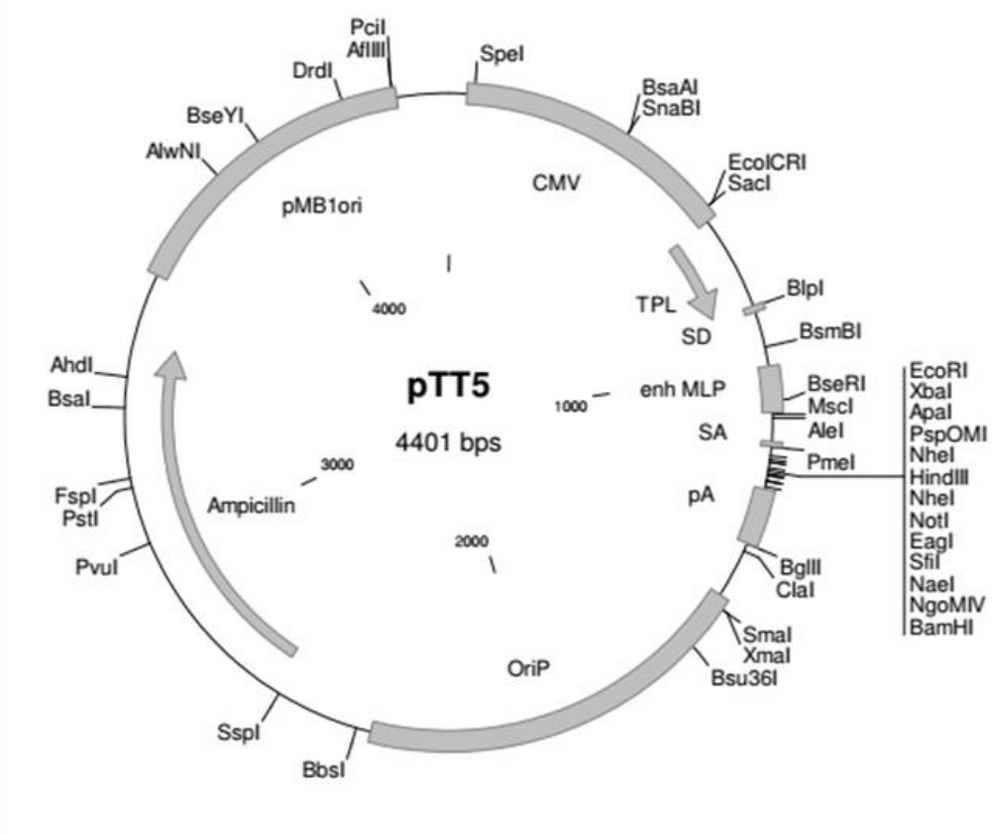

Figure 9.2 Vector map of the pTT5 plasmid. This vector was used to express different serpins in HEK 293 cells. The important features of this vector are an *E. coli* (pMB1ori) and EBV (OriP) specific origin of replication, a promotor of the cytomegalovirus (CMV), an adenovirus tripartite leader (TPL), a major late promotor (MLP), a rabbit bet-globin polyadenylation signal (pA) and an ampicillin resistance gene.

9.2 Screeing for serpina2 specific antibodies

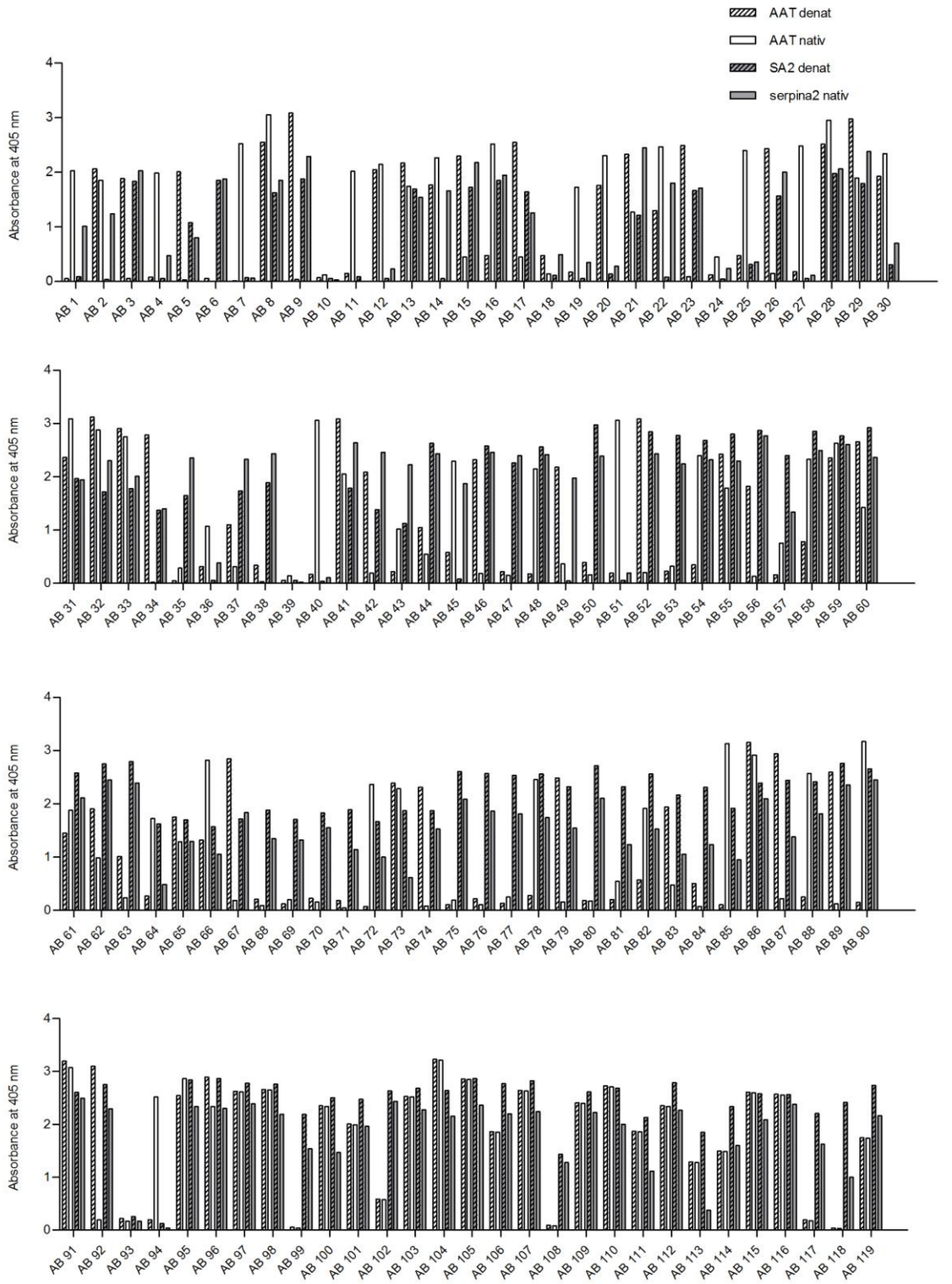

10. Publications and international meetings

10.1 Publications

Parts of this thesis are submitted for publication to the Journal of Heart and Lung transplantation:

Jessica Götzfried*, Natalia Smirnova*, Carmela Morrone, Brice Korkmaz, Ali Önder Yildirim, Oliver Eickelberg, Dieter E. Jenne.

'Preservation with alpha-1-antitrypsin improves primary graft function of murine lung transplants'

Parts of this thesis will be submitted for publication:

Jessica Götzfried, Susana Seixas, Artur Mayerhofer, Matthias Trottmann, Christoph Meyer, Agnese Petrera, Stefanie M. Hauck, Herbert Schiller, Elisabeth Kremmer, Dieter E. Jenne.

‚More than just a pseudogene: serpina2 is an epididymis specific protease inhibitor' (manuscript in preparation)

Parts of this thesis have been published:

Malik R, Dau T, Gonik M, Sivakumar A, Deredge DJ, Edeleva EV, **Götzfried J**, van der Laan SW, Pasterkamp G, Beaufort N, Seixas S, Bevan S, Lincz LF, Holliday EG, Burgess AI, Rannikmäe K, Minnerup J, Kriebel J, Waldenberger M, Müller-Nurasyid M, Lichtner P, Saleheen D; International Stroke Genetics Consortium., Rothwell PM, Levi C, Attia J, Sudlow CL, Braun D, Markus HS, Wintrode PL, Berger K, Jenne DE, Dichgans M., **2017**.

Common coding variant in SERPINA1 increases the risk for large artery stroke.

Proc Natl Acad Sci USA

10.2 Presentations at international conferences

10.2.1 Oral presentations

‘Tissue distribution and function of the putative serine protease inhibitor serpina2 and its modifying impact on lung diseases’, 32nd Winter School on Proteinases and Their Inhibitors. Italy, 2015

‘Storage and Transplantability of Donor Lungs is extended by Alpha-1-Antitrypsin as an Additive to Perfadex’, 34nd Winter School on Proteinases and Their Inhibitors. Italy, 2017 (Best presentation award)

10.2.2 Poster presentation

‘More than just a pseudogene: SERPINA2 is an epididymis specific protease inhibitor’, Gordon Research Conference: Proteolytic Enzymes an Their Inhibitors. Italy, 2016

11. Acknowledgement

Most of all I would like to thank my supervisor PD Dr. Dieter Jenne for his exquisite guidance, his continual support and for always having an open ear for me. Thank you, for all the time you took to teach me how great science is done. I truly enjoyed and learned a lot through our scientific discussion and I benefited a lot from your vast knowledge and experience. Thank you also, for allowing me to explore my own ideas and your continuous enthusiasm.

I am also very grateful to Prof. Dr. Karl-Peter Hopfner, my doctoral thesis supervisor at the faculty of chemistry and biochemistry at the Ludwig-Maximilians-Universität München. I also want to thank the members of my thesis advisory board committee, namely Dr. Øyvind L. Schönberger, Prof. Dr. Edgar Meinl and Dr. med. Ulf Schönermarck for their time, their continuous interest in my work and their helpful feedback.

Many thanks go to our collaboration partners, most of all to Susana Seixas, Prof. Dr. Arthur Mayerhofer, Prof. Dr. Trottmann and Heike Polster for their help with the ‘serpina2’ project and also to Natalia Smirnova and Carmela Morrone for their contributions to the ‘AAT in lung transplantation’ project.

I would also like to thank Prof. Dr. Oliver Eickelberg for hosting our group at the Comprehensive Pneumology Center at the Helmholtz Center Munich. Further, I want to thank the organizers of the CPC Research School for the great opportunities I had during my PhD, most of all Dr. Doreen Franke for her great support.

I want to acknowledge the financial support by the European Union Seventh Framework Program (FP7/2007-2013) under Grant Agreement 261382 (INTRICATE) and the European Union’s H2020-PHC-2015 program RELENT (668036).

I dearly want to thank all the members of the Jenne group Dr. Natascha Perera, Dr. Thérèse Dau and Dr. Lisa Allmannsberger for the warm welcome to the group and that I could always rely on your support in scientific questions and beyond. Most of all I want to thank Heike Kittel, who tragically passed away after a traffic accident, I miss you so much, but I am very

grateful that I had the chance to work with you and learn from you. I want to thank Dr. Anne Sophie Lamort for supporting our group and always making me smile. I also want to thank the new members of the Jenne lab, Stefanie Weiß und Salome Rehm for the great atmosphere in the lab, the great cooperation, their support and a lot of fun.

I also benefited greatly from my fellow PhD students and colleagues. Most of all I want to thank Larissa Knüppel for helping me to start my day early in the morning, for always having my back, and for being such a dear friend.

I also want to thank my dear friends outside science, most of all Julia Hildebrand for always being there for me.

I would like to dedicate this work to my loving family, especially my parents, my parents-in-law and my grandparents and to the best husband ever, who always believed in me and was able to motivate me whenever necessary. Thank you all for always being there for me and supporting me all the way through.